# USING ATOMIC STRUCTURES OF EXTREMOPHILIC RIBOSOMES TO STUDY BACTERIAL ADAPTATION TO STRESS

Ву

Karla Helena Bueno

A DISSERTATION
Submitted to
Newcastle University
in partial fulfilment of the requirements
for the degree of

**Doctor of Philosophy** 

2024

# **Table of Contents**

Α	BSTRACT	4
Α	CKNOWLEDGEMENTS	5
LI	ST OF FIGURES	6
LI	ST OF TABLES	. 10
Α	BBREVIATIONS AND SYMBOLS	. 11
С	HAPTER 1: INTRODUCTION	. 13
	1.1 PREFACE	. 13
	1.2 HIBERNATION IS UBIQUITOUS IN NATURE	. 14
	1.3 WHAT DO WE KNOW OF RIBOSOME HIBERNATION?	. 22
	1.4 RIBOSOME HIBERNATION FACTORS IN BACTERIA	. 28
	1.5 WHAT IS THE ROLE OF RIBOSOME HIBERNATION FACTORS? INHIBITION VS PROTECTION	. 45
	1.6 THE COLD-ADAPTED BACTERIUM PSYCHROBACTER URATIVORANS	. 48
С	HAPTER 2: MATERIALS AND METHODS	. 52
	2.1 SPECIES SELECTION	. 52
	2.2 BIOMASS PRODUCTION	. 52
	2.3 RIBOSOME ISOLATION	. 53
	2.4 GRID PREPARATION	. 55
	2.5 GRID SCREENING AND CRYO-EM DATA COLLECTION	. 55
	2.6 CRYO-EM DATA PROCESSING OF RIBOSOMES FROM P. URATIVORANS	. 56
	2.7 USING CRYO-EM MAPS TO CREATE AN ATOMIC MODEL OF COLD-ADAPTED RIBOSOM FROM P. URATIVORANS	
	2.8 IDENTIFYING A MYSTERIOUS DENSITY	. 58
	2.9 PHYLOGENETIC ANALYSIS	. 59
	2.10 MASS SPECTROMETRY ANALYSIS	. 60
С	HAPTER 3: DISCOVERY OF A NOVEL BACTERIAL RIBOSOME HIBERNATION FACTOR	. 63
	3.1 INTRODUCTION	. 63
	3.2 DETERMINING THE FIRST RIBOSOME STRUCTURE OF ANY COLD-ADAPTED ORGANISM	. 67
	3.3 CHARACTERIZING BALON: A NOVEL RIBOSOME BINDING PROTEIN	. 75
	3.4 BALON AS A RIBOSOME HIBERNATION FACTOR	. 85
	3.5 THE BALON ENCODING GENE AND ITS PHYLOGENETIC AND GENOMIC LOCALIZATIO	
	3 6 BALON BINDING TO THE RIBOSOME IS NOT LIMITED TO COLD SHOCK	

CHAPTER 4: DIFFERENT MODES OF RIBOSOME HIBERNATION	101
4.1 BINDING STATES OF THE HIBERNATING P. URATIVORANS RIBOSOME	101
4.2 BINDING STATE I: THE HIBERNATING RIBOSOME IN COMPLEX WITH BALON AND	) RaiA
	103
4.3 BINDING STATE II: THE HIBERNATING RIBOSOME IN COMPLEX WITH BALON, tRI	
4.4 BALON BINDS THE RIBOSOME IN COMPLEX WITH PROTEIN EF-Tu	114
CHAPTER 5: CONCLUSIONS AND FUTURE WORK	124
5.1 BALON POTENTIALLY ALLOWS FOR A MECHANISTICALLY DISTINCT FASTER MOI	DE OF
HIBERNATION	124
5.2 OTHER POTENTIAL FUNCTIONS OF BALON	130
5.3 BALON DISCOVERY PROVIDES AN INSIGHT INTO THE ORIGIN OF RIBOSOME	
HIBERNATION	131
5.4 HOW DO RIBOSOMES RECRUIT HIBERNATION FACTORS DURING STRESS?	133
REFERENCES	135
APPENDICES	147
PUBLICATIONS	149
PREPRINTS	153

# **ABSTRACT**

To conserve energy during starvation and stress, many organisms use hibernation factor proteins to inhibit protein synthesis and protect their ribosomes from damage. In bacteria, two families of hibernation factors have been described, but the low conservation of these proteins and the huge diversity of species, habitats and environmental stressors have confounded their discovery. Here, by combining cryogenic electron microscopy, genetics and biochemistry, we identify Balon, a new hibernation factor in the cold-adapted bacterium *Psychrobacter urativorans*. We show that Balon is a distant homologue of the archaeo-eukaryotic translation factor aeRF1 and is found in 20% of representative bacteria. During cold shock or stationary phase, Balon occupies the ribosomal A site in both vacant and actively translating ribosomes in complex with EF-Tu, highlighting an unexpected role for EF-Tu in the cellular stress response. Unlike typical A-site substrates, Balon binds to ribosomes in an mRNAindependent manner, initiating a new mode of ribosome hibernation that can commence while ribosomes are still engaged in protein synthesis. Our work suggests that Balon-EF-Tu-regulated ribosome hibernation is a ubiquitous bacterial stressresponse mechanism, and we demonstrate that putative Balon homologues in Mycobacteria bind to ribosomes in a similar fashion. This finding calls for a revision of the current model of ribosome hibernation inferred from common model organisms and holds numerous implications for how we understand and study ribosome hibernation.

# **ACKNOWLEDGEMENTS**

I would like to express my deepest gratitude to all those who supported and guided me throughout my PhD studies.

I would like to thank all past and current members of the Melnikov lab, especially Sergey, Chinenye, Lewis and Charlotte for their constant support and encouragement. You have all made this journey as enjoyable and as fun as it can be.

A special mention goes to my family, friends and Heaklig for their unwavering emotional support, understanding, and encouragement throughout the challenges of this academic pursuit.

I would also like to thank the entire NUBI staff for providing me with the knowledge and resources that laid the foundation for this research. Special thanks to Bert, Claudia, Arnaud, Simon, Douglas, August, Javier and Jack for their day-to-day help and support.

Likewise, I would like to thank the staff of the York Structural Biology lab for their support with the cryo-EM data collection and processing. Special thanks to Chris, Jamie and Sam for their guidance and contributions since the early stages of this project.

To all those who contributed to this work, whether directly or indirectly, I extend my sincere appreciation and gratitude.

# LIST OF FIGURES

Figure 1. Ribosome hibernation factors are present in the bacterial and eukaryoti	ic
domains 1	7
Figure 2. Hibernation of biological molecules is not limited to ribosomes 2	20
Figure 3. First published electron micrographs of 100S ribosomes 2	23
Figure 4. Cross section of so-called "ribosomal bodies" from oocytes in <i>L. sicul</i> a	
Figure 5. Ribosome crystal structures of <i>T. thermophilu</i> s reveals binding site o	
hibernation factor RMF to the ribosome	
Figure 6. The Shine-Dalgarno region of mRNA mediates binding of most bacteriamRNA to the ribosome	
Figure 7. Binding of RMF is incompatible with protein synthesis	3
Figure 8. Binding of RMF to the ribosome leads to formation of ribosome dimers vicentacts in the small subunit	
Figure 9. The binding of RaiA (YfiA) is in close proximity to that of RMF	39
Figure 10. Binding of HPF is incompatible with protein synthesis	łO
Figure 11. 100S ribosome formation mediated by RMF and short HPF is we conserved in gammaproteobacterial	
Figure 12. Cryo-EM analysis of <i>S. aureus</i> 100S ribosomes reveals two structural distinct types of ribosome dimers	-
Figure 13. Microscopy reveals morphological features of <i>P. urativorans</i> cells 4	18
Figure 14. Exposure to ice leads to a decrease of protein synthesis in I	<b>P.</b>

Figure 15. Screening of cryo-EM grids to assess their suitability for data collection
Figure 16. Cryo-EM processing of <i>P. urativoran</i> s ribosome from cold shocked cell72
Figure 17. Cryo-EM processing of <i>P. urativorans</i> ribosome from stationary cells72
Figure 18. Cryo-EM map of the ribosome from the <i>P.urativorans</i> ribosome 73
Figure 19. Model of the psychrophilic 70S ribosome from <i>P. urativorans</i> 74
Figure 20. Exposure to ice leads to a decrease of protein synthesis in <i>P. urativoran</i> and appears to elicit binding of a previously unidentified protein to the ribosome
Figure 21. Comparison of protein density found in the A site of <i>P. urativoran</i> ribosomes and the structure of the largest bacterial ribosomal proteins
Figure 22. Protein ligand in the A site of <i>P. urativorans</i> ribosomes does no correspond to macromolecules known to bind bacterial ribosomes
Figure 23. Result summary of Vast structure-based homology search
Figure 24. Structural comparison between the poly-Alanine model built into the unidentified density of the <i>P. urativorans</i> ribosomes (Balon) and aRF1
Figure 25. Structural comparison between the Balon density and the predicted structure of hypothetical protein A0A0M3V8U3 from <i>P. urativorans</i>
Figure 26. The identity of the protein we observed bound to our cryo-EM <i>Furativorans</i> ribosomes is protein A0A0M3V8U3 as shown by the fit of this protein into its corresponding density
Figure 27. Balon exhibits similarities to proteins aeRF1 and Pelota, suggesting a shared evolutionary origin with the aeRF1-family of translation factors found in archaea and eukaryotes
Figure 28. Balon's interactions with the ribosome is inconsistent with ribosome rescue and translation termination

Figure 29. Balon binding occludes the A site of the ribosome
Figure 30. Balon-coding genes are widespread among bacteria 91
Figure 31. Comparison of AlphaFold-predicted structures of proteins detected in
our homology search reveal similarity among Balon homologs in bacterial species across different phyla93
Figure 32. Balon homologs lack conservation of functional motifs present in aeRF1
95
Figure 33. Atomic model of Balon (coloured by sequence conservation) illustrates
high conservation of residues responsible for ribosome recognition
Figure 34. Balon is often encoded within stress response operons
Figure 35. Bacteria may be able to express different isoforms of Balon under distinct environmental conditions
Figure 36. Balon binds the ribosome during stationary phase
Figure 37. Cryo-EM maps reveal the two main states of ribosomes derived from bacteria <i>P. urativorans</i> during cold shock
Figure 38. Most cold shock <i>P. urativorans</i> ribosomes are associated to two hibernation factors
Figure 39. Balon homolog, eRF1, cannot bind the ribosome concurrently with RaiA due to steric clashes
Figure 40. Focussed classification analysis of cold shock <i>P. urativorans</i> ribosomes
reveals hibernating ribosomes bound to factors of protein synthesis 107
Figure 41. Cross sectional view of <i>P. urativorans</i> ribosome bound to Balon and Pa
site tRNA
Figure 42. Balon-associated ribosomes with P-site tRNA, and mRNA also show
density for the nascent peptide 109

Figure 43. Comparison of the ribosomal protein bL27 in active ribosomes (left Balon bound ribosomes (right)	
Figure 44. Balon-associated ribosomes showed density of P-site tRNA and mRNA	
Figure 45. EF-Tu in complex with Balon is found in its "open" conformation 115	
Figure 46. Structural comparison of Balon binding to EF-Tu and their homologous proteins in archaea and eukaryotes	
Figure 47. EF-Tu contacts hibernation factor Balon and the small and large subuniof the ribosome	
Figure 48. Balon-associated EF-Tu interacts with the sarcin-ricin loop 119	
Figure 49. Balon interacts with EF-Tu at a distinct site compared to its eukaryotic homologs	
Figure 50. EF-Tu in its GTP bound or "closed" conformation in complex with Balor would not be able to bind the ribosome	
Figure 51. Balon could not establish sufficient contacts with GTP bound EF-Tu to maintain a stable interaction	
Figure 52. Balon-mediated hibernation represents a unique mechanism or ribosome hibernation in bacteria	
Figure 53. Balon allows ribosomes to enter hibernation using a novel mechanism or ribosome dormancy	

# LIST OF TABLES

Table 1. List of all representative species with full ribosome structures availabl	le in
Protein Data Bank previous to this project	65

# **ABBREVIATIONS AND SYMBOLS**

0	degree
Å	Angstrom
aeRF1	archaeo-eukaryotic release factor
AFIS	aberration-free image shift
aRF1	archaeal release factor
ATP	adenosine triphosphate
BLAST	basic local alignment search tool
C	Celsius
CA1P	2-Carboxy-D-arabitinol 1-phosphate
Cryo-EM	cryo-electron microscopy
CTBP	2-carboxytetritol-1,4-bisphosphate
CTF	contrast transfer function
DC	decoding centre
DNA	deoxyribonucleic acid
EF-G	elongation factor G
EF-Tu	elongation factor temperature unstable
eRF1	eukaryotic release factor
HPF	hibernation promoting factor
IF1	inhibitory factor 1
IF1	initiation factor 1
IF2	initiation factor 2
g	g-force
g	gram
kDa	kilodalton
kV	kilovolt
LC-MS/MS	Liquid chromatography-tandem mass spectrometry
MDa	megadalton
mL	millilitre
mM	millimolar
Mr	molecular mass
mRNA	messenger ribonucleic acid

ODoptical density
PDBprotein data bank
PDBPD-glycero-2,3-pentodiulose-1,5-bisphosphate
PEGpolyethylene glycol
pHpotential of hydrogen
PTCpeptidyl transferase centre
r.p.mrevolutions per minute
RaiAribosome associated inhibitor A
RFrelease factor
RMFribosome modulating factor
rRNAribosomal ribonucleic acid
Ssvedberg
SRAstationary-phase-induced ribosome-associated protein
tRNAtransfer ribonucleic acid
v/vvolume/volume
w/vweight volume
XuBPD-xylulose-1,5-bisphosphate
μLmicrolitre

# **CHAPTER 1: INTRODUCTION**

## 1.1 PREFACE

Initially the main goal of this project was to reveal mechanisms of adaptation of biological molecules to cold environments. Our experimental system involved cryo-EM studies of ribosomes from psychrophilic (cold-adapted) bacteria. While this remains true, the scope of this work has been expanded to consider not only how bacteria slowly adapt to the environmental changes through evolutionary changes in their genomes, but also how bacteria adapt to sudden changes in temperature by controlling the activity and stability of ribosomes. The change in the breadth of this project was motivated by an unexpected discovery of what happens to ribosomes when bacterial cells are suddenly exposed to ice.

By isolating ribosomes from cold-shocked bacteria, we have discovered a previously unidentified protein that binds to the ribosome in response to stress. We found that this protein associates with most of the ribosomes present in our sample, making this protein the main ribosome partner in stressed cells. Within the ribosome, this protein occupies key active centres of the ribosome, such as the decoding centre and the peptidyl transferase centre.

We have termed this new protein Balon (1), and its discovery highlights an important aspect of ribosomal adaptation to cold: adaptation of the protein synthesis machinery to cold environments occurs at various timescales and through various mechanisms, ranging from irreversible long-term evolutionary changes in the molecular structure of ribosomal proteins and rRNA, to the short-term reversible interactions of the ribosomes with regulatory and currently unstudied proteins. In this context, the following section will focus on providing an introduction to ribosome hibernation— a phenomenon responsible for the reversible association of ribosomes with regulatory

proteins in metabolically inactive or stressed cells. By providing an overview of ribosome hibernation in the bacterial domain of life, I will explain how bacteria can use this process to adapt environmental stress.

## 1.2 HIBERNATION IS UBIQUITOUS IN NATURE

While most biological research focuses on active metabolic processes in living organisms, the study of life in a resting state has received little attention. However, a large portion of Earth's organisms are in hibernation or dormant at any given time. It is estimated that at least 60% of the global microbial biomass exists in some form of dormancy — (1). Certain bacteria can remain dormant for incredibly long periods, in some cases exceeding 250 million years(2) (3). Dormancy, however, is not limited to microbial life.

For a wide range of multicellular organisms, such as bears, arctic squirrels, raccoons, snakes, snails, and spiders, hibernation plays a vital role in their natural life cycle (4) (5) (6). This period of dormancy allows these species to conserve energy, survive harsh environmental conditions, and resume activity when favourable conditions return. Even in organisms that do not undergo full hibernation, dormancy can still occur in specific parts of the body. In humans, for example, oocytes can remain dormant for over 30 years, showing no outward signs of life, yet retaining the ability to start a new life once fertilized. This demonstrates that for many organisms, a state of inactivity is not only common but often represents the dominant form of life. Hibernation and dormancy, therefore, are widespread strategies for survival across both macroscopic and microscopic life forms.

## Hibernation is also common for certain enzymes

Hibernation, however, is not restricted to living organisms; it can also occur at the molecular level. Today we know that various biological molecules are capable of entering a state of dormancy. Early studies focused on the characterization of an array of biological assemblies began to uncover that dormant cells contain dormant molecular machines. However, these discoveries were often made independently by scientists focused on the study of different biological assemblies, such as ribosomes, RNA polymerases, proteasomes, or ATP synthetases, and often without knowledge of each other's work (7) (8) (9) (10) (11) (12) (13). Despite this, research starting on the late 1950s to has revealed strong evidence of a common molecular mechanism that enables organisms to survive in a state of hibernation. This mechanism, known as "hibernation of biological molecules," is a self-preservation strategy found in organisms ranging from the simplest bacteria to complex eukaryotes such as humans. It involves the production of special type proteins called hibernation factors, which either inhibit or protect essential biological molecules from degradation during periods of starvation and stress. These hibernating proteins are crucial for allowing organisms to withstand extended periods of reduced metabolic activity (often, but not necessarily upon stress exposure) without breaking down the essential molecular structures needed for survival.

By that time, it was well established that oocytes have the ability to endure dormancy for several decades while still retaining the capacity for rapid reactivation upon fertilization. In an effort to understand this exceptional ability for self-preservation, early studies conducted in the 1970s began to identify certain "factors" of unknown molecular identity. These factors were found to bind to ribosomes in unfertilized eggs and inhibit protein synthesis *in vitro* (14) (9) (15). As early as 1973, it became evident that ribosomes in dormant, unfertilized eggs could associate with these unidentified factors. These factors appeared to play a role in inhibiting protein synthesis, highlighting a mechanism that contributes to the preservation of oocytes in their dormant state.

After the identification of ribosome hibernation factors in bacteria, functionally similar proteins were discovered in eukaryotes. The first of these factors, Stm1, was identified in 2011 as a protein that binds to virtually all cellular ribosomes in yeast *Saccharomyces cerevisiae* in response to sudden glucose starvation (16).

Subsequently, the Stm1 homolog, Serbp1, was found to bind to ribosomes in cold-shocked cells of humans and *Drosophila melanogaster* (17). Later studies revealed five more families of ribosome hibernation factors. These included proteins Lso2/CCDC124 in humans, yeasts and parasitic fungi microsporidia (18) (19) (20), proteins IFRD1/IFRD2 in rabbit reticulate extracts and Drosophila cells (21) (22), proteins MDF1 and MDF2 in metabolically inactive spores of fungal parasites microsporidia (23), and protein Dap1b in frogs/Dapl1 in xenopus that participates in ribosome hibernation in oocytes of frogs or zebrafish (24).

All ribosome hibernation factors identified in eukaryotes were shown to function in a similar manner compared to bacterial hibernation factors. Specifically, they bind to the functional centres of all or most ribosomes in cells that are either metabolically inactive or under stress (**Figure 1**). Despite this functional similarity, there is a notable lack of structural resemblance between eukaryotic ribosome hibernation factors and their bacterial counterparts (**Figure 1**). This lack of similarity suggests that ribosome hibernation factors evolved independently in the two domains of life, indicating distinct evolutionary origins for these factors in bacteria and eukaryotes.

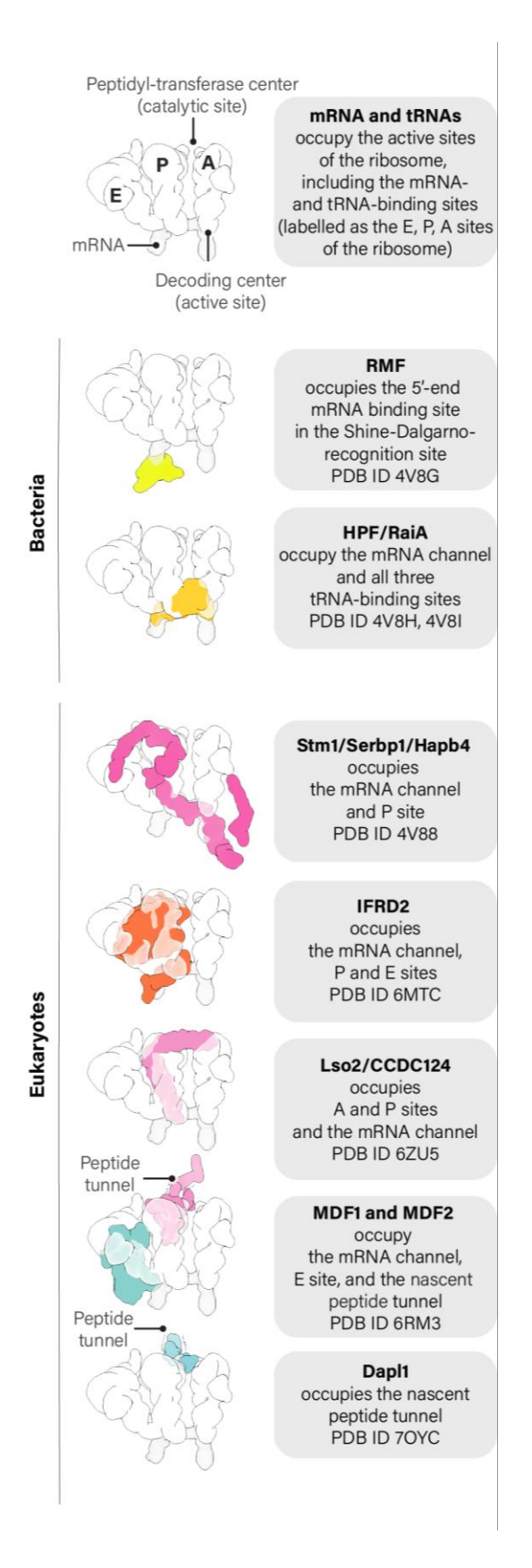


**Figure 1. Ribosome hibernation factors are present in the bacterial and eukaryotic domains.** Comparison of the binding sites of structurally characterized hibernation factors shows the wide diversity of these proteins in terms of overall three-dimensional folding of these factors and their binding sites within the ribosome. Adapted from (25).

Studies of bacterial and eukaryotic hibernation factors revealed two important facts. First, it became clear that most characterized species possess more than one family of hibernation factors. *Escherichia coli*, the most extensively studied organism in this context, is notable for containing at least four families of ribosome hibernation factors: RMF, HPF/RaiA, and the putative hibernation factors Sra (26) and YqjD/ElaB/YgaM (27). The reasons underlying the apparent need for multiple families of these proteins remain unclear. Although experimental studies of this redundancy are currently missing, it is possible that each family of factors exhibits a preference for specific environments or stressors, thus making it possible for bacteria to effectively adapt to a variety of hostile environments. Another possible benefit of these parallel ribosome hibernation pathways in a single organism may be related to a more effective protection they may provide: if one system is compromised or overwhelmed, the other can still function to provide a protective effect.

Secondly, despite the crucial role of ribosome hibernation in cell survival, these proteins are not conserved across all species. Bacteria and eukaryotes each have their own distinct sets of ribosome hibernation factors. In eukaryotes, these include Stm1/Serbp (16), Lso2/CCDC124 (18), IFRD1/IFRD2 (21), MDF1, MDF2 (23), and Dap1b (24) in eukaryotes, and HPF/RaiA (28), (29), (30), and RMF (26) in bacteria.

In the absence of evolutionary or experimental studies that involve a larger number of non-model organisms, the extent of conservation for each family of ribosome hibernation factors across species remains unclear. Specifically, it is currently unknown whether these factors are broadly conserved across all bacteria or eukaryotes, or if different lineages of bacteria and eukaryotes possess their own unique sets of hibernation factors.

One challenge in resolving this issue is the notably higher rate of sequence evolution for these proteins compared to other ribosome-binding proteins. This rapid evolution makes traditional homology search methods, such as BLAST searches or Markov Models-based approaches, less effective for identifying their homologs across species (31). However, studies of the most conserved hibernation factors, such as HPF and RaiA, suggest they likely appeared shortly after the divergence of bacteria from

archaea and eukaryotes. If the current estimates of this evolutionary split are accurate, ribosome hibernation has been present in living cells for about 3.5 billion years (32).

Molecular hibernation extends beyond ribosomes to include other essential enzymes (**Figure 2**). RNA polymerases, for instance, are well-characterized examples of hibernating enzymes. In both eukaryotes (*S. cerevisiae*) and bacteria (*Mycobacterium smegmatis*), RNA polymerases enter a hibernation state by forming inactive dimers or octamers (13), (33), (34), (35), (36), (37). In yeasts, the hibernation of RNA polymerase I has been studied both *in vitro* and *in vivo* (38). This process involves the formation of dimers where the flexible stalk of one RNA polymerase I molecule inserts into the DNA-binding channel of another molecule within the dimer, leading to inactivity. When dormant yeast cells are returned to optimal conditions, RNA polymerase I dimers are disassembled with the help of the protein Rrn3. This protein prevents the stalk from acting as a DNA tunnel-binding factor and has additional functions (38).

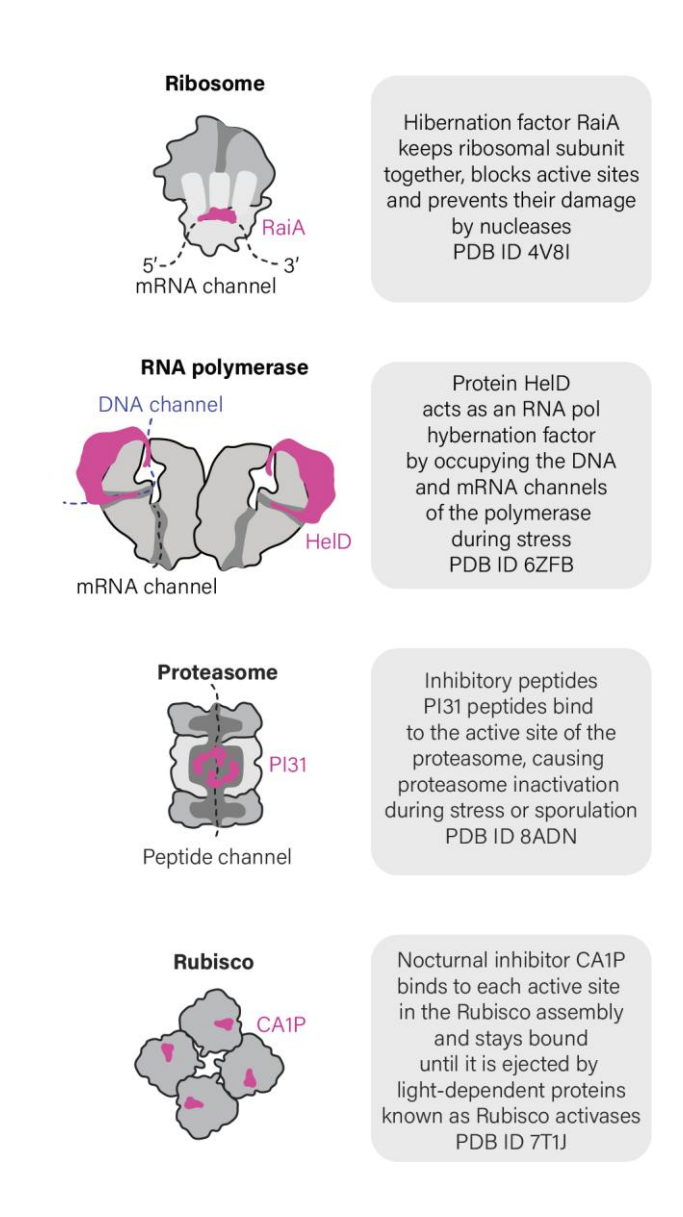


**Figure 2. Hibernation of biological molecules is not limited to ribosomes.** In addition to ribosomes other complex molecular assemblies are known to hibernate in a process mediated by the binding of endogenous proteins (RNA polymerase and proteasomes) or small molecules (Rubisco). Adapted from (25).

Recent studies have shown that the bacteria *M. smegmatis* and *Bacillus subtilis* have a specific hibernation factor for RNA polymerase, known as protein HelD (33), (34). During periods of starvation and stress, HelD functions similarly to ribosome hibernation factors by binding to the active sites of RNA polymerase, including the DNA-and RNA-binding channels (**Figure 2**). Therefore, it has been demonstrated that at least two molecular machines within a living cell—ribosomes and RNA polymerases—hibernate with the help of dedicated, genetically encoded hibernation factor proteins.

Aside from RNA polymerases, certain enzymes, including plant catalases and the Rubisco enzyme, have been shown to enter a hibernation-like state when they associate with small molecules produced endogenously by plant cells in response to cold shock or darkness (10), (11). In the case of Rubisco, this enzyme is essential for converting carbon dioxide into organic compounds during the daytime. However, during night-time, when photosynthesis is not possible due to the lack of light, Rubisco's activity significantly decreases. This decrease is attributed to the accumulation of the small molecule 2-carboxy-D-arabinitol 1-phosphate (CA1P) in the cell, which binds to Rubisco's active site during darkness and low light (39), (40).

As in the case with ribosomes and RNA polymerases, this inactivation of Rubisco is reversible. As light becomes available, CA1P is removed from Rubisco by the protein Rubisco activase. Additionally, the phosphatase CA1Pase deactivates CA1P through dephosphorylation, producing a CA molecule that cannot bind to Rubisco (40). In addition to CA1P, other small molecules are being studied as condition-specific endogenous inhibitors of plant Rubisco, including phosphorylated sugar molecules like XuBP (41), PDBP (42), and CTBP (43). While it remains to find out how many enzymes use a similar hibernation mechanism, this example shows that, in addition to genetically encoded hibernation factor proteins, some enzymes can hibernate by interacting with endogenously produced small molecules.

Because molecular hibernation has become a research focus only on the past few years, the exact number of enzymes that can hibernate remains unknown. However, increasing evidence suggests that molecular hibernation might be a common characteristic among essential enzymes, allowing them to endure and recover from various cellular stresses. For example, specific inhibitors induced by stress and starvation have been identified not only for ribosomes and RNA polymerases but also for the ATP synthase in eukaryotic mitochondria (protein IF1) (8), (44) and proteasomes (protein PI31) (12), (45), The role of these inhibitors in molecular hibernation remains debated. Nonetheless, the growing number of cellular components that are able to hibernate suggests that living cells likely use a range of yet-to-be-discovered and complex mechanisms to prepare their vital molecules for prolonged periods of inactivity.

### 1.3 WHAT DO WE KNOW OF RIBOSOME HIBERNATION?

## Hibernating ribosomes: an outline of their discovery

The phenomenon of molecular hibernation has been most extensively studied in ribosomes, which are essential ribonucleoprotein complexes that catalyse protein synthesis. Hibernating ribosomes were first described in the scientific literature in 1958 by James Watson and Alfred Tissières. At the time, the exact composition, structure and properties of ribosomes were not precisely known. In their efforts to help characterize these complex macromolecular assemblies Watson and Tissières analysed cell lysates of actively growing *E. coli* cells using sedimentation assays, and electron microscopy. They observed that ribosomal particles with a sedimentation coefficient of 100S were present in their cell lysate samples, and that changing the concentration of magnesium resulted in a reversible transition between 70S (monomeric) and 100S (dimeric) ribosomes *in vitro* (46).

While Watson and Tissières made no assertions about the potential biological significance of 100S ribosomes in the cell and attributed the detection of 100S ribosomes solely to magnesium concentration, it is possible that other conditions could have contributed to the formation of 100S ribosomes in their samples. According to the methods described the cells were cultured at optimal growth conditions and collected while the cells were actively growing, and therefore not hibernating.

However, before the ribosome samples were collected, as part of their ribosome purification protocol (46) these cells were exposed to conditions—such as low temperatures—that we now know lead to the expression of genes that are related to the formation of 100S ribosomes *in vivo* (47) (48).

One key piece of information that Watson and Tissière stated in their publication was their conclusion that 100S ribosomes are formed by 2 70S particles (46). This became evident when Huxley and Zubay published the first electron micrographs

showing 100S ribosomes from *E. coli* cells where two distinct ribosome particles are bound by the small subunit and form ribosome dimers (**Figure 3**) (49).

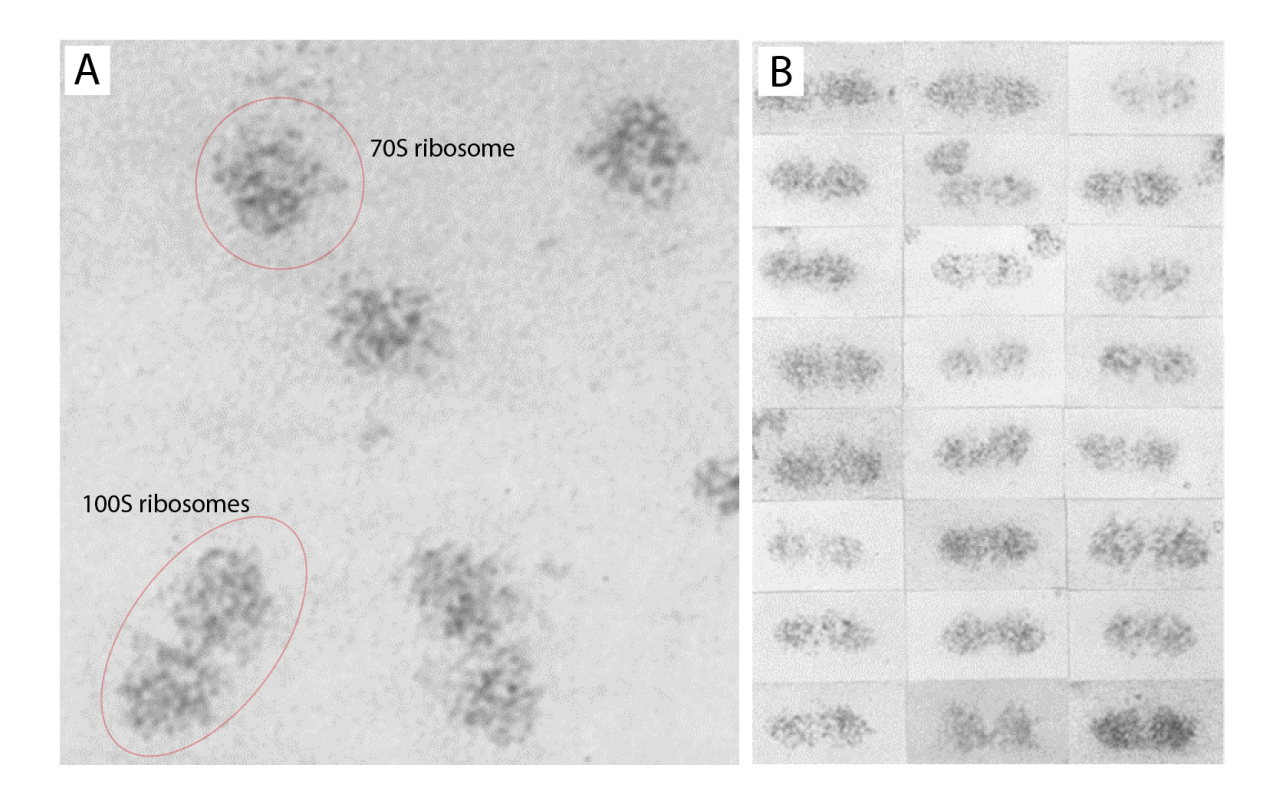


**Figure 3. First published electron micrographs of 100S ribosomes.** Panels (**A**) and (**B**) show ribosome dimers (100S ribosomes) from *E. coli* as a response to changes in magnesium concentration *in vitro*. While this phenomenon also occurs in *E. coli* cells in vivo as a response to stress this would remain unknown until later experiments showed that formation of 100S ribosomes can occur during stationary phase in *E. coli* cells. Adapted from (49).

The relationship between environmental stress, 100S ribosomes and protein synthesis would be first proposed and demonstrated by McCarthy in 1960. His analysis of cell lysates from *E. coli* cells showed that during nutrient deprivation and stationary phase the majority of the ribosomes in the cell were 100S ribosomes, and that these 100S ribosomes were only present in cell lysates obtained from "resting cells" (7).

Another important aspect related to ribosome hibernation became evident by McCarthy's experiments on protein synthesis and environmental stress. He noted that resumption of cellular growth appeared to reestablish the "normal ratios" of different classes of ribosomes to pre-starvation levels. More specifically, addition of glucose to the media containing starved cells caused the appearance of 70S, 51S and 32S

particles within 1.5 min. This was accompanied by a continuous decrease and eventual disappearance of 100S particles which were not detected after 11 min after addition of glucose, and it coincided with the reestablishment of protein synthesis between 7-11 min after glucose addition (5).

Despite the fact that hibernating ribosomes were first detected in bacteria, one of the earliest observations of hibernating ribosomes *in vivo* was made in 1972 from oocytes and follicular cells of lizards (*Lacerta sicula*) (**Figure 4**) (50). These images showed that during winter rest, the ribosomes of this species of lizard form aggregates referred to as "ribosome bodies." Each ribosome body consists of crystalline sheets made up of thousands of ribosome tetramers arranged in a periodic pattern. During spring, these "ribosome bodies" disassociate into individual ribosomes, so that ribosome bodies are completely absent in summer.

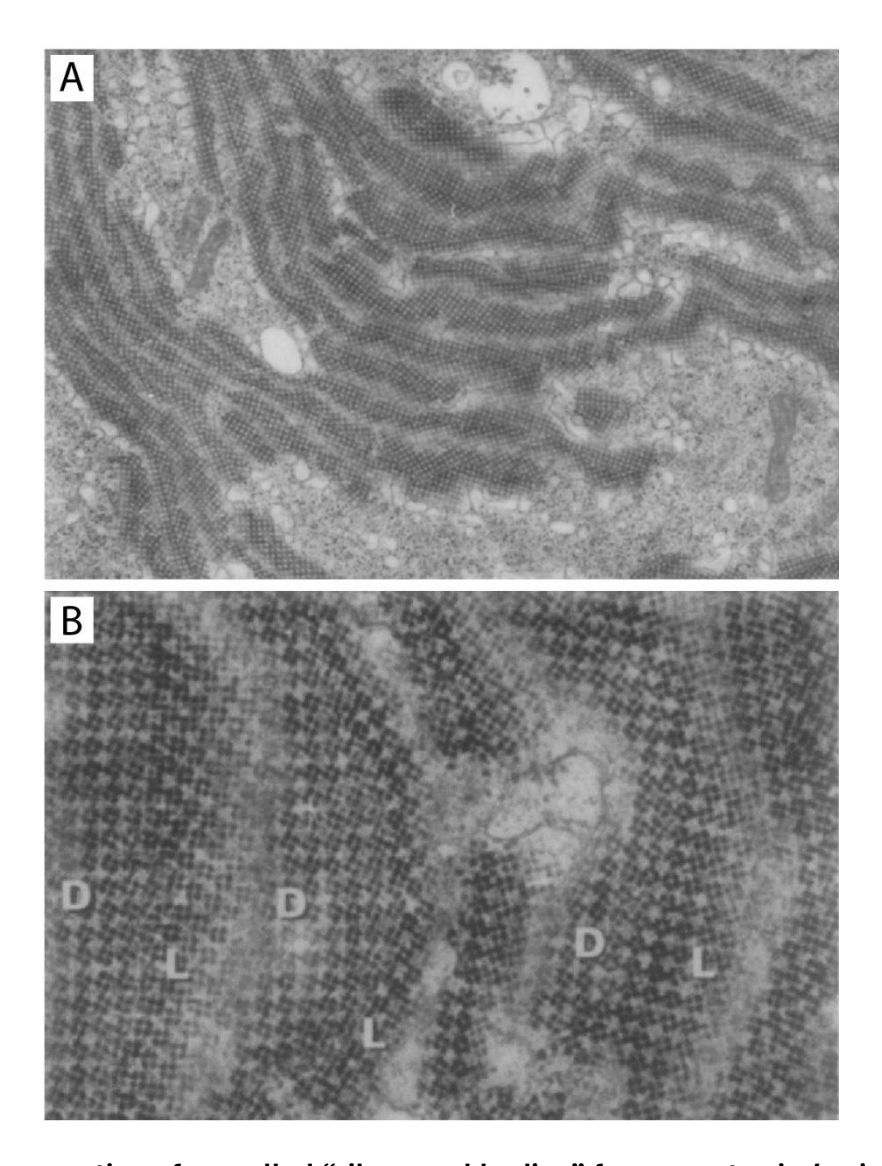


**Figure 4. Cross section of so-called "ribosomal bodies" from oocytes in** *L. sicula* shown in panel (**A**), a zoomed-in view shown in panel (**B**). Electron microscopy of oocytes from *L. sicula* showed that when this species of lizard hibernates its ribosomes are arranged in crystalline sheets likely as a mechanism to "store" ribosomes during prolonged periods of cellular inactivity. Adapted from (50).

Similar patterns were also observed in oocytes from mice (51) and an ascidian *Ciona intestinalis* (52), as well as in cold-shocked chick embryos (53). In these cases, ribosomes were found to be orderly arranged on the inner side of the cell membranes, further demonstrating that ribosomes can form complex and periodic structures *in vivo*.

In her Nobel Prize lecture, Ada Yonath, a pioneer in ribosome structural studies, explained that early imaging studies of ribosomes using transmission electron microscopy were a key inspiration for her to attempt crystallizing ribosomes. She

explained that the fact that ribosomes could form crystal-like aggregates in a cell hinted at the possibility of their crystallization *in vitro*. (54).

The initial observations of ribosome aggregates *in vivo* have been largely overlooked and rarely mentioned in the literature. However, the introduction of cryoelectron tomography has reignited interest in the supramolecular organization of hibernating ribosomes, bringing more attention to this fascinating phenomenon in ribosome biology.

In the past year, cytosolic ribosomes in yeast cells have been found to associate with the outer membrane of mitochondria during glucose starvation (55). Likewise, ribosomes were shown to assemble into helical sheets comprised of dozens or hundreds of ribosomes per sheet in metabolically inactive spores of parasitic fungi microsporidia (56). Currently, the biological significance and mechanisms underlying these supramolecular assemblies of hibernating ribosomes remains unclear. However, it seems plausible that this aggregation provides an additional level of protection of ribosomes from degradation by nucleases or proteases, thereby ensuring the preservation of ribosomes during extended periods of dormancy.

#### Mathematics of ribosome hibernation

Bacterial cells are capable of modulating ribosome activity as a response to stress in three ways: 1) by adjusting the number and concentration of ribosomes per cell, 2) by changing the oligomeric status and intracellular localization of ribosomes, and 3) by increasing the number of ribosome hibernation factors in the cell.

When cells deplete available nutrients and enter the stationary phase, ribosome synthesis slows, and a significant portion of ribosomes is degraded shortly after nutrient exhaustion (61).

Quantitative analysis of ribosome levels in *E. coli* grown in different media revealed that in rich media, *E. coli* has a division time of 24 minutes and contains about 72,000 ribosomes per cell (59). In minimal media, the same strain has a division time of 100 minutes with only 6,800 ribosomes per cell. However, comparisons showed that faster-dividing *E. coli* cells are generally much larger. As a result, the ribosome concentration in the cytoplasm of actively growing *E. coli* remains nearly constant, making up approximately one-third of the dry cellular weight in both fast- and slow-growing *E. coli* cultures (59).

Recent quantitative proteomics studies estimate that an actively growing *E. coli* cell contains about 28,000–36,000 ribosomes, along with similar amounts of hibernation factors, including 2,000 copies of HPF, 7,900 copies of RaiA, and just 199 copies of RMF (60). This indicates that actively growing cells maintain a substantial pool of hibernation factors, sufficient to bind approximately one-third of the cellular ribosomes. (25).

*E. coli* cells are estimated to translate an average protein in 20 seconds, while the shift to ribosome hibernation takes about 1 minute. Mass spectrometry studies show that after 24 hours in the stationary phase, *E. coli* cells contain roughly 2,000 ribosomes, while the levels of hibernation factors—HPF, RaiA, and RMF—increase to 4,000, 11,700, and 3,500, copies respectively (60). This means that hibernation factors greatly outnumber ribosomes in these conditions, enabling them to bind nearly all cellular ribosomes during prolonged metabolic inactivity.

It is worth noting that hibernation factors also considerably outnumber other factors involved in ribosome-associated stress responses. For example, stationary phase *E. coli* cells contain just 2 detectable copies of the protein RelA that is involved in cellular responses to stress or nutrient depletion (60), which corresponds stoichiometrically to just 0.01% of cellular ribosomes (25). This suggests that in bacteria ribosome hibernation is a key stress response mechanism and that cells dedicate a substantial number of resources to the production of ribosome hibernation factors upon stress exposure.

Before this study, 2 families of ribosome hibernation factors had been structurally characterized in bacteria. These are RMF, and the RaiA/HPF protein family.

The next section includes a detailed description of the main findings on the mechanisms of ribosome hibernation in bacteria as revealed by structural studies on RMF and RaiA/HPF.

### 1.4 RIBOSOME HIBERNATION FACTORS IN BACTERIA

### Ribosome modulation factor (RMF)

The first bacterial ribosome hibernation factor described in the literature was isolated by Wada et al. from stationary phase *E. coli* cells. This 55 amino acid protein was described as a Ribosome modulation factor (RMF) and was found to only associate with 100S ribosomes of resting (stationary phase) *E. coli* cells and was therefore only detected in stationary phase samples (26).

Wada and colleagues later proposed that binding of RMF was responsible for ribosome dimerization of 70S ribosomes. Furthermore, they showed that 100S ribosomes from stationary phase cells return to their monomeric state once transferred to fresh media. It is worth noting that the discovery of RMF was prompted by an earlier discovery by Wada et al. of 4 previously undescribed ribosomal proteins (pre-L31, L35, L36 and protein D which was not completely characterized) in 1986 (61). This earlier discovery led them to investigate the "physiological significance of the structural heterogeneity of ribosomes in *E. coli*" for which they analysed ribosomes from *E. coli* at different stages of growth, including stationary phase, and thus found RMF (26).

Later experiments investigating the role of the RMF gene during stationary phase in ribosome dimerization showed that disruption of the RMF gene results in the cells inability to form 100S ribosomes during the stationary phase (62). Expression of RMF was found to be transcriptionally regulated: the RMF gene remains silent during exponential growth in *E. coli* cells. However, the level of expression of this gene

increases as cells transition from the log to the stationary phase. The RMF gene was also found to be expressed in the log phase of slow-growing *E. coli* cells (likely due to mild levels of nutrient depletion) (62).

One particularly important finding by Yamagashi and colleagues is that cells with a mutated/disrupted RMF gene exhibited a significant loss of viability after cells enter stationary phase, highlighting the importance of this gene for cell survival during prolonged stationary phase (62).

Subsequent studies by Wada et al. showed that ribosome dimerization in *E. coli* occurs in an RMF-concentration dependent manner *in vitro*. Importantly, *in vitro* protein synthesis experiments showed that binding of RMF to the ribosome, and consequently ribosome dimerization resulted in protein synthesis inhibition (63). These findings not were not only in agreement with McCarthy's early experiments on the relationship between ribosome dimerization in *E. coli* during stationary phase and its effects on protein synthesis (7), but they also provided the first pieces of evidence towards a mechanistic understanding of ribosome hibernation as a response to stress.

It is worth noting that Wada and colleagues correctly hypothesized that RMF must bind at the active centres of the ribosome, however its exact binding location would be uncertain for over two decades after its discovery.

Initially, it was thought that RMF binds the large ribosomal subunit, in close proximity to the peptidyl-transferase centre as indicated by protein cross linking experiments using 100S ribosomes from stationary phase *E. coli* (64).

Later, *Thermus thermophilus* ribosome structures bound to hibernation factor RMF, showed that RMF binds not in the large subunit, but in the small ribosomal subunit. More specifically, RMF binds the ribosome in the mRNA channel where 4 residues from RMF (Thr33, Gly32, Tyr31 and Arg11) directly interact with nucleotides A1531, U1532, and C1533 in 16S rRNA, at the anti-Shine-Dalgarno region in 16S rRNA (**Figure 5**) (65).

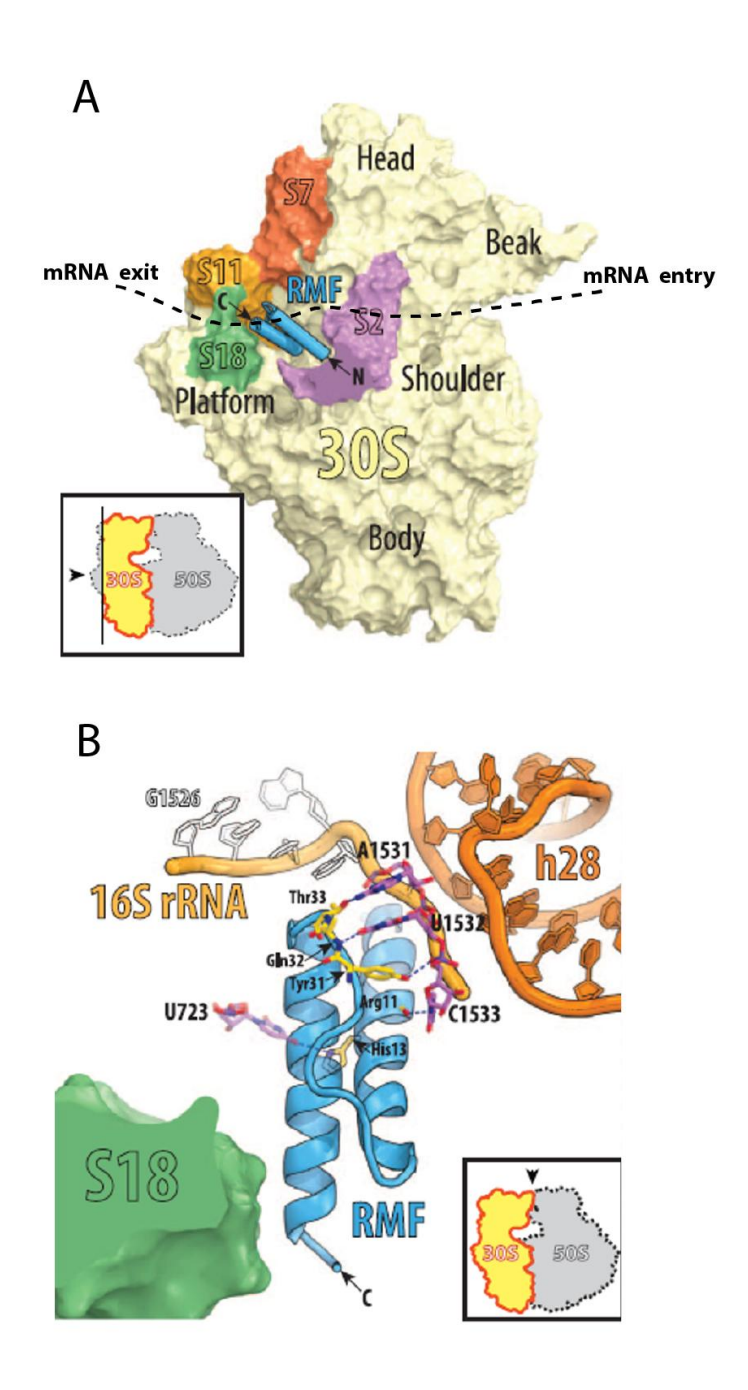
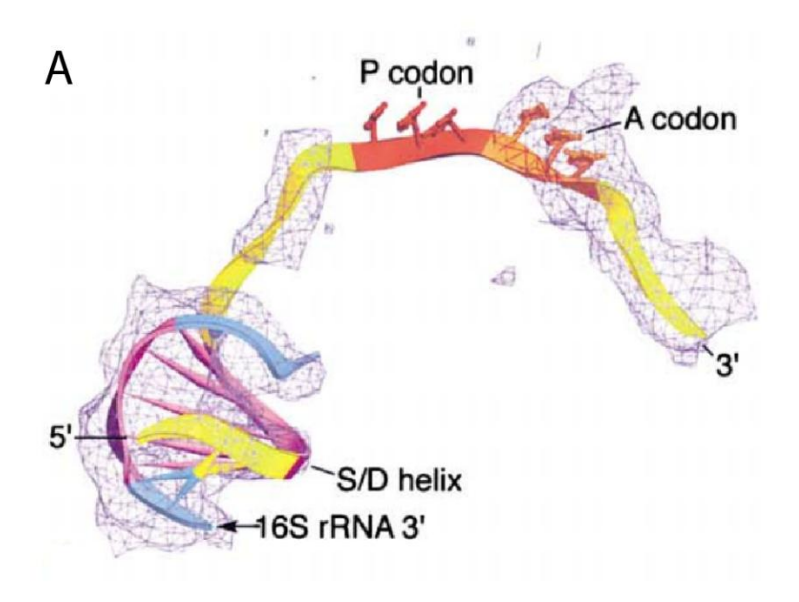


Figure 5. Ribosome crystal structures of *T. thermophilus* reveals binding site of hibernation factor RMF to the ribosome. (A) Hibernation factor RMF binds at the mRNA channel (indicated with a dashed line) in a region of 16S rRNA known as the anti-Shine-Dalgarno region, which is critical for translation of most mRNAs in bacteria. (B) Zoom-in view of RMF binding site shows directs contacts between this hibernation factor and h28 of 16S rRNA in the small ribosomal subunit. Adapted from (65).

The anti-Shine-Dalgarno region refers to a specific sequence of nucleotides that is located at the 3' end of 16S rRNA (66). In *E. coli*, the anti-Shine-Dalgarno sequence is 5'-CCUCCU-3' and comprises residues 1535 to 1540 (67). This region of 16S rRNA is of particular importance for ribosome function, as it plays a key role in the most tightly

regulated step of translation: protein synthesis initiation (68). During initiation, the nucleotides that form the anti-Shine-Dalgarno region form base pairs with the Shine-Dalgarno nucleotides in mRNA to form a double helix upstream of the start codon (69).

The Shine-Dalgarno sequence is a purine-rich, highly conserved sequence of nucleotides located at the 5' untranslated region in most bacterial mRNAs (70). The interaction between the mRNA's Shine-Dalgarno sequence and the anti-Shine-Dalgarno region in the ribosome is thought to help stabilize the pre-initiation complex and place the start codon in the P-site in preparation for peptide bond formation (**Figure 6**) (71).



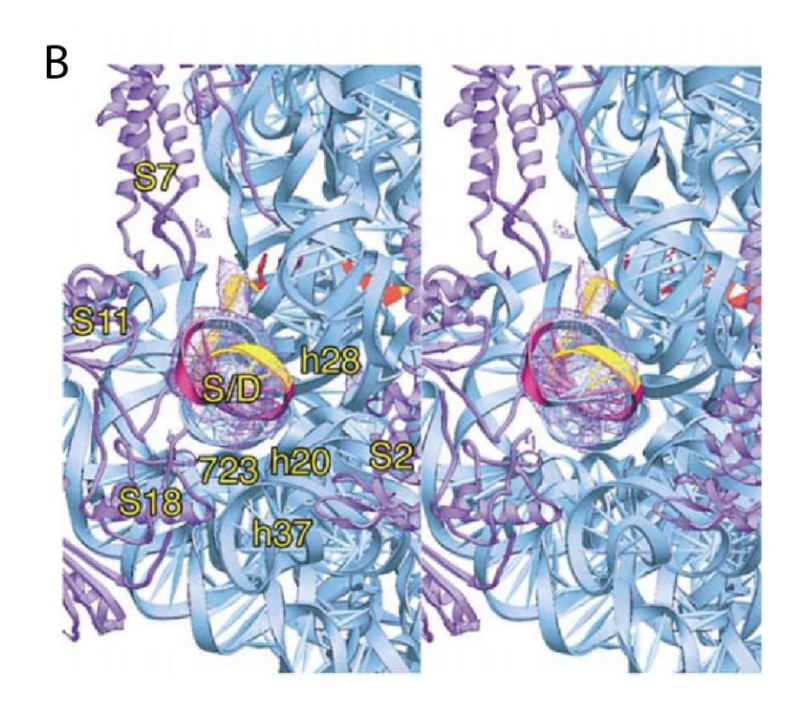
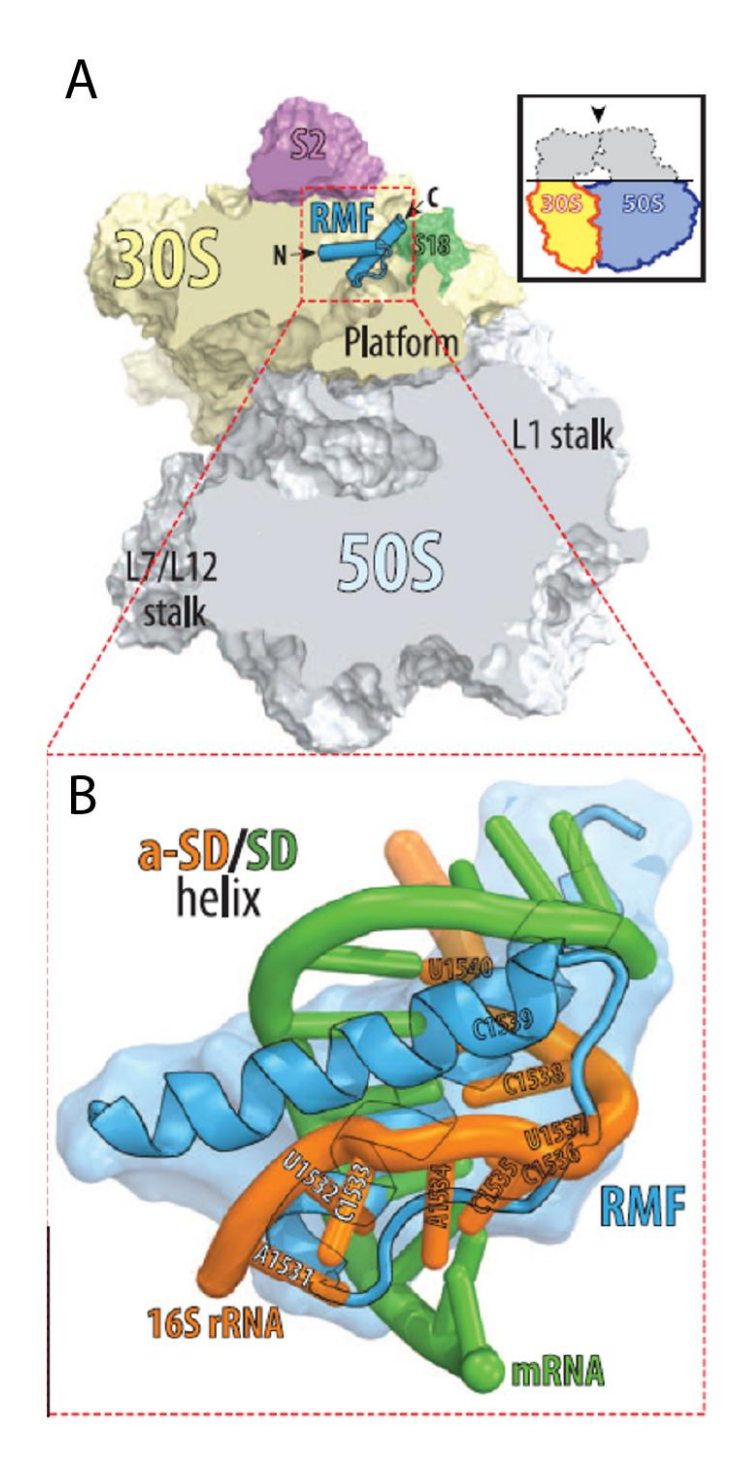


Figure 6. The Shine-Dalgarno region of mRNA mediates binding of most bacterial mRNA to the ribosome. (A) mRNA model shows Shine-Dalgarno:anti-Shine-Dalgarno helix interaction (shown in purple) between mRNA (yellow) and 16S (blue). Also shown is the A codon (orange) which corresponds to the mRNA codon positioned in the A site, and the P codon or start codon (red) positioned at the P site of the ribosome during translation initiation. (B) Zoomed-in view of mRNA in complex with the ribosome showing the Shine-Dalgarno helix. Adapted from (69).

The binding site of RMF suggests that this hibernation factor prevents protein synthesis initiation by preventing Shine-Dalgarno:anti-Shine-Dalgarno interactions. This

becomes evident when observing the steric clash that would result from the binding of mRNA to the ribosome during initiation when RMF is bound to the ribosome (**Figure 7**) (65).



**Figure 7. Binding of RMF is incompatible with protein synthesis.** Structure of *T. thermophilus* ribosome in complex with hibernation factor RMF shows that binding of this protein would result in a steric clash with the Shine-Dalgarno region of mRNA, thereby preventing the translation of most cellular mRNAs in bacteria. Adapted from (65).

Notably, RMF binding to the ribosome triggers a conformational change of the so-called "head" of the small ribosomal subunit. The head of the 30S subunit makes up about one third of the small subunit, and it includes 9 ribosomal proteins (72). Upon binding of RMF the head of the small subunit moves 10 Å away from the large subunit. This "forward movement" allows for the formation of ribosome dimers via two main contact points between the small subunits of two ribosomes bound to RMF. The first mediated by a protein-protein interaction between the ribosomal proteins S2 from both 70S ribosomes, and the second by RNA interactions between helices 39 from both ribosomal particles (**Figure 8**) (65).

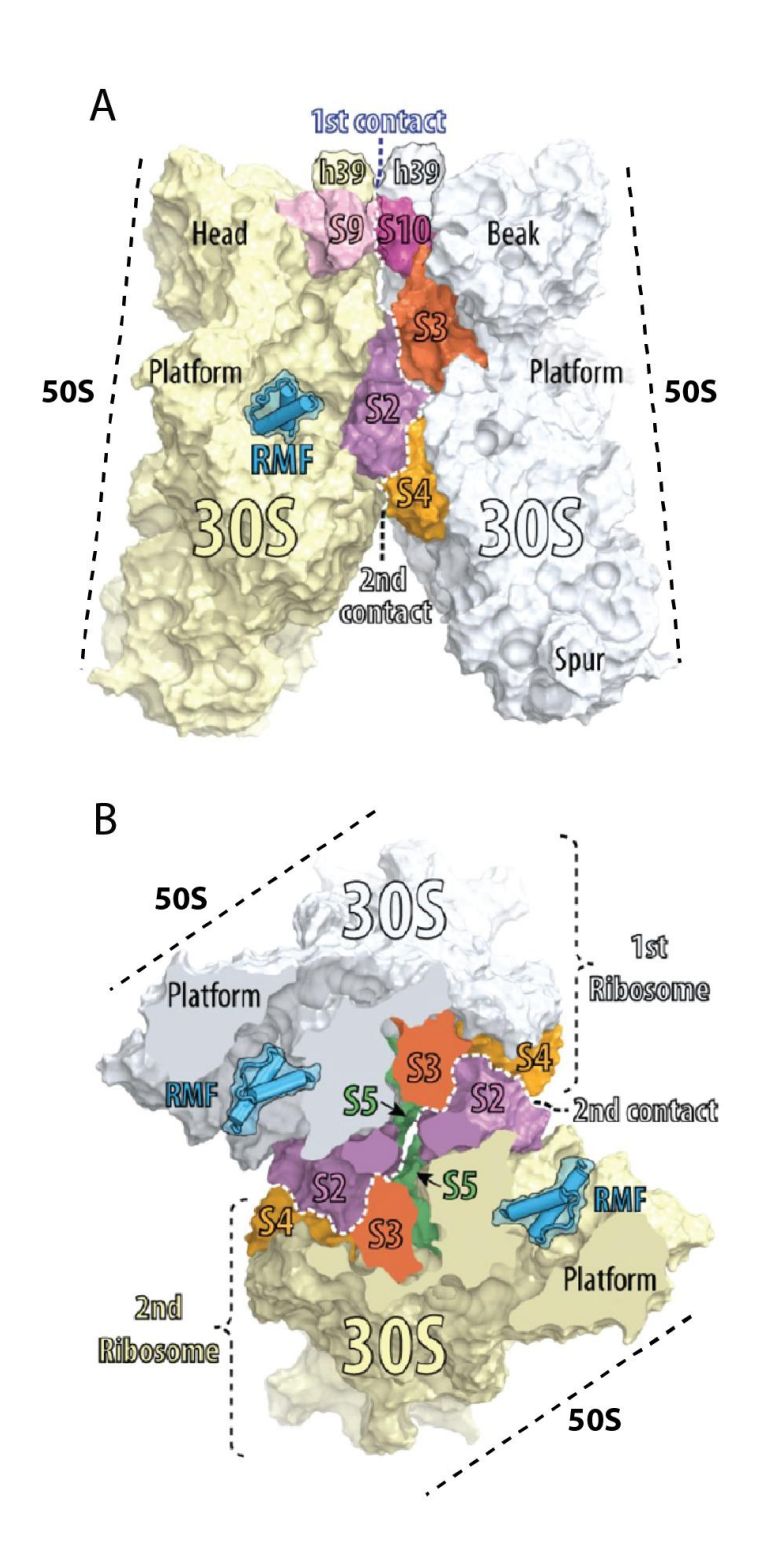


Figure 8. Binding of RMF to the ribosome leads to formation of ribosome dimers via contacts in the small subunit. (A) 100S ribosome structure bound to RMF shows how contacts between helices 39 in 16S rRNA of each monomer help mediate ribosome dimerization. (B) Cross section of 100S ribosomes shown in panel A viewed from the top of the 100S complex details how protein-protein interactions (involving proteins S2, S3, S4 and S5) help stabilize the entire complex. Adapted from (65).

This ribosome dimerization mechanism is thought to be conserved in those species of bacteria that bear the RMF gene. Interestingly, the presence of RMF on the bacterial tree of life is rather limited as it has only been detected among the gamma-proteobacteria class (73). In this bacterial class the formation of RMF-mediated100S ribosome formation is thought to occur first by the binding of RMF to the ribosome, thereby eliciting ribosome dimerization into *so-called* 90S ribosomes. These 90S ribosome dimers are further stabilized into 100S ribosome dimers by the binding of a second class of bacterial hibernation factor, HPF (hibernation promoting factor).

#### RaiA/HPF

The second family of structurally characterized hibernation factors in bacteria is that of RaiA/HPF. Ribosome associated inhibitor A, RaiA (initially called protein Y or YfiA) was discovered by Agafonov et al. in 70S *E. coli* ribosomes where it was found to bind at the small ribosomal subunit. At the time of its discovery RaiA was found to be present in 10 other bacterial species. While RaiA was not initially classified as a hibernation factor, the authors of the study posited that RaiA may have been involved in subunit association given its proposed location at the interface of the small subunit and the stabilizing effect RaiA showed on subunit association. Nevertheless, the authors could only speculate about the function of the newly discovered protein and made no assertions as to the biological significance of RaiA (28).

However, in a follow-up study Agafonov and colleagues found two key characteristics of RaiA related to its status as a hibernation factor. First, they were able to conclude that RaiA binding to the ribosome was elicited by conditions of stress. RaiA was not detected in the ribosome fractions obtained from actively growing *E. coli* cells that were incubated at 37°C, and only appeared in the ribosome fractions obtained from *E.coli* cells that were exposed to low temperatures (either by a sudden decrease to 15°C or a slow temperature decrease down to 4°C) (29).

Likewise, ribosomes from stationary phase *E. coli* cells contained comparable levels of RaiA than the ribosomes from cold stressed cells. The authors themselves asserted that the detection of RaiA in their 1999 study may have been a consequence of the cooling down of the cells during ribosome isolation (29).

The second key finding in this study that solidifies RaiA as a hibernation factor has to do with one of the functions of this protein: protein synthesis inhibition. *In vitro* translation experiments showed that in the presence of RaiA inhibits ribosome function in a dose-dependent manner with a 65% decrease in protein synthesis when present in a 1:1 ratio with the ribosome. This prompted the authors of this study to rename YfiA to RaiA to highlight the inhibitory properties of this protein (29).

While unknown at the time, the discovery of RaiA represents a key milestone in our understating of ribosome hibernation, as it showed that ribosome hibernation in bacteria is not exclusive to dimeric or 100S ribosomes and that monomeric (70S) ribosomes can also hibernate. This provided the first piece of evidence against a unified model of ribosome hibernation in bacteria and hinted at the possibility that bacteria can adopt more than one strategy to modulate their ribosomes as a response to environmental stress.

Subsequent biochemical and structural studies suggested that binding of RaiA is incompatible with 100S formation via RMF binding (74) (64). However, protein HPF (hibernation promoting factor), a homolog of RaiA has been detected in 100S ribosomes that are also bound to RMF.

Maki et al. described protein HPF (initially named YhbH), a ribosome hibernation factor homologous to RaiA. This protein was detected when researchers used 2D gel electrophoresis to analyse the 100S ribosome fraction obtained from stationary phase *E. coli* cells. (75).

In *E. coli*, ribosome dimers are thought to first form by the binding of RMF to the ribosome as illustrated in the previous section. Once this so-called 90S ribosome dimer complex forms, binding of HPF is thought to stabilize the dimerized ribosomes to form "mature" 100S ribosomes. This model is supported by *in vitro* experiments with *E. coli* ribosomes that show that upon binding of RMF alone formation of 90S ribosome dimers

are detected (76) (74). However, HPF alone does not elicit dimerization of ribosomes in *E. coli* cells (74). Given that only RMF alone is sufficient for ribosome dimerization (90S ribosome formation), and lack of HPF results in failure to form ribosome dimers, it is thought that HPF has a supporting role in the formation of 100S ribosomes. However, the mechanism behind the proposed "stabilizing" effect of HPF in 100S ribosome formation has yet to be elucidated.

#### RaiA and HPF binding to the ribosome

Structural studies have revealed that RaiA binds the ribosome at the mRNA channel, where tRNAs would normally bind during protein synthesis. More specifically, in *E. coli* RMF and RaiA cannot bind the ribosome simultaneously. This is because RaiA has an extension at the C-terminal domain that would presumably cause a steric clash with RMF (**Figure 9**) (65).

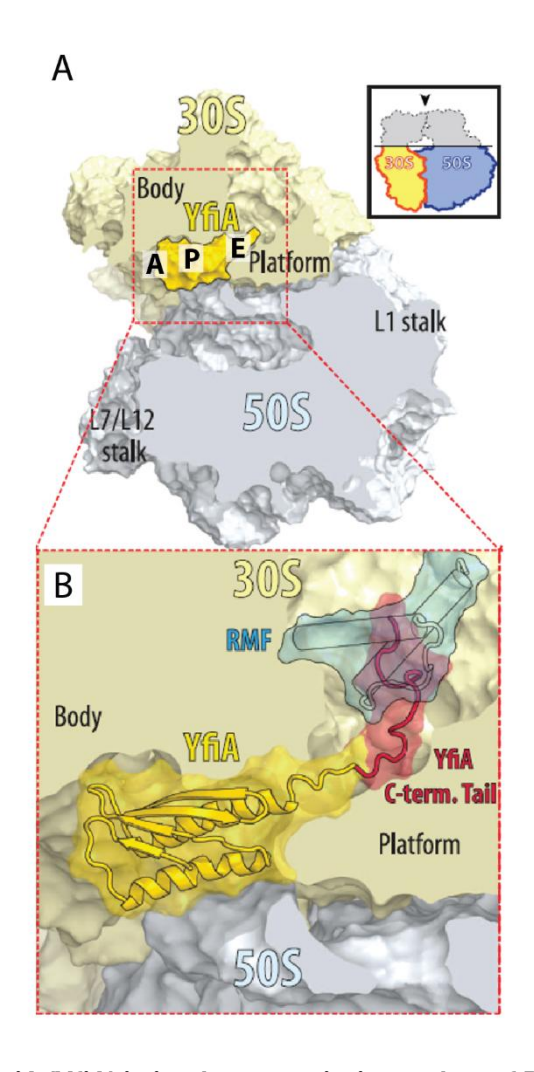


**Figure 9.** The binding of RaiA (YfiA) is in close proximity to that of RMF. RaiA(YfiA)/HPF bind in the mRNA binding channel in near the binding site of P-site tRNA. Note that the long isoform of HPF would form a steric clash with RMF in accordance with current models of 100S ribosome formation in bacteria which explain that ribosome dimerization in bacteria is mediated either by binding of RMF and short HPF or long HPF. Adapted from (65).

Binding of RaiA in the mRNA channel precludes binding of mRNA to the ribosome, thereby preventing protein synthesis, in agreement with the previous studies discussed on the inhibitory function of RaiA on translation.

Similarly, HPF is known to also bind at the mRNA channel, extending from the A site through the E site, meaning that its binding site overlaps with that of its homolog RaiA. Binding of HPF to the ribosome would result in a steric clash with canonical factors of protein synthesis such as initiation factors IF1, IF3, and elongation factor EFG as well as preclude the binding of tRNAs (**Figure 10**) (65).

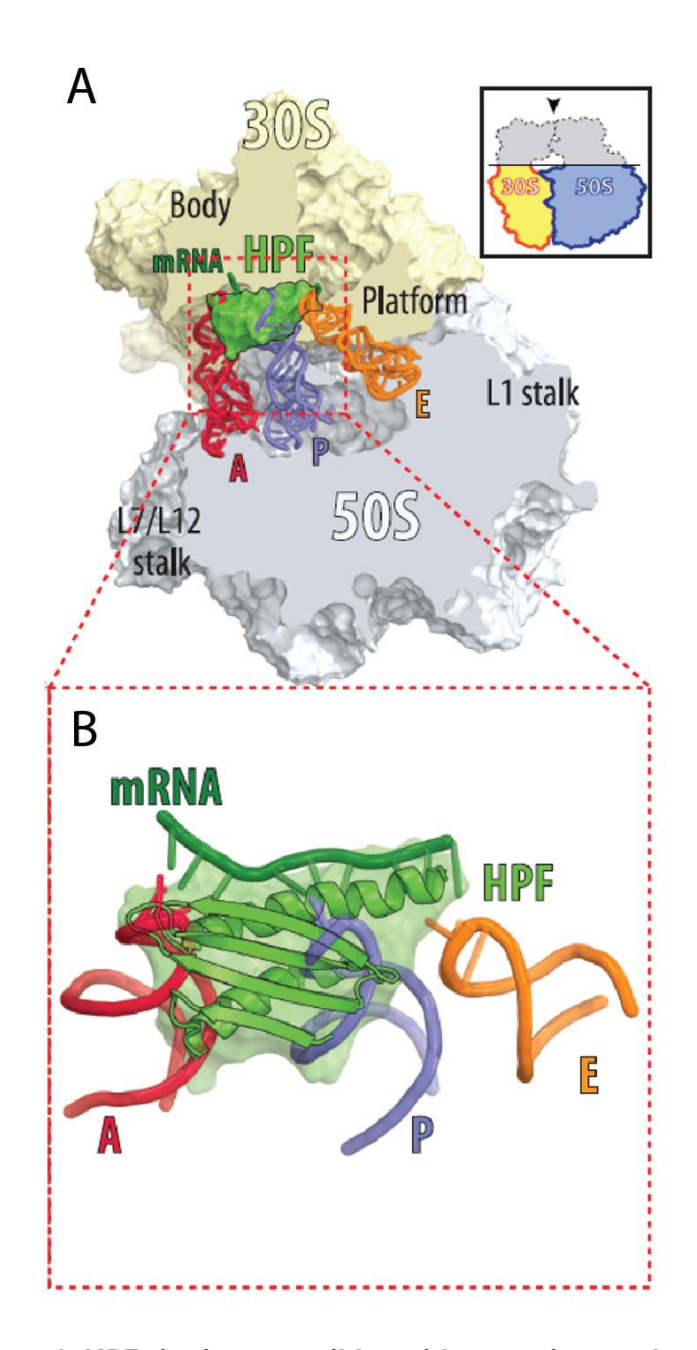


Figure 10. Binding of HPF is incompatible with protein synthesis. Structure of T. thermophilus ribosome in complex with hibernation factor HPF shows that the binding site of this protein spans the binding sites of tRNAs during protein synthesis. Adapted from (65).

It is worth noting that HPF sits in close proximity to the decoding centre with residues Arg 75, Arg 23, Lys 26 and Lys 29 interacting directly with the four nucleotides adjacent to the decoding centre (G1494, U1495, C1496 and G1497) (65). The decoding centre is one of the active centres of the ribosomes where mRNA codons interact with tRNA anti-codons during protein synthesis. The decoding centre plays a crucial role in protein synthesis as it dictates whether the correct cognate tRNA has bound the

ribosome based on specific codon that is being "decoded" or read at any given time. This process (referred to as "decoding") helps ensure that the right amino acids are added at the right positions within the nascent polypeptide chain (77).

As mentioned earlier HPF helps mediate 100S formation in bacteria that encode both RMF and HPF. This proposed mechanism, however, contemplates one of the isoforms of this protein commonly referred to as short HPF.

Previous studies looking into the distribution of HPF across bacterial species identified that this protein has two distinct isoforms based on the length of the C-terminal tail of HPF. According to Ueta and colleagues, short HPF (which was primarily found in gamma and some beta-proteobacteria) lacks the C-terminal extension that is present in long HPF beyond the first 95 amino acid residues that are present in both isoforms of the protein (74).

Formation of 100S ribosomes has been detected in several species of gamma-proteobacteria during stationary phase including *E. coli*, *Salmonella typhimurium*, *Proteus mirabilis*, *Pectobacterium carotovorum*, *Klebsiella pneumoniae* and *Serratia marcescens* (**Figure 11**). By contrast, in the beta-proteobacterium *Burkholderia multivorans* (which does not encode RMF and has a distinct isoform of short HPF that differs from short HPF in gamma-proteobacteria) 100S ribosomes were not detected even during stationary phase (78). This suggests that 100S formation mediated by RMF and short HPF may be a mechanism that is best conserved among the gammaproteobacterial, particularly the *Enterobacteriaceae* family to which all the species mentioned above belong to.

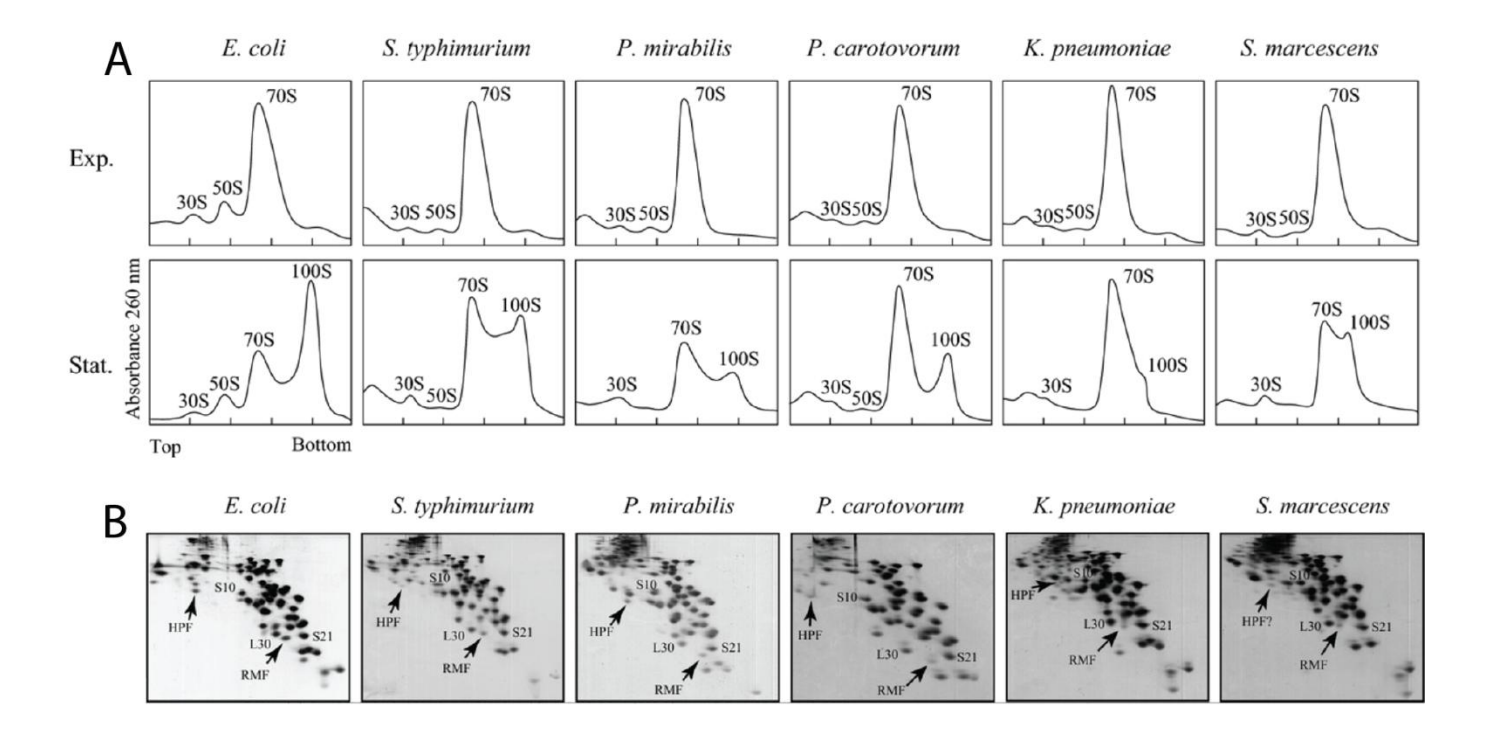


**Figure 11. 100S ribosome formation mediated by RMF and short HPF is well conserved in gammaproteobacterial.** (**A**) Analysis of ribosome samples by sucrose density gradient centrifugation from *E. coli, S. typhimurium, P. mirabilis, P. carotovorum, K. pneumoniae* and *S. marcescens* reveals that 100S formation is a conserved mechanism of ribosome hibernation in these species during stationary phase. (**B**) Gel electrophoresis analysis 100S ribosome fractions in the species mentioned above suggests that ribosome dimerization during stationary phase is mediated by binding of RMF and HPF. Adapted from (78).

While it may seem that the distinction between short and long HPF is rather trivial, structural studies suggest that each isoform of the protein may be involved in different mechanisms of ribosome hibernation in bacteria. One example of the role of long HPF in ribosome hibernation is illustrated by structural studies by Franken and colleagues of hibernating ribosomes of the bacterium, *Lactococcus lactis*. In this study, a protein annotated as RaiA (HPF homolog) in *L. lactis* was shown to be required for 100S formation during stationary phase. While ribosome dimers were only observed in wild type *L. lactis* cells as they transitioned to stationary phase, *L. lactis* that lacked the RaiA gene did not have the ability to form ribosome dimers under the same stress conditions as the wild type and were only able to form 100S ribosomes after transforming the knockout cells with a plasmid that contained the RaiA gene. Notably, RaiA with a truncated C-terminal domain were found to be able to bind the ribosome but did not elicit dimerization (79).

In vitro dimerization experiments by Puri et al. of *L. lactis* ribosomes later showed that ribosomes dimerized when incubated with HPF purified from *E. coli* and *L. lactis* RaiA. However, overexpression of HPF from *E. coli* in *L. lactis* did not result in ribosome dimerization (80). This is of particular importance if we consider that unlike *E. coli* which has genes for RMF and HPF, the only ribosome hibernation factor that *L. lactis* was known to encode at the time that this study was conducted was RaiA. This could explain how formation of 100S ribosomes occurs in *L. lactis* (and possibly other organisms) which do not possess genes for RMF or short HPF.

It is important to note that Puri and colleagues proposed the reclassification of *L. lactis* encoded RaiA into HPF, (specifically into long HPF) because of its higher sequence similarity to HPF in *E. coli* (64%) as opposed to RaiA in E. coli (32%) and its structural similarity to HPF in *E. coli*, particularly in their extended C-terminal domain (80).

Another example of the role of long HPF in ribosome hibernation in bacteria comes from studies in *Staphylococcus aureus* showing that the long isoform of HPF is responsible for ribosome dimerization. Similarly to *L. lactis*, *S. aureus* does not encode for either RMF or the short isoform of HPF, and relies only on long HPF to form dimers (81). The 100S ribosome structures from *S. aureus* revealed that in this organism ribosomes form dimers in two structurally distinct manners (**Figure 12**). In both conformations the ribosome dimers are bound by the small subunit where the C-terminal domain of one of the copies of HPF bound to the ribosome interacts not directly with a second ribosome, but instead with the C-terminal domain of the second copy of HPF in complex with the ribosome. This protein-protein interaction does not require a conformational change at the head of the small subunit as it is the case with RMF, but still allows to position both subunits in enough proximity for additional interactions that stabilize the entire complex (81).

In the so-called "tight" conformation helices 26 interact to create additional contacts between the ribosomes. These interactions are absent in the "loose" conformation which seem to only rely on the C-terminal domain to stabilize the dimer (79). The fact that long HPF is capable of forming 100S ribosomes without the need of any additional proteins could potentially explain why organisms that encode long HPF

do not also encode RMF and short HPF (73), and can therefore bypass the 90S intermediate conformation prior to short HPF binding and the 100S complex is stabilized (82).

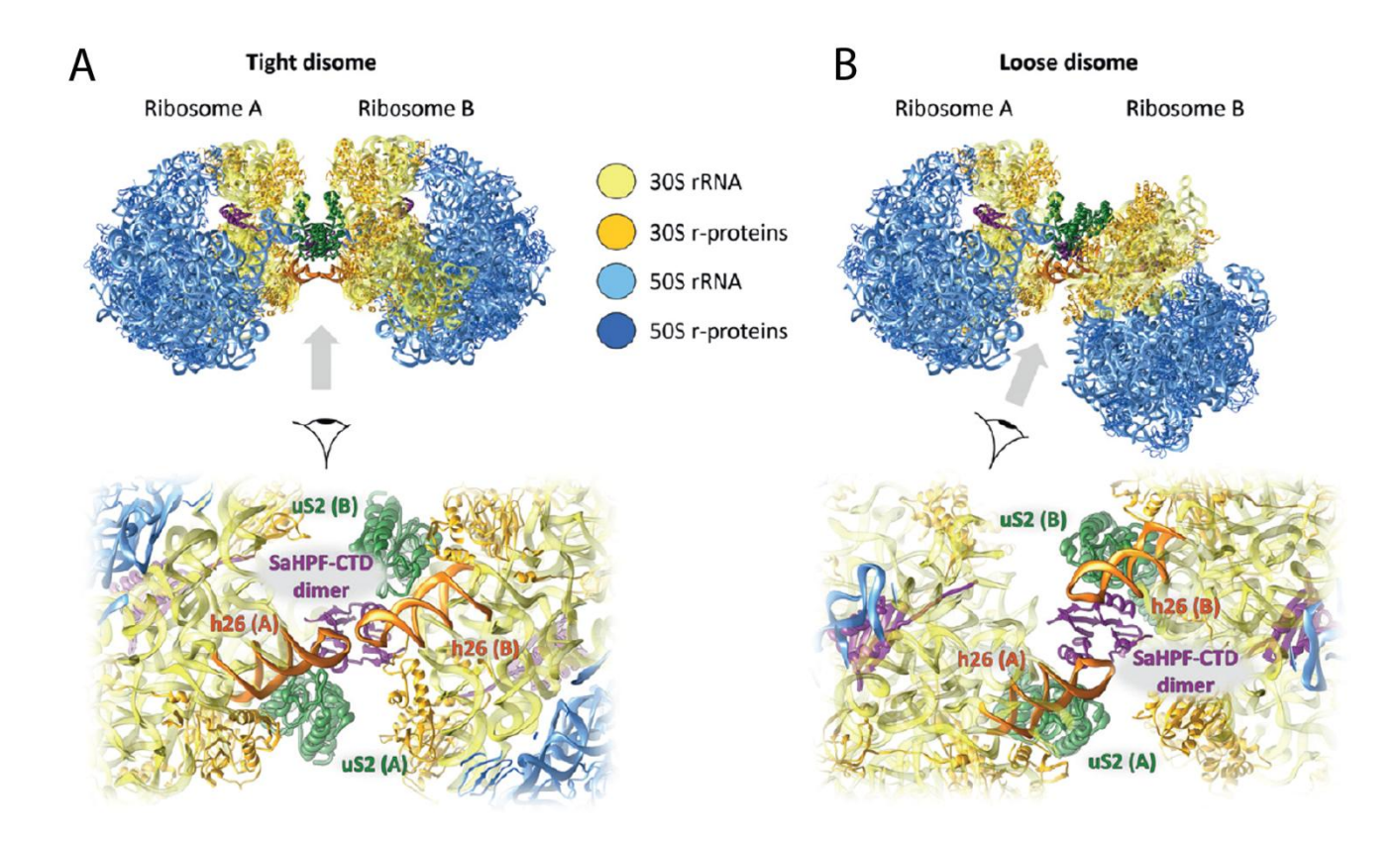


**Figure 12.** Cryo-EM analysis of *S. aureus* 100S ribosomes reveals two structurally distinct types of ribosome dimers. (A) In the so-called "tight" ribosome dimers in *S. aureus* helices 26 in 16S rRNA are brought in close proximity to one another closely resembling 100S ribosomes in other species, such as *T. thermophilus* and *E. coli*. By contrast, the so-called "loose" ribosome dimer shown in panel (B) adopts a different conformation as is evident by the relative placement of both small subunits, the relative distance of helices 26, and conformational change of proteins S2. Adapted from (81).

In summary, structural and biochemical studies on the mechanisms of bacterial ribosome hibernation have uncovered three distinct mechanisms by which bacteria are able to modulate ribosome activity in response to stress. These are the following:

- 1) 100S dimerization by binding of RMF and short HPF to the ribosome
- 2) 100S dimerization by binding of long HPF to the ribosome
- 3) 70S hibernating ribosomes by binding of RaiA

Given the limited number of bacterial species that have been studied in relation to ribosome hibernation, and the lack of structural data of putative hibernation associated factors such as SRA, YqjD, ElaB, among others, it is to be expected that the number of mechanisms that govern ribosome hibernation in bacteria is much higher than we currently know.

# 1.5 WHAT IS THE ROLE OF RIBOSOME HIBERNATION FACTORS? INHIBITION VS PROTECTION

When ribosome hibernation factors were first identified in *E. coli*, they were hypothesized to play a role of protein synthesis inhibitors that arrest ribosome activity in order to prevent their undesired activities or preserve energy in metabolically inactive cells. However, growing evidence suggests that beyond their inhibitory properties, hibernation factors may serve an additional or an alternative role—that may be as important for the cell as it is to conserve energy during times of stress, —that is to protect the integrity of the ribosome during stress.

The possibility that hibernation factors may serve a protective role was first proposed by the team of scientists that described the first hibernation factor to be

discovered. Wada and colleagues hypothesized that 100S ribosomes represented "a storage form of ribosomes" (63), and that these ribosomes might exhibit a higher degree of resistance to degradation, particularly by nucleases or proteases which are known to be more abundant during stationary phase, the primary stressor that seemed to trigger 100S ribosome formation (26).

In a subsequent publication by the same group, ribosome hibernation factor RMF is described as "stationary growth phase specific inhibitor" (62) highlighting the idea that the primary function of these proteins is to halt translation. Soon this would become the prevalent narrative in the scientific literature, and the potential protective role of hibernation factors would be relegated to a second plane and even become a matter of debate. One of the reasons behind why this idea became controversial has to do with how difficult it can be to detect lower levels of ribosome degradation in the absence of ribosome hibernation factors. By contrast, testing the inhibitory effects of ribosome hibernation factors has proven to be much easier, as shown by early experiments in which ribosome hibernation factors were assessed using the so-called *in vitro* translation system (29) (63).

Nevertheless, the effects of hibernation factors on cell fitness or recovery after stress (and by extension evidence to support that these proteins may be involved in conservation of essential components of the cell, such as ribosomes) has been known since shortly after the discovery of ribosome hibernation factors. For instance, lack of RMF has been linked to decreased levels of viability in *E. coli* cells during stationary phase (62). More recently, formation of 100S ribosomes has been associated with a higher degree of viability and tolerance to stress in *E. coli* cells during the stationary phase (48).

Genetic knockouts of RMF in *E. coli* not only accelerate rRNA decay but cause a 100-fold decline in cellular survival rate after a 5-day toxic exposure to acid (83). The survival of RMF-deficient cells largely depends on the time that cells spend in stationary phase or under starvation. While RMF was dispensable for a relatively short-term stress of up to 4 days, the impact of RMF on the ability of cells to recover increased dramatically with longer periods of stress. A similar, time-dependent impact was

observed in other model organisms, including HPF/RaiA-depleted *E. coli* (84), *S. aureus* (85), and *M. smegmatis* (86).

In *B. subtilis*, lack of ribosome hibernation factor HPF does not affect the viability of these knockout cells, however their ability to resume growth once placed in fresh media following stationary phase is considerably impaired in comparison to the wild-type cells (87). Other studies on the role of HPF in *B. subtilis* have reported a significant loss of ribosomal proteins uS2 and uS3 during stationary phase (88) likely due to the degradation of the small ribosomal subunit by RNAse R (89). Similarly, in *S. aureus* HPF has been shown to prevent degradation of ribosomes and decrease cell viability over extended periods of time (90).

These findings were replicated by other laboratories that have shown that the deletion of genes encoding RaiA/HPF and RMF leads to accelerated rRNA decay in metabolically inactive cells of *E. coli*, *S. aureus*, and *M. smegmatis* (86), (85), (73).

More mechanistic experiments investigating the absence of hibernation factors in stationary phase bacterial cultures of *S. aureus* have shown that lack of hibernation factors can lead to ribosomal dissociation into individual subunits, followed by nucleolytic degradation of ribosomal subunits by the RNA-degrading enzyme RNase R (85). Remarkably, these ribosomes tend to accumulate rRNA nicks precisely at the sites where hibernation factors bind, leading to the conclusion that the primary role of ribosome hibernation factors is to safeguard the vulnerable active centres of the ribosome against cellular nucleases (84) as hypothesized decades ago by Wada et al.

Collectively, these data revealed that the fitness cost of hibernation factors depends on the duration of metabolically inactive states. The longer cells remain metabolically inactive in the absence of hibernation factors, the less likely they are to recover, indicating that protecting ribosome from degradation, rather than arresting their activity, is the major beneficial activity of ribosome hibernation factors. Given that many cells can remain dormant for several years, hibernation factors are therefore a matter of life or death during such states of long-term dormancy.

#### 1.6 THE COLD-ADAPTED BACTERIUM PSYCHROBACTER URATIVORANS

Psychrobacter urativorans is Gram-negative coccus that belongs to the bacterial class of the gamma-proteobacteria. Like many cocci bacteria, *P. urativorans* cells grow in in a cluster-like fashion resulting in large aggregates of cells (**Figure 13**). The earliest observations of *P. urativorans* describe this organism as "multicellular" due to their tendency to grow in clusters of two, four or more cells with a shared cell wall (91).

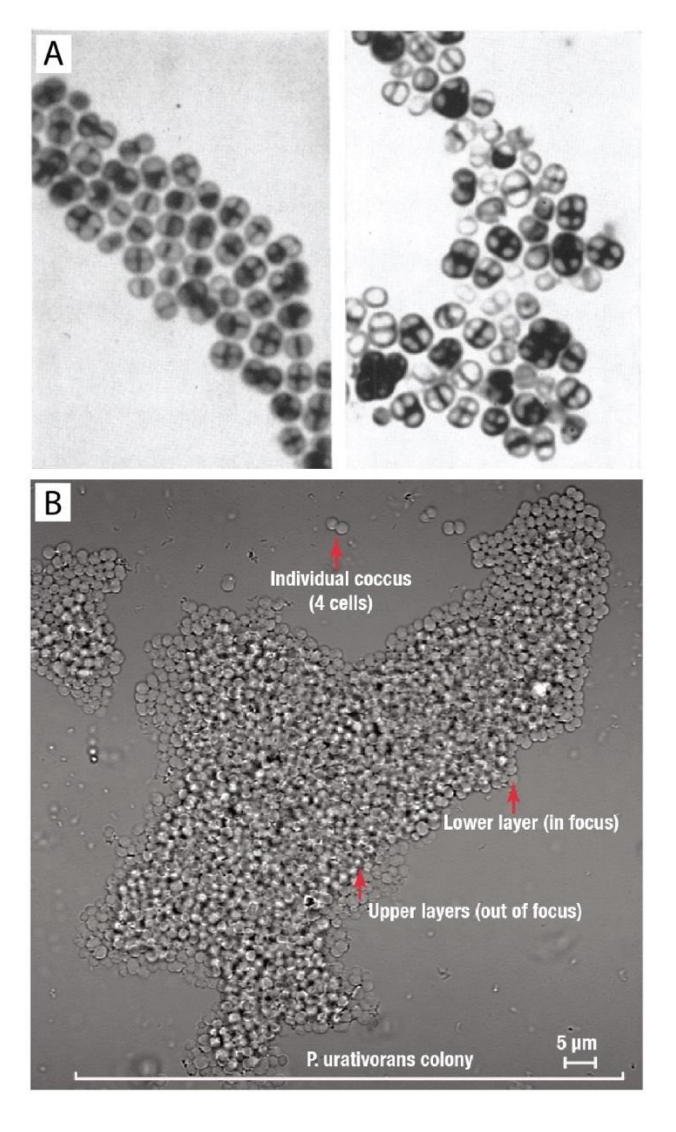


**Figure 13. Microscopy reveals morphological features of** *P. urativorans* **cells. (A)** Staining *P. urativorans* cells shows that these cells often present in groups of 2 and 4 cocci that appear to share a cell wall. (**B**) Brightfield microscopy shows the tendency of *P. urativorans* to grow in a cluster-like fashion and to form large aggregates of cells. Adapted from (91), (31).

One of the most prominent characteristics of *P. urativorans* is its ability to grow at low temperatures. This is evident when we look at the range of temperatures that allow for the growth of this organism as well as the different environments were this species has been isolated from.

*P. urativorans* was first isolated in 1951 from sausages prepared from frozen pork meat and named *Micrococcus cryophilus* due to its characteristic morphology and ability to grow at low temperatures (92). While the absolute lowest growth temperature for this organism has not been tested it was initially reported that it can grow at temperatures as low as -4°C with a maximum growth temperature of 24°C. *M. cryophilus* was reported to grow in a pH range between 5.5 and 9.5, and be incapable of growth in the absence of oxygen (92).

In 1996 the species was redescribed after being isolated from ornithogenic soil samples from Antarctica, and reclassified ad *Psychrobacter urativorans* due to its 16S rRNA sequence similarity to other members of this genus (93). Ornithogenic soils are formed from the deposition of faeces from birds that inhabit Antarctica (most notably penguins), providing organic matter rich in essential elements to sustain life in an otherwise nutrient deficient environment. These soils are a source of great bacterial diversity with members of the *Psychrobacter* genus being one of the most dominant bacterial species detected in these soils and other Antarctic environments (94) (95) (96).

The presence of *Psychrobacter* in ornithogenic soils suggests that these organisms can be found not only in environmental samples but can also inhabit the gut of various marine animals. In fact, several species of *Psychrobacter* have been isolated in the digestive tract of penguins (97) fish, sea snails (98), seals (99) as well as in storks (100) and polar bears (101).

It is thought that the *Psychobacter* genus evolved from a mesophilic ancestor that was associated with animal hosts, particularly those comprising gut microbiota. Cold adaptation within *Psychrobacter* species was acquired as these organisms became more abundant in the environment and adopted free-living lifestyles as opposed to being host associated (101), likely explaining the relatively wide range of temperatures at which different species of *Psychrobacter* can grow (-18 to 40°C) (102).

One environmental survey looking at the distribution of the *Psychrobacter* found that members of this genus are present in natural habitats with a diverse range of temperatures. *Psychrobacter* species were detected in environmental samples from some of the coldest locations of our planet (Antarctica, and Siberian permafrost), to tropical habitats (Brazil, Puerto Rico and Hawaii), as well as template habitats (Michigan and Iowa, USA) (103).

The ability of *Psychrobacter* species to grow at a wide range of temperatures as evidenced by environmental sampling and laboratory tests (102) points not only to a seemingly complex relationship between cold adaptation and the evolution of this genus.

Cold adapted organisms, also referred to as psychrophilic (psychro = old; philic = loving) are often classified in 2 categories: strict psychrophiles (sometimes referred to as "eupsychrophiles" or "true psychophiles") and psychrotolerant or psychrotrophic organisms. One of the most widely accepted definitions for psychrophiles was proposed by Richard Morita in 1975 who defined psychrophilic organisms as having a maximum growth temperature of 20°C with an optimal growth temperature of 15°C or lower and are capable of growth at 0°C or lower (104). Psychrotrophs on the other hand are defined as organisms that have an optimal growth temperature 15°C or higher and can sustain growth at temperatures above 20°C (105).

Based on the temperature range at which *P. urativorans* can sustain life it is classified as a psychrotroph or psychrotolerant bacterium. While the specific adaptations that allow *P. urativorans* to grow at low temperatures have not been widely described, most of the research focused on these adaptations relate to fatty acid composition of this organism. One of these adaptations include a decrease in the fatty acid chain that comprises the cell wall of this organism (106), a common response in bacteria upon exposure to low temperatures (107).

By contrast, the question of how *P. urativorans* (and other cold adapted organisms) adapt their protein synthesis machinery in response sudden changes in temperature remained largely unexplored. This question is particularly important because most cold-adapted bacteria grow significantly slower than common model organisms like *E. coli*. For instance, *P. urativorans* divides at least five times slower than

*E. coli*. This makes it impossible for this cold-adapted organism to instantly adjust its metabolism, including ribosomal protein synthesis, to abrupt changes in temperature.

The following chapters will focus on describing one mechanism by which *P. urativorans* (and likely other bacterial species) are able to quickly alter their ribosomes in response to rapid decreases in temperature.

### **CHAPTER 2: MATERIALS AND METHODS**

#### 2.1 SPECIES SELECTION

The decision to use *P. urativorans* as a model organism relates to the initial aim of this project, which was to use ribosomes from cold adapted bacteria to investigate how biological molecules adapt to low temperatures. In this context, *P. urativorans* was selected based on the following criteria:

- 1. Adaptation to cold: the species selected must be classified as either psychrophilic or psychrotolerant based on their minimum growth temperature and their optimal growth temperature.
- 2. Sequenced genome: the species selected must have had a fully sequenced genome to enable building ribosome models using cryo-EM maps.
- 3. Commercial availability and defined laboratory growth conditions.

#### 2.2 BIOMASS PRODUCTION

#### "Cold shock" dataset

Freeze-dried cells of *P. urativorans* were obtained from the American Type Culture Collection (ATCC 15174). The cell pellet was rehydrated in 15 mL of pre-chilled marine broth 2216 medium (Sigma-Aldrich) and incubated in a shaker (SciQuip Incu-Shake Mini) at 150 r.p.m. at 10°C for 7 days, according to the American Type Culture

Collection protocol. This culture was then used to inoculate 1 L of pre-chilled marine broth 2216 medium and incubated at 150 r.p.m. for 4 days at 10 °C until the culture reached an optical density at 600 nm ( $OD_{600}$ ) of 0.272. The cells were then placed on ice for 10 min and centrifuged for 5 min at 4 °C and 5,000g, yielding approximately 1 g of cell pellet.

#### "Stationary phase" dataset

To isolate ribosomes from stationary cells, P. urativorans cells were cultured in marine broth 2216 medium (Sigma-Aldrich) at 20°C and at 150 r.p.m. The culture was allowed to reach the stationary phase (OD<sub>600</sub> of 1.5) and remain in this phase for 4 days before pelleting these cells for 5 min at 4 °C and 5,000g and using this pellet for ribosome isolation.

#### 2.3 RIBOSOME ISOLATION

To lyse the cells, the pellets were resuspended in 1 mL of buffer A (50 mM Tris-HCl pH 7.5, 20 mM magnesium acetate and 50 mM KCl), transferred to 2-mL microcentrifuge tubes containing approximately 0.1 mL of 0.5 mm zirconium beads (Sigma-Aldrich BeadBug), and disrupted by shaking for 30 s at 6.5 ms<sup>-1</sup> speed in a bead beater (Thermo FastPrep FP120 Cell Disrupter). The sample was then centrifuged for 5 min at 4 °C and 16,000g to remove cell debris, and the resulting supernatant was collected and centrifuged for 1 min at 16,000 r.p.m. and 4 °C to remove the remaining debris.

To separate ribosomes from most other cellular components, we employed a stepwise precipitation of the lysate with PEG20,000, which is known to reduce solubility of biological molecules in cellular extracts (108). The cell lysate corresponding to 30 min of ice treatment was then mixed with PEG 20,000 (25% w/v) to a final concentration of 0.5% (w/v) and centrifuged for 5 min at 4 °C and 16,000g to precipitate insoluble aggregates. Precipitation was repeated using a stepwise increase of PEG 20,000 concentration until visible signs of ribosome precipitation was observed (formation of a white pellet and/or increase in opacity of the sample). Optical density at 260 nm and 260/280 ratio measurement were taken after the addition of PEG20,000 to monitor the precipitation of ribosomes in the sample. The supernatant was mixed with PEG 20000 (powder) to the final concentration of about 12.5% (w/v) and centrifuged for 5 min at 4 °C and 16,000g to precipitate ribosomes. Then the supernatant was mixed with PEG 20,000 (powder) to the final concentration of about 12.5% (w/v) and centrifuged for 5 min at 4 °C and 16,000g to precipitate ribosomes.

To confirm the presence of ribosomes in the purified samples, the precipitated fractions of cell lysates were analysed using size exclusion chromatography with a Superdex 200 10/300 GL column (GE Healthcare). This column allows the separation of particles with a molecular weight above 10-600 kDa by size. 100  $\mu$ L of crude ribosome samples of *P. urativorans* were analysed. Most particles detected had a molecular weight above 0.6 MDa, indicating possible presence of ribosomes (**Appendix 1**).

To remove any unwanted molecules that may have potentially been present in the samples PD Spin Trap G-25 microspin columns (GE Healthcare) with an exclusion limit of 5,000 Mr were used as a clean-up step. The columns were equilibrated according to the manufacturer's instructions and loaded with the precipitated P. urativorans ribosome sample twice to clear crude ribosomes from small molecules. The obtained solution had an  $OD_{260}$  of 34.89 and an  $OD_{260}/_{280}$  of 1.71, corresponding to a ribosome concentration of 512 nM. This solution was split into 10- $\mu$ L aliquots and frozen at -20 °C for subsequent cryo-EM and mass spectrometry analyses.

To analyse polysome profiles, we analysed 0.1 mL of crude *P. urativorans* lysates per time point, using 10–40% sucrose gradients in buffer A after 3 h of centrifugation at 35,000 r.p.m. and 4 °C in a SW40 rotor (Beckman Coulter).

#### 2.4 GRID PREPARATION

To prepare ribosome samples for cryo-EM analyses, 8–10- $\mu$ L aliquots of crude ribosomes were thawed on ice and loaded onto glow-discharged (20 mA, 60 s or 90 s, PELCO easiGlow) Quantifoil grids (R1.2/1.3, 200 mesh, copper), using 2  $\mu$ L of the sample per grid. The grids were then blotted for 1 or 2 s at 100% humidity (using blotting force –5) and vitrified using liquid nitrogen-cooled ethane in a Vitrobot Mark IV (Thermo Scientific).

#### 2.5 GRID SCREENING AND CRYO-EM DATA COLLECTION

The grids for both the cold shock and stationary phase datasets were screened using Smart EPU (Thermo Scientific) with a 200-kV Glacios electron cryo-microscope (Thermo Scientific) with a Falcon 4 detector located at the York Structural Biology Laboratory, University of York, UK.

#### "Cold shock" dataset

The dataset was collected on a 300-kV Krios cryogenic electron microscope (Thermo Scientific) located at the electron Bio-Imaging Centre, Diamond Light Source, UK. A total of 9,637 micrograph videos were recorded in aberration-free image shift (AFIS) mode using defocus targets of -2.4, -2.1, -1.8, -1.5, -1.2 and -0.9  $\mu$ m. The grids were exposed to a total dose of 40 electrons Å-2 across 2.55 s. A nominal magnification of ×165,000 was applied, resulting in a final calibrated object sampling of 0.723 Å pixel size.

#### "Stationary phase" dataset

The dataset corresponding to the stationary phase sample of *P. urativorans* ribosomes was collected using a 200-kV Glacios cryogenic electron microscope (Thermo Scientific) with a Falcon 4 detector located at the York Structural Biology Laboratory, University of York, UK. For each video, the grids were exposed to a total dose of 50 electrons Å–2 across 5.65 s. A nominal magnification of ×150,000 was applied, resulting in a final calibrated object sampling of 0.94 Å pixel size. A total of 4,997 micrograph videos were recorded in AFIS mode using defocus targets of -1.4, -1.2, -1.0, -0.8 and 0.6  $\mu$ m.

#### 2.6 CRYO-EM DATA PROCESSING OF RIBOSOMES FROM P. URATIVORANS

#### "Cold shock" dataset

Cryo-EM data for the *P. urativorans* dataset were initially processed using cryoSPARC v4.2.0. In brief, after patch motion correction and CTF estimation, a total of 1,410,883 particles were picked from the 11,196 micrographs using cryoSPARC blob picker (Minimum particle diameter 180 Å, Maximum particle diameter 230 Å). Particles were then extracted using a box size of 500 pixels and subjected to 2 rounds of 2D classification. The resulting classes (106,019 particles) were selected for ab-initio reconstruction and non-uniform refinement with C1 symmetry, which resulted in the map with a resolution of 3.02 Å. At this point, some heterogeneity was observed at the Balon binding site and decoding centre. To resolve this, masked 3D classification was carried out around the densities corresponding to Balon, tRNA, RaiA and EF-Tu. The following custom parameters were used: 2 classes, 5 Å low-pass filter, forced

classification, class similarity: 0. After 3D classification, non-uniform refinement with default parameters was carried out in the resulting maps. To better resolve domain I of EF-Tu further local refinement was carried out for EF-Tu after 3D classification. The following custom parameters were used: 5 Å low-pass filter, recentre rotations and shifts in each iteration, pose/shift gaussian prior during alignment: 7 degrees, SD prior over rotation and 4 Å, SD prior over shifts, Rotation search extent: 10 degrees. Shift search extent: 5 Å.

#### "Stationary phase" dataset

Cryo-EM data for the *P. urativorans* dataset were initially processed using cryoSPARC v4.2.0. In brief, after patch motion correction and CTF estimation, a total of 909,391 particles were picked from the 4,997 micrographs using cryoSPARC blob picker (Minimum particle diameter 190 Å, Maximum particle diameter 260 Å). Particles were then extracted using a box size of 400 pixels and subjected to 3 rounds of 2D classification. The resulting classes (corresponding to 80,882 particles) were selected for ab-initio reconstruction and homogeneous refinement with C1 symmetry, which resulted in a map with a resolution of 5.14 Å. To test for the presence of Balon in this map, masked 3D classification with default parameters separating into 2 classes was performed around the Balon density.

#### 2.7 USING CRYO-EM MAPS TO CREATE AN ATOMIC MODEL OF COLD-ADAPTED RIBOSOMES FROM *P. URATIVORANS*

The atomic models of *P. urativorans* ribosomes and the ribosome-binding proteins were produced using *Coot* v0.8.9.256 (109) and AlphaFold (110). As a starting model, the atomic model of ribosomal proteins generated by AlphaFold2 and the

atomic model of rRNA from the coordinates of *T. thermophilus* ribosomes (PDB ID 4Y4O) (111) were used. These rRNA and protein models were morph-fitted into the cryo-EM maps using ChimeraX 1.458 (112) and Phenix 1.20.159 (113) and then rebuilt using *Coot* on the basis of the information about the genomic sequence of *P. urativorans* (RefSeq GCF\_001298525.1). In the ribosome complex with Balon, mRNA and tRNA, the mRNA molecule was modelled as poly-U, and the tRNA molecule was modelled as poly-U<sub>1-72</sub>A<sub>73</sub> C<sub>74</sub> C<sub>75</sub> A<sub>76</sub> (where the last three nucleotides correspond to the universally conserved CCA-terminal sequence in all tRNA molecules).

#### 2.8 IDENTIFYING A MYSTERIOUS DENSITY

The density corresponding to Balon was initially identified as a non-ribosomal protein, which was initially modelled as a poly-alanine chain to determine its backbone structure. This poly-alanine backbone model was then used as an input file for a search of proteins with similar fold in the PDB using the National Center for Biotechnology Information tool for tracking structural similarities of macromolecules, Vast (114). This search identified the archaeal protein aeRF1 from Aeropyrum pernix as the most similar known structure to Balon, suggesting that Balon is a bacterial homologue of aeRF1. Next, proteins with a similar sequence to that of A. pernix aeRF1 were searched for P. urativorans. After three iterations of Markov model-based search with HHMER in the UniProt database, a hypothetical protein encoded by P. urativornas (UniProt ID A0A0M3V8U3) with sequence similarity to aeRF1 and Pelota was found. This protein, which we termed Balon, had a sequence that matched the cryo-EM map and was used to create its atomic model. The resulting atomic structures of Balon in complex with the ribosome, RaiA and EF-Tu or Balon in complex with the ribosome, tRNA and mRNA were then refined using Phenix real-space refinement, and the refined coordinates were validated using MolProbity (115).

#### 2.9 PHYLOGENETIC ANALYSIS

To assess phylogenetic distribution of Balon in bacterial species, three iterations of homology search were carried out using the sequence of Balon from *P. urativorans* (UniProt ID A0A0M3V8U3) as an input for a profile hidden Markov model-based analysis with HMMER (116). For each search iteration, the following search options were used: - E 1 --domE 1 --incE 0.01 --incdomE 0.03 --seqdb uniprotrefprot. The resulting dataset was reduced first by removing protein sequences that lacked information about their Phylum (21 sequences), then by removing sequences that were shorter than 300 amino acids as they typically lacked one or two of the three domains of Balon/aeRF1 (which included 806 sequences), then by removing sequences that were annotated as a protein fragment (34 sequences), and finally by removing duplicated sequences (31 sequences). This resulted in the dataset including 1,896 sequences of Balon homologues from 1,565 bacterial species.

To gain insight into a possible evolutionary origin of Balon from the archaeo-eukaryotic family of aeRF1 proteins, a complementary search for bacterial homologues of the archaeal aeRF1 was carried out using three iterations of HMMER. As an input for the first iteration, the sequence of aeRF1 from the archaeon *A. pernix* (UniProt ID Q9YAF1) was used, which we identified as being one of the closest structural homologues of Balon. For each iteration, the database of reference proteomes restricted to the bacterial domain of life was used using these search options: -E 1 --domE 1 --incE 0.01 --incdomE 0.03 --seqdb uniprotrefprot. The resulting dataset was reduced first by removing sequences lacking information about their phylum (21 sequences), then by removing sequences that were lacking at least one of the three domains of aeRF1 proteins (sequences shorter than 300 amino acids, which included 1,422 sequences), then by removing sequences annotated as a protein fragment (5 sequences), and finally by removing duplicated sequences (104 sequences). This resulted in the dataset of 1,617 sequences of bacterial aeRF1 homologues from 1,353 bacterial species.

To map the identified Balon homologues on the tree of life, the results of the previous searches were combined and repetitive entries, were removed, which resulted in a dataset of 1,898 protein sequences from 1,572 bacterial species. These sequences were aligned using Clustal Omega (117) with default parameters, which resulted in a multiple sequence alignment and a phylogenetic tree. To compare phylogenetic distribution of Balon, RMF and RaiA-type hibernation factors, the homology search was repeated using HMMER (with the same parameters as for our Balon homologues searches) for RaiA (using the *E. coli* sequences of RaiA as an input); and RMF (using the *E. coli* sequence of RMF as an input).

#### 2.10 MASS SPECTROMETRY ANALYSIS

Mass spectrometry analysis of crude samples of *P. urativorans* ribosomes was carried out at the Centre of Excellence in Mass Spectrometry at the University of York.

For each measurement taken a 10-µL aliquot of crude *P. urativorans* ribosome solution was reduced with 4.5 mM dithiothreitol and heated at 55 °C. The sample was alkylated with the addition of 10 mM iodoacetamide before proteolytic digestion with 0.2 µg Promega sequencing-grade trypsin and incubation at 37 °C for 16 h. The resulting peptides were desalted by Millipore C18 ZipTip, following the manufacturer's protocol, with final elution into aqueous 50% (v/v) acetonitrile. Desalted peptides were dried under vacuum before being resuspended in aqueous 0.1% trifluoroacetic acid (v/v) for LC–MS/MS.

Peptides were loaded onto a mClass nanoflow UPLC system (Waters) equipped with a nanoEaze M/Z Symmetry 100-Å C18, 5- $\mu$ m trap column (180  $\mu$ m × 20 mm, Waters) and a PepMap, 2  $\mu$ m, 100 Å, C18 EasyNano nanocapillary column (75  $\mu$ m × 500 mm, Thermo). The trap wash solvent was aqueous 0.05% (v/v)

trifluoroacetic acid and the trapping flow rate was 15  $\mu$ l min–1. The trap was washed for 5 min before switching flow to the capillary column. Separation used gradient elution of two solvents: solvent A—aqueous 0.1% (v/v) formic acid; solvent B—acetonitrile containing 0.1% (v/v) formic acid. The flow rate for the capillary column was 330 nL min<sup>-1</sup> and the column temperature was 40 °C. The linear multi-step gradient profile was: 3–10% B over 7 min, 10–35% B over 30 min, 35–99% B over 5 min and then proceeded to wash with 99% solvent B for 4 min. The column was returned to initial conditions and re-equilibrated for 15 min before subsequent injections.

The nanoLC system was interfaced with an Orbitrap Fusion Tribrid mass spectrometer (Thermo) with an EasyNano ionization source (Thermo). Positive ESI-MS and MS2 spectra were acquired using Xcalibur software (v4.0, Thermo). Instrument source settings were: ion spray voltage—1,900 V; sweep gas—0 a.u.; ion transfer tube temperature—275 °C. MS1 spectra were acquired in the Orbitrap with 120,000 resolution, the scan range of m/z 375–1,500, the AGC target of 4 × 105, and the maximum fill time of 100 ms. Data-dependent acquisition was carried out in top speed mode using a 1-s cycle, selecting the most intense precursors with charge states >1. Easy-IC was used for internal calibration. Dynamic exclusion was carried out for 50-s post precursor selection and a minimum threshold for fragmentation was set at 5 × 103. MS2 spectra were acquired in the linear ion trap with: scan rate—turbo; quadrupole isolation—1.6 m/z; activation type—HCD; activation energy—32%; AGC target—5 × 103; first mass—110 m/z; maximum fill time—100 ms. Acquisitions were arranged by Xcalibur to inject ions for all available parallelizable time.

Peak lists in Thermo.raw format were converted to .mgf using MSConvert (v3.0, ProteoWizard) before submitting to database searching against the *P. urativorans* subset of the UniProt database (3 August 2022, 2,349 sequences; 769,448 residues)52 appended with 118 common proteomic contaminants. Mascot Daemon (v2.6.0, Matrix Science) was used to submit the search to a locally running copy of the Mascot program (Matrix Science, v2.7.0). Search criteria specified: enzyme—trypsin; maximum missed cleavages—2; fixed modifications—carbamidomethylation of protein C termini; variable modifications—acetylation of protein N-termini, deamidation of Asn and Gln residues, N-terminal conversion of Gln and Glu to pyro-Glu, oxidation of Met and

phosphorylation of Ser, Thr and Tyr residues; peptide tolerance—3 ppm; MS/MS tolerance—0.5 Da; instrument—ESI-TRAP. Peptide identifications were passed through the percolator algorithm to achieve a 1% false discovery rate assessed against a reverse database. The search data for which molar percentages of each identified protein were calculated from Mascot emPAI values by expressing individual values as a percentage of the sum of all emPAI values in the sample, as previously described (118). To calculate the relative abundance of each cellular protein before and after 30 min of ice treatment, their total spectrum counts in the ice-treated sample were divided by the corresponding total spectrum counts of the control (non-ice-treated) sample. An infinite value for a few proteins means that in the control sample we have not been able to detect evidence for a protein by spectral counting.

# CHAPTER 3: DISCOVERY OF A NOVEL BACTERIAL RIBOSOME HIBERNATION FACTOR

#### 3.1 INTRODUCTION

The initial aim of this project was to describe the molecular adaptations that allow cold-adapted organisms to survive and thrive at extremely low temperatures. To address this question, we chose to determine the ribosome structure of the cold-adapted bacterium *P. urativorans*. The rationale behind the decision to use ribosomes to study molecular adaptation to cold relates to the following three key characteristics of this macromolecule:

- 1. Complexity: Compared to an average cellular bacterial protein, which has a molecular weight of approximately 35 kDa (119), ribosomes have a molecular weight of 2.5 MDa. Furthermore, the ribosome is comprised of 54 different proteins, over 4,000 RNA bases (120), and several hundreds of small molecules (121) and metal ions (122), making ribosomes one of the most complex assemblies in the cell (123). Therefore, by studying ribosome structure we can simultaneously observe how molecules of different folds and different chemical natures (protein and RNA) have adapted to cold.
- 2. Ubiquity: Compared to most cellular components that are present only in a subset of organisms on the tree of life, ribosomes belong to a very small group of ubiquitous cellular macromolecules (124). Given that ribosomes are present in all forms of life, they can be isolated from any organism of our interest that is adapted to any given intervals of temperatures at which life is possible.
- 3. **Essentiality:** Compared to most cellular molecules that can be eliminated from the cell without causing lethality, ribosomes are absolutely required for life as

they perform the vital process of protein synthesis. We, therefore, hypothesized that organisms must adapt their ribosomes to extreme environments to allow organisms to inhabit and thrive in these environments.

Despite the fact that cold environments represent a major portion of our planet's ecosystems (with 90% of our oceans having temperatures of 5°C or below (125), and 80% of the Earth's biosphere being at constantly low temperatures (126)), cold environments remain largely understudied (127).

Bioinformatic studies that have surveyed the impact of thermal adaptation on DNA and amino acid sequence composition often include a considerably lower number of cold-adapted organisms, likely due to a lower number of genomic sequences available for cold adapted organisms (128) (129) (130).

Currently, our understanding of how biological molecules adapt to low temperatures stems largely from the study of only 6 families of relatively small enzymes (131) that have been studied primarily due to their applications in various sectors including food and textile production, the pharmaceutical industry (132), and biotechnology, (133). However, despite their wide array of industrial applications, structural information about these cold-adapted enzymes remains limited (131) (134).

The scarcity of structural information of molecules from cold adapted organisms extends to other components of the cell, including the ribosome. To date, scientists have determined ribosome structures for 44 distinct organisms, nearly all of which are mesophilic (**Table 1**). The only exceptions are the thermophilic bacterium *Thermus thermophilus* (optimal growth temperature: 65-72°C) (135) (136), the thermophilic archaeon *Thermococcus kodakarensis* (85°C) (137) (138), and the thermophilic fungus *Chaetomium thermophilum* (50-55°C) (139) (140). Notably, in the case of *T. thermophilus*, *T. kodakarensis*, and *C. thermophilum* these ribosomes were chosen for convenience to work with their samples at room temperature, and they were used as a generalized model of bacterial, archaeal, and fungal ribosome, respectively, with little attention to how the ribosomes from these organisms have adapted to high temperatures. On the opposite side of the thermal spectrum, ribosomes from cold adapted organisms have never been systematically assessed in terms of their

adaptation to cold. In fact, before the start of this project there were no ribosome structures available for any cold-adapted organism.

Table 1. List of all representative species with full ribosome structures available in Protein Data Bank (PDB) previous to this project. While there are hundreds of ribosome structures publicly available on PDB, (before the completion of this study) there were only 44 species for which we have full ribosome structures (containing both the small and large subunits). Note that there are 48 species listed, for 4 of which there are both cytosolic and plastid derived (mitochondrial or chloroplast) ribosome structures available. All species listed are either mesophilic or thermophilic.

Archaea			
Accession number	Species	Classification	
4V6U	Pyrococcus furiosus	Hyperthermophile	
4V4N	Methanocaldococcus jannaschii	Thermophile	
6TH6	Thermococcus kodakarensis	Thermophile	
4ADX	Methanothermobacter thermautotrophicus	Thermophile	
1FFK	Haloarcula marismortui	Thermotolerant	
Bacteria			
Accession number	Species	Classification	
4V4Q	Escherichia coli	Mesophile	
4V42	Thermus thermophilus	Thermophile	
5061	Mycolicibacterium smegmatis	Mesophile	
3J9W	Bacillus subtilis	Mesophile	
6SPG	Pseudomonas aeruginosa	Mesophile	
5NGM	Staphylococcus aureus	Mesophile	
5MYJ	Lactococcus lactis	Mesophile	
6O8Z	Enterococcus faecalis	Mesophile	
7JIL	Flavobacterium johnsoniae	Mesophile	
5V93	Mycobacterium tuberculosis	Mesophile	
2ZJR	Deinococcus radiodurans	Mesophile	
6YHS	Acinetobacter baumannii	Mesophile	
Eukaryotes			
Accession number	Species	Classification	
4V8P	Tetrahymena thermophila	Thermotolerant	
5DC3	Saccharomyces cerevisiae	Mesophile	
4UG0	Homo sapiens	Mesophile	
4V6W	Drosophila melanogaster	Mesophile	
3JAJ	Oryctolagus cuniculus	Mesophile	
3J7P	Sus scrofa	Mesophile	
6ZJ3	Euglena gracilis	Mesophile	
5T2A	Leishmania donovani	Mesophile	
3J79	Plasmodium falciparum	Mesophile	

6RM3	Vairimorpha necatrix	Mesophile
6ZU5	Paranosema locustae	Mesophile
4V7H	Thermomyces lanuginosus	Thermophile
6SWA	Mus musculus	Mesophile
4V91	Kluyveromyces lactis	Mesophile
5XXB	Toxoplasma gondii	Mesophile
5XY3	Trichomonas vaginalis	Mesophile
4V5Z	Canis lupus familiaris	Mesophile
5T5H	Trypanosoma cruzi	Mesophile
4V7E	Triticum aestivum	Mesophile
5OQL	Chaetomium thermophilum	Thermophile
9BH5	Caenorhabditis elegans	Mesophile
Mitochondria		
Accession number	Species	Classification
6HIV	Trypanosoma brucei brucei	Mesophile
6Z1P	Tetrahymena thermophila	Thermotolerant
6YWY	Neurospora crassa	Mesophile
5MRC	Saccharomyces cerevisiae	Mesophile
6XYW	Arabidopsis thaliana	Mesophile
5AJ4	Sus scrofa	Mesophile
7AM2	Leishmania tarentolae	Mesophile
7AIH	Leishmania major	Mesophile
3JD5	Bos taurus	Mesophile
3J9M	Homo sapiens	Mesophile
Chloroplasts		
Accession number	Species	Classification
5MMM	Spinacia oleracea	Mesophile

## 3.2 DETERMINING THE FIRST RIBOSOME STRUCTURE OF ANY COLD-ADAPTED ORGANISM

To determine the structure of *P. urativorans* ribosomes we first sourced these cells from the American Type Culture Collection (ATCC) and precultured cells according to ATCC instructions, which included using the Marine Broth, a media formulated to mimic the natural conditions of seawater to support the growth of marine microorganisms. Then, because our initial goal was to characterize the molecular adaptations that allow cold adapted organisms to remain active at low temperatures we decided to culture *P. urativorans* below its reported optimal growth temperature of 18 to 20°C (93). Therefore, our experimental system involved maintaining *P. urativorans* cultures at 10°C to produce the bacterial biomass needed for ribosome isolation.

To avoid enriching our samples with dead cells, we collected *P. urativorans* cells during their logarithmic growth. We then placed these cultures on ice for approximately 30 minutes before ribosome isolation as part of the standard protocols for ribosome isolation (141). This means that we exposed our bacterial samples to cold shock, which is known to arrest protein synthesis and induce a state of ribosome hibernation (142) (143). Consistent with this notion, we observed a gradual reduction in protein synthesis as the duration of ice exposure increased, as indicated by our polysome profiling analysis (**Figure 14**).

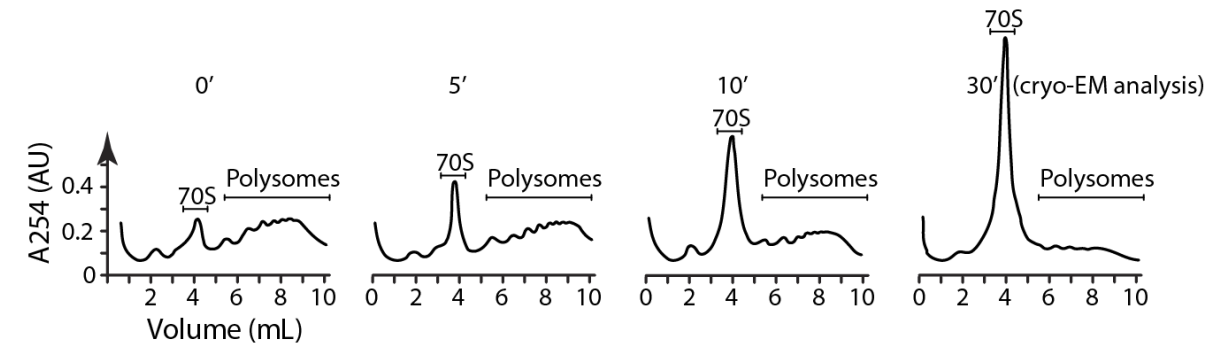


Figure 14. Exposure to ice leads to a decrease of protein synthesis in *P. urativorans*. Polysome profiling in sucrose gradients shows progressive increase of monomeric ribosomes, and a decrease of polysomes within 30 minutes of response to ice exposure of *P. urativorans* cells. This is evident based on the fraction pattern obtained over different time points showing how the polysome fractions, shown as peaks of varying molecular weight over the x-axis (elution volume) become almost undetectable.

In order to purify the ribosomes from the cold-shocked *P. urativorans*, we first needed to produce sufficient amount of biomass of these bacteria. Although, in theory, it should be physically possible to determine the structure of ribosomes using as little as 12,000 particles (144)—a smaller number of ribosomes in a single bacterial cell such as *E. coli* (145)—in practice, we needed at least 50 mg of biomass to handle the material in a convenient fashion and without the risk of ribosome loss due to non-specific absorption on the surfaces of Eppendorf tubes and pipette tips. We therefore produced approximately 1g of bacterial biomass, collected a cell pellet and lysed these cells as stated in the **Methods sections 2.2 and 2.3**.

Next, at the stage of cell lysis, we aimed to minimize the dilution of the cell lysate, which could create a risk of dissociation of ribosomes from ribosome-binding proteins. Therefore, prior to cell disruption with glass beads, we resuspended the cells in a minimal volume of lysis buffer, using a 1:1 weight-to-volume ratio between the biomass and the buffer. We also ensured that the lysis buffer contained components to support a neutral pH (20 mM Tris-HCl, pH 7.5) and magnesium ions (in the form of 20 mM MgCl<sub>2</sub>) to prevent the dissociation of ribosomes into individual subunits and unfolding of rRNA.

After breaking cells and centrifugating the cell lysate to remove cellular debris and lipid components present in the lysate, we proceeded to purify the ribosomes, assuming that ribosomes are present in the aqueous fraction of the cell lysate (supernatant) due to their hydrophilic and soluble nature. To isolate ribosomes, we adopted a previously established protocol that relies on using polyethylene glycol (PEG) to precipitate biological molecules, as this polymer is known to reduce the solubility of organic compounds in aqueous solutions (108). We added PEG20,000 to the lysate in a stepwise manner as described in the **Methods section 2.3**, while using optical density readings (at 260 nm) to monitor whether ribosomes had precipitated or not. Previously, rRNA has been reported to account for about 85% of the cellular RNA (146). We, therefore, reasoned that optical readings at 260 nm would correspond mainly to the absorbance of rRNA in our lysate. We also monitored the optical readings of the 260nm/280nm ratio to monitor the purity of our sample. After adding PEG20,000 to a concentration of 12.5%, We observed a sudden decrease in lysate transparency,

indicative of formation of insoluble aggregates and possible ribosome precipitation. We precipitated this sample using centrifugation and detected a sudden loss of absorbance at 260 nm ( $OD_{260}$ ), which dropped from approximately 3 to below 0.5. Therefore, we anticipated that the obtained pellet contained ribosomes. We resuspended the pellet and subjected the obtained solution to an additional purification step: we passed it through a mini-gel-filtration column to separate ribosomes from small molecules that could potentially contaminate the ribosomes and prevent more accurate measurements of the ribosome concentration based on the  $OD_{260}$  readings. Thus, we obtained a sample with the following optical density readings:  $OD_{260} = 34.89$  and an  $OD_{260/280}$  of 1.71. This suggested that our sample contained a substantial amount of nucleic acids as shown by the absorbance at 260 nm the absorbance at 260/280 nm (147).

To verify the presence of ribosomes in the obtained sample, we performed size exclusion chromatography as described in the **Methods section 2.3**. As shown in **Appendix 1**, we observed that the main peak corresponded to that of particles with a molecular weight exceeding 0.9 MDa, consistent with the presence of ribosomes in our sample. Therefore, we decided to use this sample for cryo-EM analysis.

Our next goal was to prepare grids for cryo-EM analysis of our *P. urativorans* ribosome samples. We first used glow discharging copper Quantifoil grids as described in the **Methods section 2.4**. Glow discharging the grids aids in increasing the hydrophobicity of the surface of the grids, which is comprised of carbon, a hydrophobic material. This helps ensure an even distribution of the sample throughout the grid. We then applied 2µL of *P. urativorans* ribosome sample onto the grids, removed the excessive amounts of sample using blotting paper and vitrified the grids using ethane that had been condensed using liquid nitrogen. The use of liquid ethane results in a rapid cooling of the sample, resulting in vitreous ice, as opposed to crystalline ice which is not suitable for cryo-EM data collection.

After preparing the grids we screened them as described in the **Methods section**2.5. We first inspected the overall grid views, known as grid atlases, to verify that we successfully removed the excessive amounts of sample, creating a sufficiently thin vitreous ice in the grid that is penetrable by the electron beams used for cryo-EM imaging (**Figure 15**).

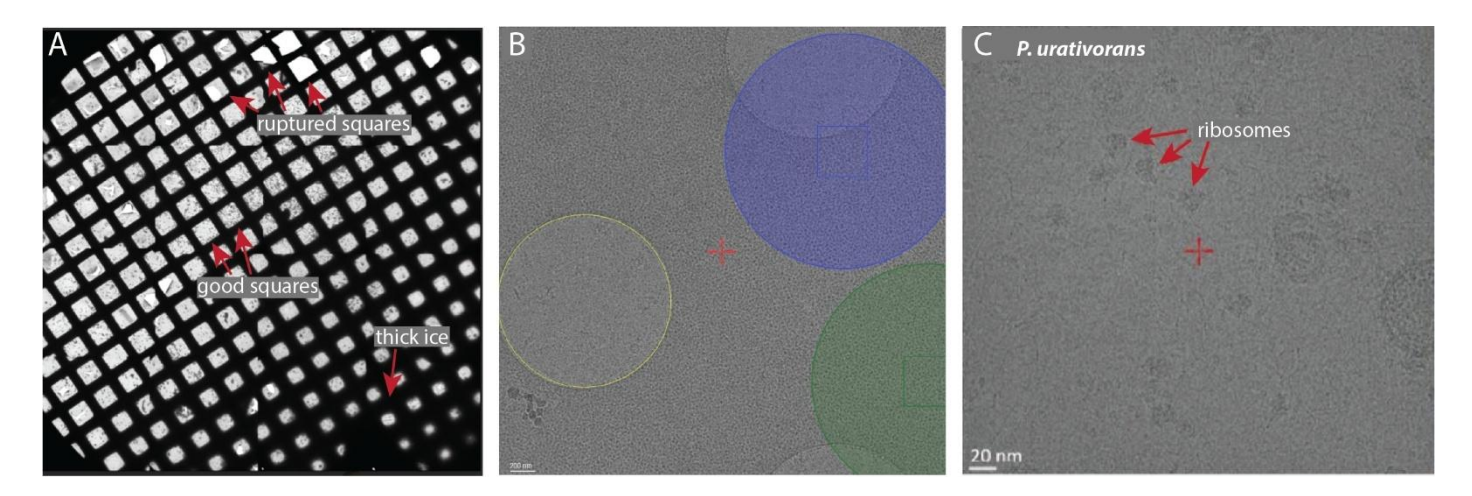


Figure 15. Screening of cryo-EM grids to assess their suitability for data collection. (A) Atlas view showing an overall snapshot of the grid used for data collection. The atlas, created by stitching together overlapping low magnification images, provides a comprehensive map of the grid. Some areas of the grid show squares appear transparent, indicating that excessive sample was removed, preventing optimal ice thickness. Other areas of the grid show squares where the carbon coating of the grid has been ruptured, precluding data collection in these squares. Areas of the grid with ice that is too thick is also indicated. Ice that is too thick could interfere with data collection due to excessive electron absorption. We collected data from "good squares" with optimal ice thickness, and where the carbon layer was preserved. (B) Zoom-in view focusing on specific grid holes illustrates the preparation of the microscope for data collection. The blue circle indicates the desired positions for the electron beam. It is focused not on the grid holes (our area of interest) but on the carbon, which serves as a stable reference point around the areas of interest on the grid. Focusing on this area is crucial because it allows the microscope to find the optimal beam intensity and focus before targeting the actual sample. The green circle indicates the position of the electron beam for the actual data collection. The green circle should be aligned with the grid hole to direct the beam accurately at the sample. (Note: the green circle is not properly aligned in this example, as we did not have a better example available). (C) Test movie illustrates the presence of ribosomes in the grid hole. Ribosomes appear as high-contrast particles that have characteristic features of two subunits and measuring approximately 20 nm in size.

We then examined individual grid holes, which confirmed the presence of ribosome particles and allowed us to estimate their concentration (**Figure 15**). This was important for devising our data collection plan, as we aimed to collect at least 20,000 images of individual ribosomes. Our test images, taken from a few random grid squares

with optimal ice thickness, revealed approximately 50 ribosome particles per movie (**Figure 15**) indicating that we had sufficient time allocated for data collection to collect images (movies) of over 100,000 ribosome particles. Therefore, we proceeded with the data collection.

In total, we aimed to collect two datasets: one for cold shock condition, and a second for stationary phase condition in order to compare and contrast how ribosomes respond to an abrupt versus gradual changes in cellular environment. We also wanted to accelerate our data collection to maximize the total number of observed ribosome particles in our dataset. For this purpose, we exposed our grids to the electron beam in aberration-free image shift (AFIS) mode to bypass movement of the microscope stage and thereby helping minimize image aberrations and increase the rate of data collection (148).

To process the resulting movies, we used CryoSPARC to confirm the presence of sufficiently high numbers of ribosome particles in our sample. After the standard procedures of motion correction and CTF estimation, we performed particle picking by specifying the expected size of our ribosomal particles (approximately 20 nm) and grouped the extracted particles into 2D "classes" containing similar images (images of similar particles in a similar orientation relative to the electron beam). We then proceeded to select the classes that appeared to comprise ribosome images based on the characteristic morphology, including the size of about 20 nm and the presence of two uneven subunits. In total, these classes comprised over 100,000 ribosome particles. Therefore, we concluded that we had obtained enough particles to determine the ribosome structure.

To obtain a three-dimensional reconstruction of the average ribosome present in our samples, we merged all the manually selected 2D classes of the ribosome particles from different angles. To increase the resolution of this reconstruction or cryo-EM map we used non-uniform refinement. This allowed us to obtain our first map of the *P. urativorans* ribosomes at approximately 3 Å resolution, which was sufficiently high for our goal: to determine the molecular structure of ribosomal proteins and rRNA in this species. A visual summary of this processing pipeline is shown in **Figure 16**.

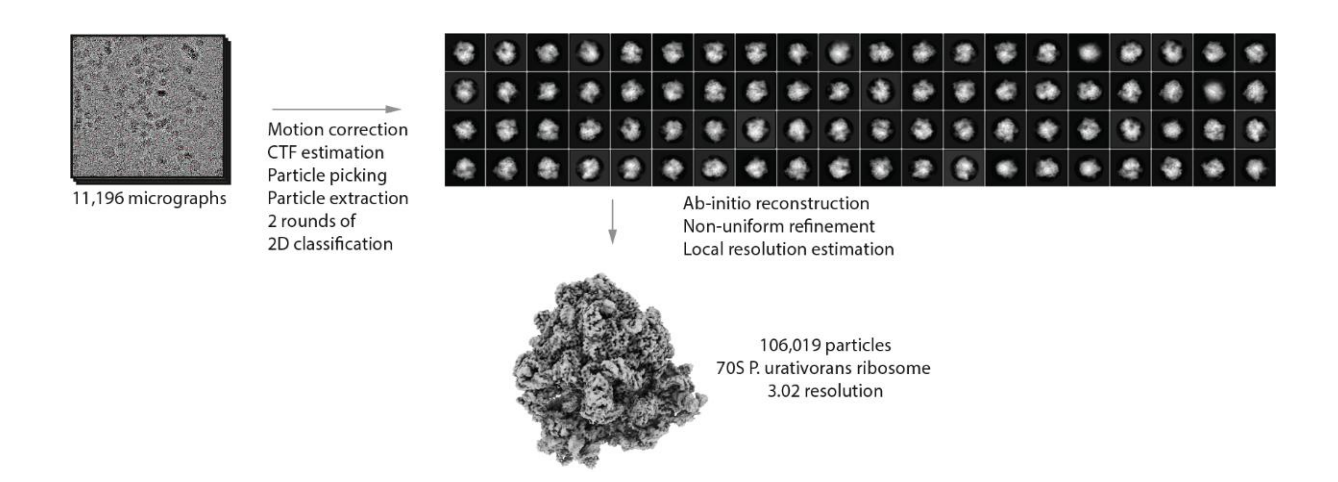
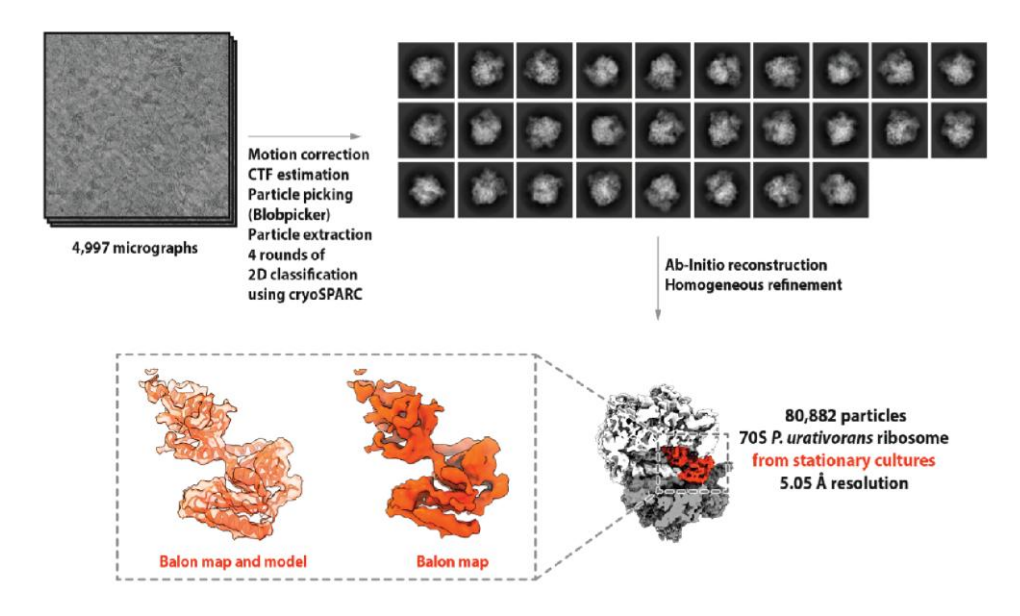


Figure 16. Cryo-EM processing of *P. urativorans* ribosome from cold shocked cells. Graphical summary of cryo-EM data processing pipeline shows a representative micrograph at 165,000x, 2D classes, 3D reconstructions and major steps of data processing using CryoSPARC.

A similar workflow was used to process movies of the *P. urativorans* ribosome sample from stationary cells (**Figure 17**, **Methods section 2.6**).



**Figure 17. Cryo-EM processing of** *P. urativorans* **ribosome from stationary cells.** Graphical summary of cryo-EM data processing pipeline shows a representative micrograph at 150,000x, 2D classes, 3D reconstructions and major steps of data processing using CryoSPARC.

Having obtained a cryo-EM density map of ribosomes isolated from cold-shock *P. urativorans*, we visually inspected the map and estimated its local resolution (**Figure 18**).

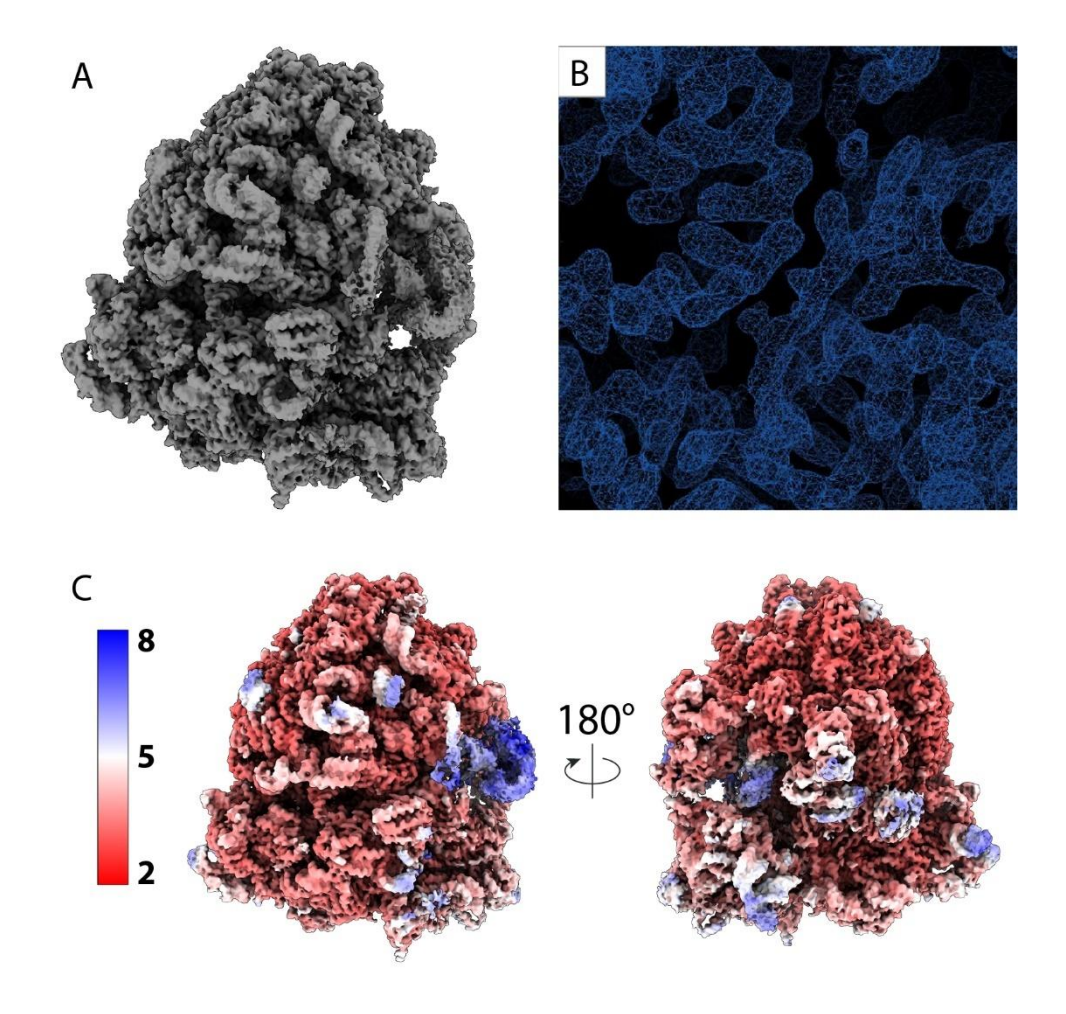


**Figure 18. Cryo-EM map of the ribosome from the** *P.urativorans* **ribosome.** (**A**) This panel shows the overall structure of the *P. urativorans* 70S ribosome. (**B**) Amplified view of the cryo-EM map showing segments of RNA and protein from the cryo-EM map depicted in panel A. (**C**) Local resolution map showing the estimated resolution of the *P. urativorans* ribosome.

Our manual examination of the cryo-EM map shown in **Figure 18** showed that it had sufficient resolution to build the molecular model of the *P. urativorans* 70S ribosome (**Figure 19**). We therefore proceeded to build the model using a model of the *T. thermophilus* ribosome (PDB ID 4Y4O) as a starting template (note that we completed this work just before AlphaFold 2 made publicly available structure predictions for over 200 million proteins (149)). This allowed us to generate the

molecular structure of *P. urativorans* ribosomes. A table with refinement values for the obtained models can be found in **Appendix 2**.

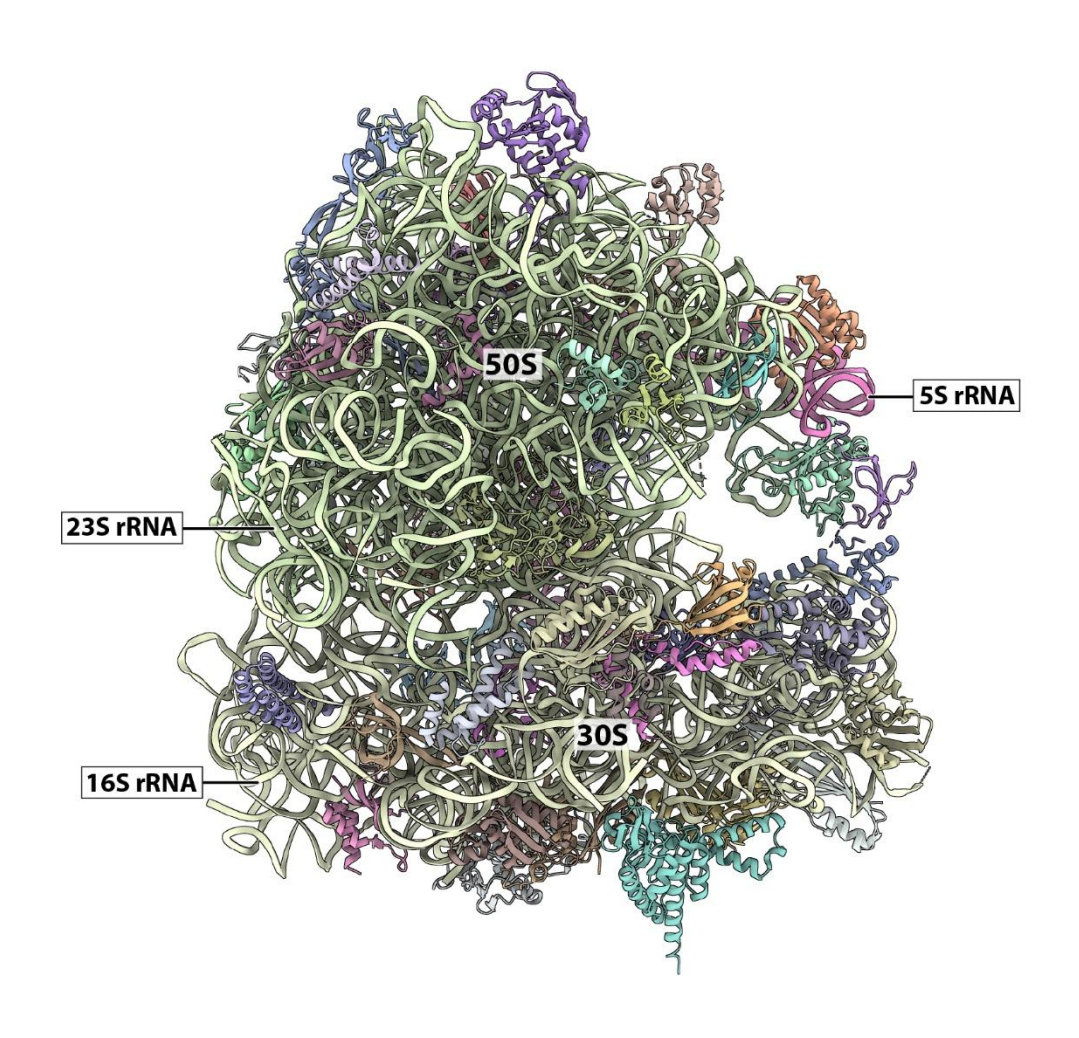


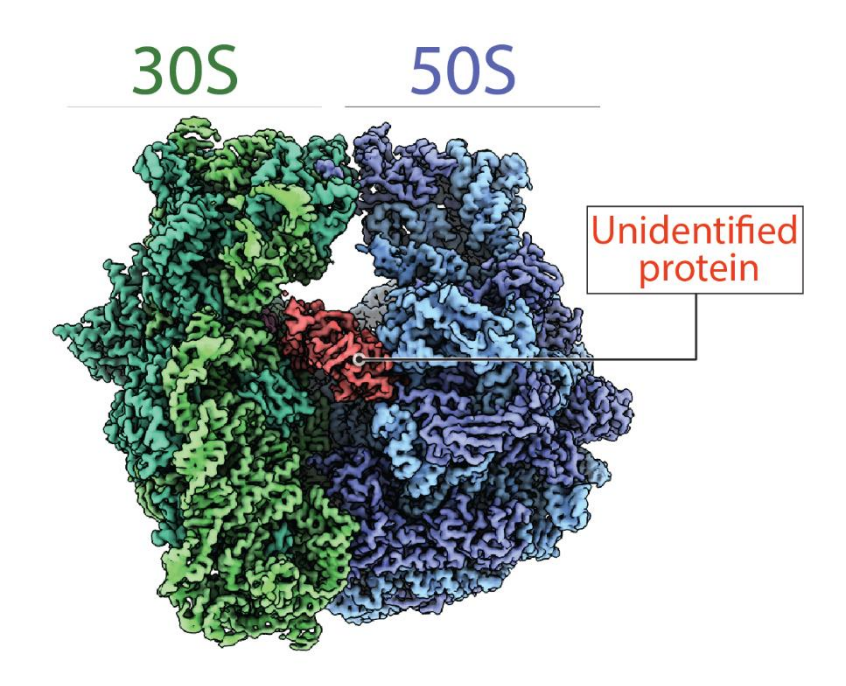
**Figure 19. Model of the psychrophilic 70S ribosome from** *P. urativorans.* This 2.5 MDa assembly is the first atomic structure of a complex assembly from any cold-adapted organism.

The model shown in **Figure 19** is the first atomic structure determined for a complex cellular component from any cold-adapted organism. It is comprised of 50 ribosomal proteins, 3 rRNA chains, and a total of 5 ligands. These ligands are found in complex with the ribosome at varying levels of occupancy and correspond to distinct binding states. A full description of these binding states is detailed in chapter 4. The remainder of this chapter will focus on the ligand with the highest level of occupancy, a previously unidentified bacterial ribosome hibernation factor.

#### 3.3 CHARACTERIZING BALON: A NOVEL RIBOSOME BINDING PROTEIN

Virtually all organisms can adapt to stress using two distinct strategies: a long-term strategy that takes millions of years and requires slow accumulation of mutations in a genome, and a short-term strategy that allows them to survive transient environmental stressors. This section describes an unexpected opportunity to shed light into a previously unknown mechanism by which *P. urativorans* adapts to sudden stress: Balon-mediated ribosome hibernation.

While building the model for *P. urativorans* ribosome, it became evident that the interface of the ribosome, more specifically, the A site of the ribosome (where canonical factors of protein synthesis are recruited to the ribosome (150) ) was occupied by a protein ligand (**Figure 20**).



### P. urativorans ribosome

Figure 20. Exposure to ice leads to a decrease of protein synthesis in *P. urativorans* and appears to elicit binding of a previously unidentified protein to the ribosome. Cryo-EM map of *P. urativorans* ribosome bound to previously unidentified protein that binds the A site.

The density corresponding to this protein was unlikely to be that of a ribosomal protein given its localization, size and overall structure. Ribosomal proteins are not known to bind the A site of the ribosome because this site is used for binding the main substrates of protein synthesis, known as aminoacyl-tRNAs. Furthermore, the density observed was considerably larger than most ribosomal proteins which in bacteria have on average about 130 amino acids (151). The larger ribosomal proteins (those with over 200 amino acids) have a structure that is inconsistent with our unidentified density (**Figure 21**).

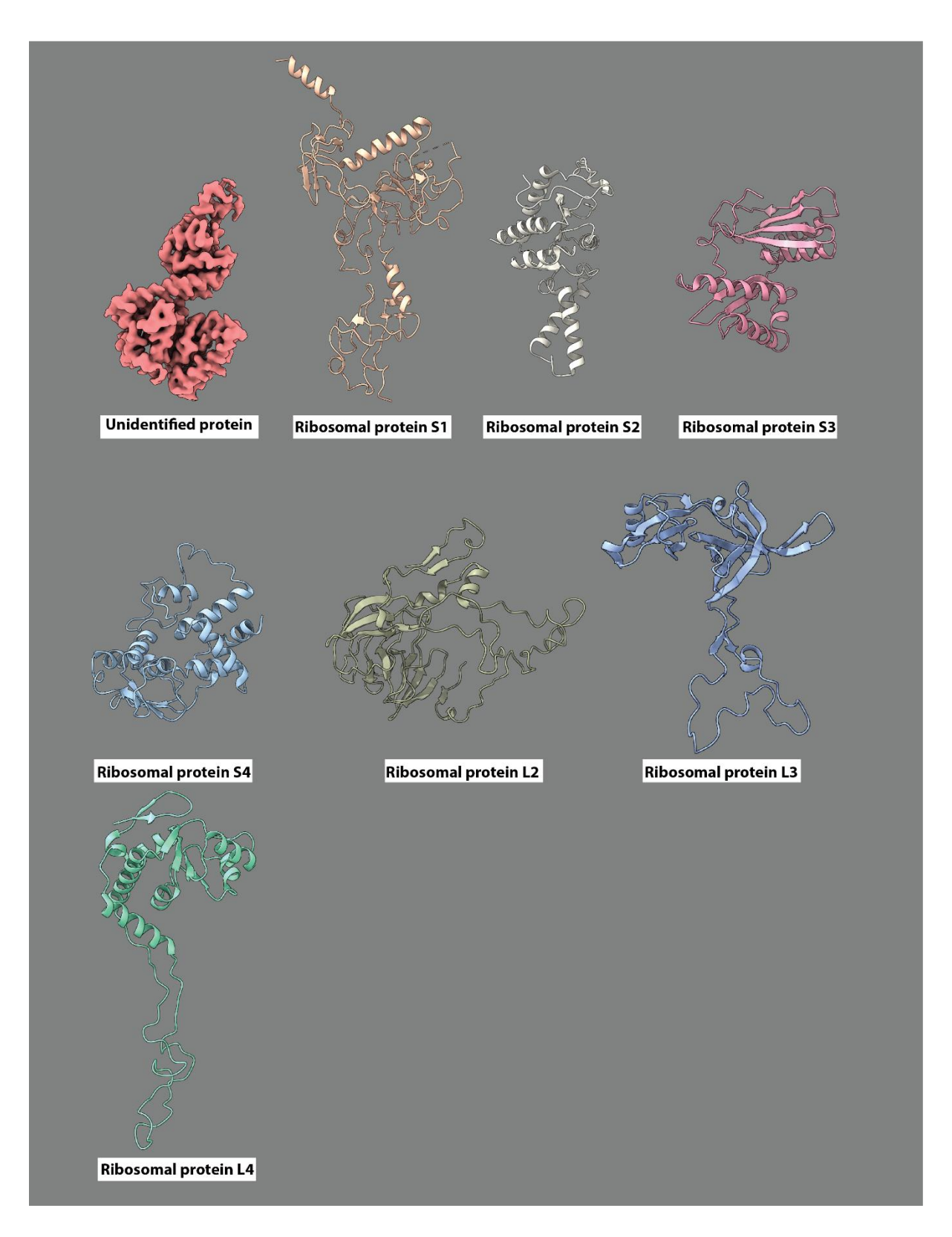
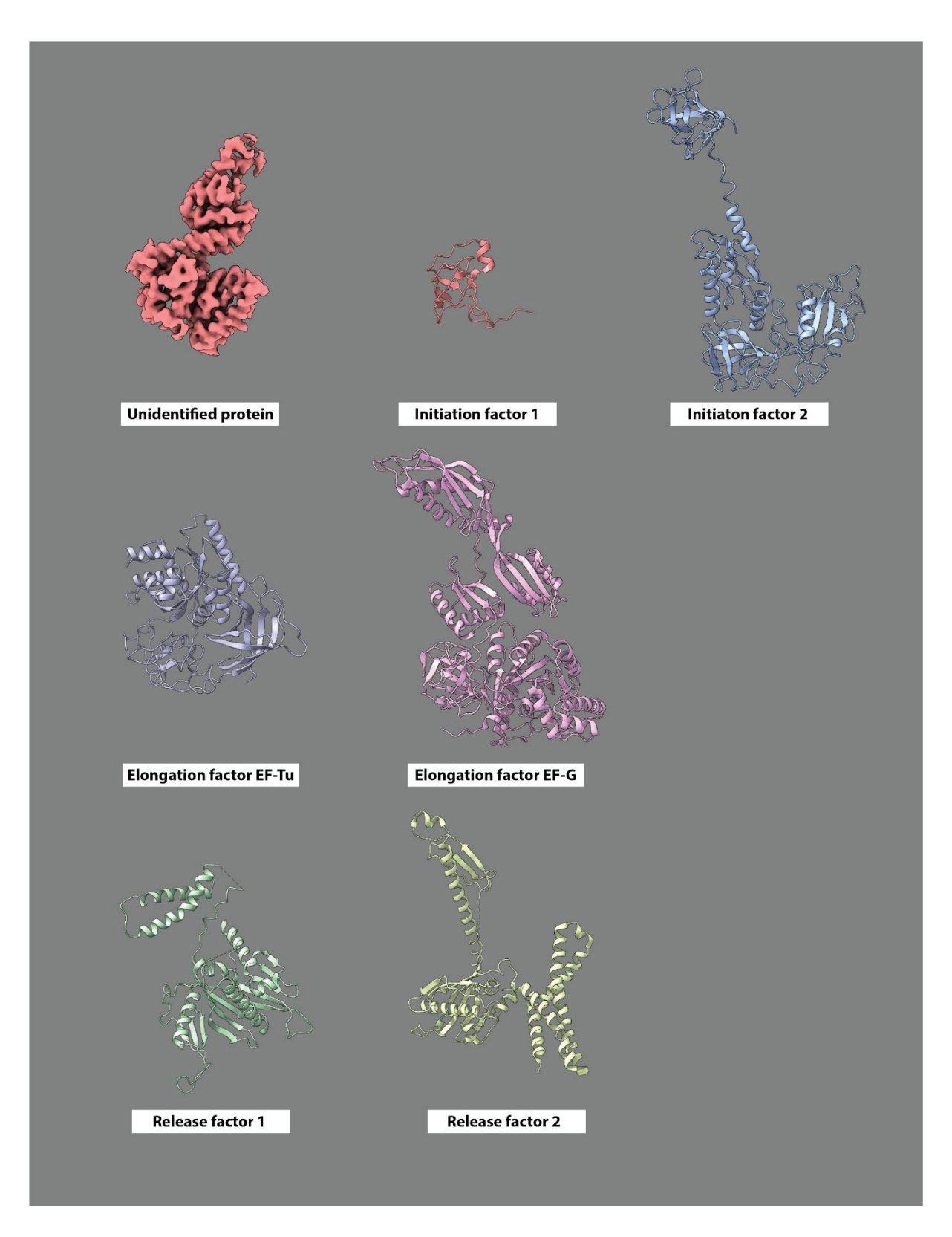


Figure 21. Comparison of protein density found in the A site of *P. urativorans* ribosomes and the structure of the largest bacterial ribosomal proteins. The density observed appeared to be larger than the average ribosomal protein. Structural comparison of the largest ribosomal proteins in *E.coli*, S1, S2, S3, S4, L2, L3, L4 (PDB 6H4N) shows no resemblance to the unidentified protein.

When comparing the overall structure of known ribosome binding molecules to the density we observed in the A site of the *P. urativorans* ribosomes, it is clear that it does not resemble any previously described molecule that has been observed in complex with the bacterial ribosome. This includes factors of translation initiation factors (e.g. IF1, IF2), and elongation (EF-Tu, EF-G) and termination factors (RF1, RF2) (**Figure 22**).



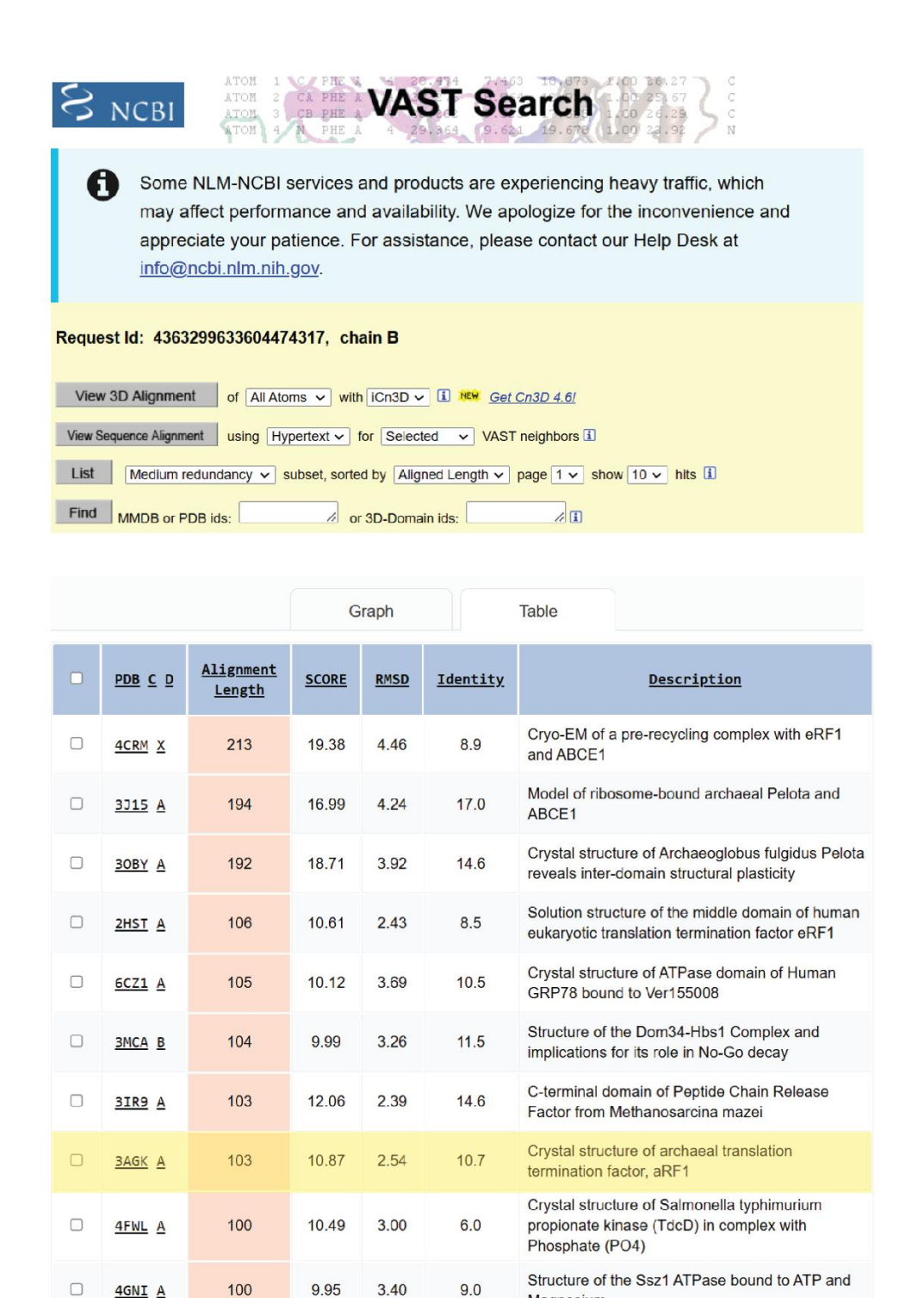
**Figure 22.** Protein ligand in the A site of *P. urativorans* ribosomes does not correspond to macromolecules known to bind bacterial ribosomes. Density of unidentified protein in *P. urativorans* ribosomes is not consistent with the overall three-dimensional structure of known ribosome binding proteins, including bacterial translation termination factors (Release factor 1: PDB 2B3T, Release factor 2: PDB 5H5U) initiation factors (Initiation factor 1 and initiation factor 2 PDB 1ZO1), elongation factors (EF-Tu, PDB: 1EFT, EF-G, PDB 4M1K).

To identify and characterise this ribosome binding protein, we first constructed a poly-Alanine model within its corresponding density in our cryo-EM map of the *P. urativorans* ribosome. This approach allowed us not only to visualize the overall three-dimensional structure of the protein based on its carbon backbone, but also to get an approximation of the size of this protein. Based on the poly-Alanine model we estimated that it is comprised of about 370 amino acids.

Next, we utilised the poly-Alanine model coordinates to search for the protein's identity and any potential homologs. Using Vast (114), a structure-based homology search tool, we compared the resulting structure with previously experimentally determined structures available in the Protein Data Bank.

Interestingly, the proteins with the highest degree of structural similarity to our unidentified protein according to our homology search analysis are ribosome binding proteins that are present only in Archaea and Eukaryotes.

Our results revealed that the aRF1 termination factor aRF1 from the archaeon *Aeropyrum pernix* exhibited the highest structural similarity to the factor observed in our cryo-EM map. The ribosome rescue factor Pelota was also identified as a structural homolog to our unidentified protein (**Figure 23**). aRF1 from *A. pernix* shares an appreciable level of structural similarity to the factor we observed in our cryo-EM maps, especially considering that these proteins are found in organisms that belong to entirely separate domains of life (**Figure 24**).



Citing VAST: Gibrat JF, Madej T, Bryant SH, "Surprising similarities in structure comparison", Curr Opin Struct Biol. 1996 Jun; 6(3):377-85.

Magnesium

Disclaimer | Write to the Help Desk NCBI | NLM | NIH

**Figure 23. Result summary of Vast structure-based homology search.** Structure-based homology search identified aRF1 from *A. pernix* (PDB 3AGK) as the most structurally similar structure on PDB to the factor we observed in cryo-EM *P. urativorans* ribosomes based on RMSD estimates. Note that while structures of human eRF1 (PDB 2HST) and peptide chain release factor in *Methanosarcina mazei* (PDB 3IR9) showed a lower RMSD than aRF1 from *A. pernix*, these structures only include one of the domains of these proteins. In contrast, the structure for aRF1 in *A. pernix* (PDB 3AGK) includes all three domains that comprise this protein.

Archaeal release factor 1 (aRF1) is a termination factor that belongs to the archaeo-eukaryotic class I release factor protein family. These proteins are responsible for stop codon recognition in mRNAs, and promote polypeptide release during termination of protein synthesis by the ribosome (152) (153). They share close evolutionary relation with the ribosome rescue factor Pelota, which is also only present in archaea and eukaryotes (154) (155). Pelota recognizes aberrant mRNAs in ribosomes that have become stalled during translation as a result of truncations or other structural defects in mRNAs (156) (157).

Given the structural similarity between Pelota (Spanish for "Ball") and our unidentified protein, we have named our protein "Balón" (also Spanish for "Ball"), by which I will refer to this protein for the remaining of my thesis.

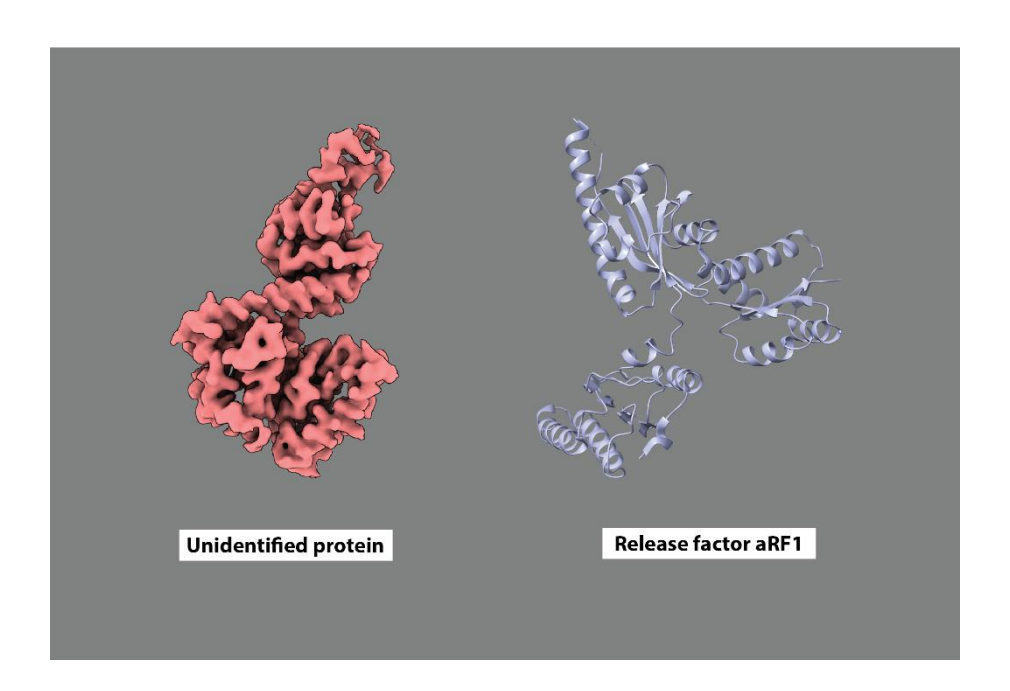


Figure 24. Structural comparison between the poly-Alanine model built into the unidentified density of the *P. urativorans* ribosomes (Balon) and aRF1. Structure-based homology search revealed that the most structurally similar protein to the ligand we observed in the *P. urativorans* ribosomes was the termination factor aRF1 from the thermophilic archaeon *A. pernix*.

To determine the precise sequence identity of Balon and its corresponding gene in *P. urativorans*, we utilized the sequence of aRF1 from *A. pernix* as an input for a sequence-guided homology search using HMMER, a Markov model-based homolog search tool (116). Our aim with this search was to identify the protein in *P. urativorans* that most closely resembled that of aRF1 in *A. pernix*. After three search iterations, we found that one of the homologs identified was a protein from *P. urativorans* which had been annotated as a hypothetical protein (Uniprot ID A0A0M3V8U3). This hypothetical protein was about the same length as we expected based on our poly-alanine model estimate with 369 amino acids in length, and had an overall structure (as predicted by AlphaFold (110)) that matched the density we observed in our cryo-EM maps (**Figure 25**). Furthermore, mass spectrometry analysis by LC/MS-MS conducted at the Centre of Excellence in Mass Spectrometry, University of York confirmed the presence of this protein in our *P. urativorans* ribosome sample (**Appendix 3**).

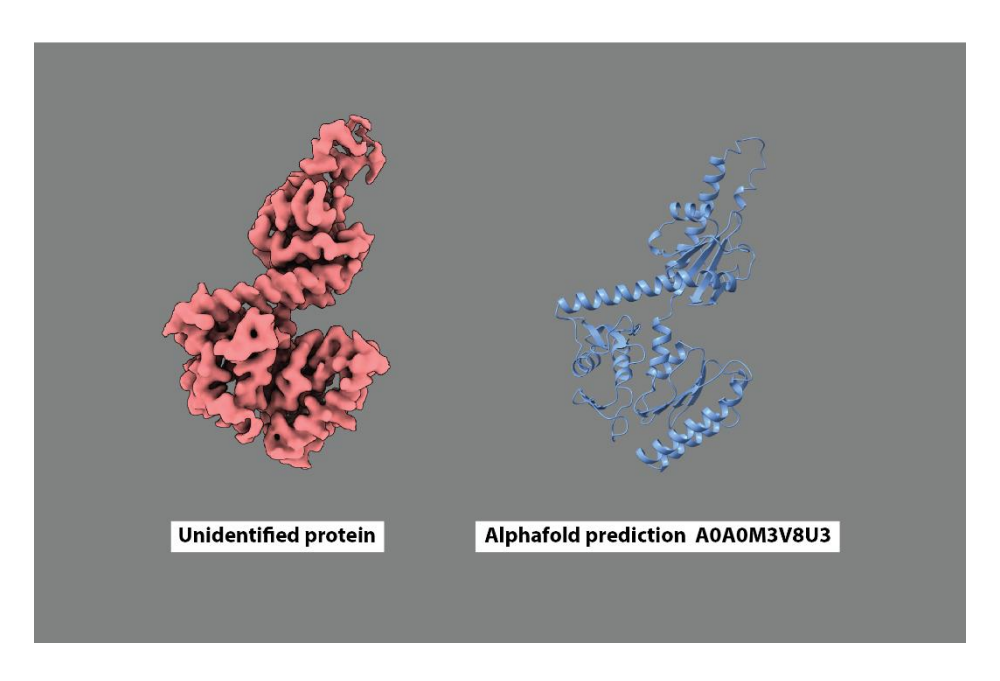


Figure 25. Structural comparison between the Balon density and the predicted structure of hypothetical protein A0A0M3V8U3 from *P. urativorans*. AlphaFold prediction of hypothetical protein identified using HMMER shows a high degree of similarity to Balon density from *P. urativorans* ribosomes.

Taken together, the homology search analysis (both structure and sequence based), as well as the mass spectrometry and structural analysis we have carried out

suggest that the identity of Balon is indeed protein A0A0M3V8U3 from *P. urativorans*. Consistent with this conclusion, our subsequent building of the atomic model of this "hypothetical protein" showed an agreement between its sequence and the Balon density in our cryo-EM map (**Figure 26**).

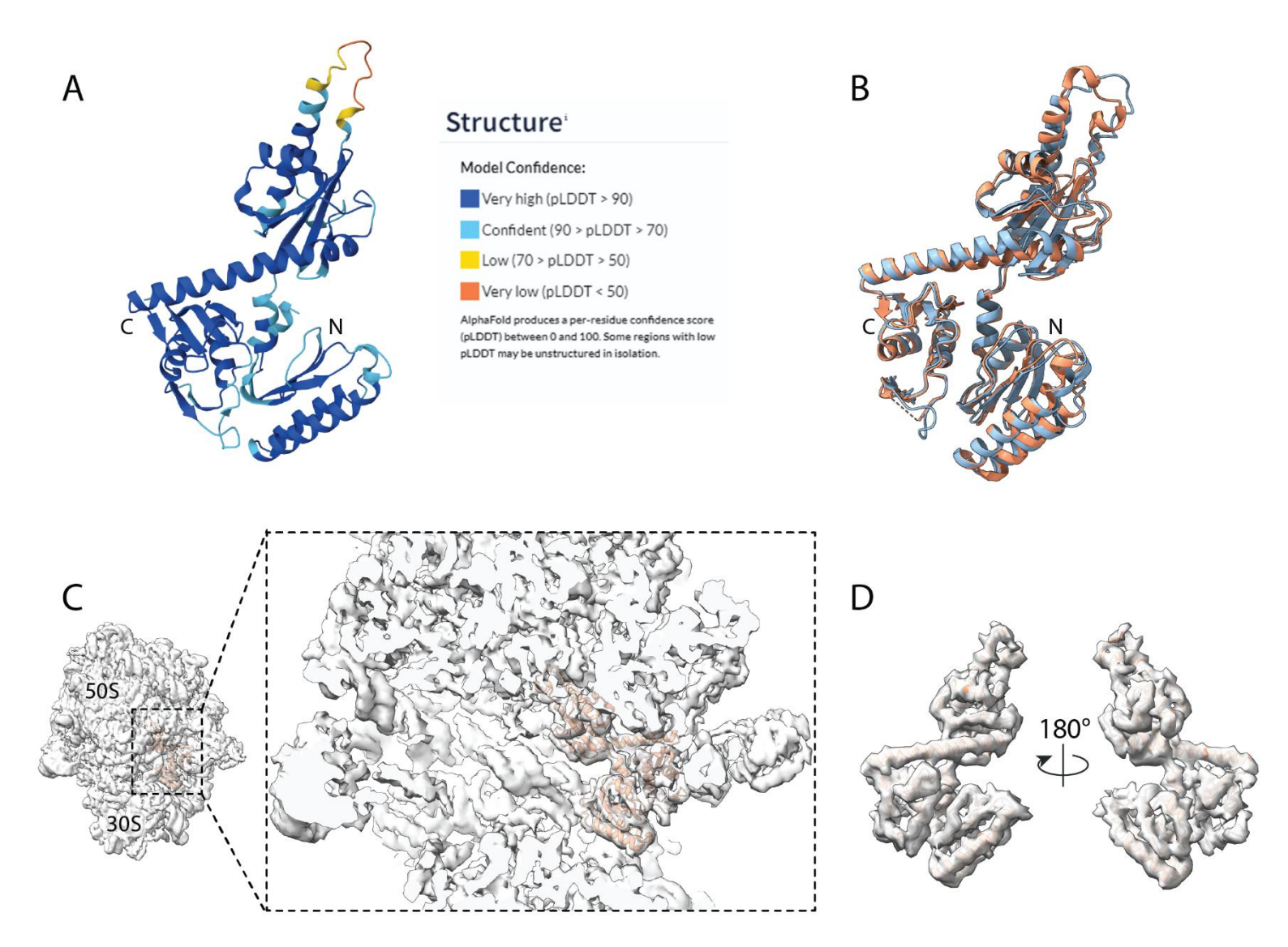


Figure 26. The identity of the protein we observed bound to our cryo-EM *P. urativorans* ribosomes is protein A0A0M3V8U3 as shown by the fit of this protein into its corresponding density. (A) AlphaFold predicted structure for protein A0A0M3V8U3. (B) AlphaFold predicted structure for protein A0A0M3V8U3 (blue) superimposed with model built for unidentified protein based on our cryo-EM map (orange). (C) Model for unidentified protein built into *P. urativorans* cryo-EM map shows the binding site of this protein. (D) Orthogonal views of the section of the cryo-EM *P. urativorans* ribosome that corresponds to unidentified protein shows in detail the overall fit of the model built for protein A0A0M3V8U3.

#### 3.4 BALON AS A RIBOSOME HIBERNATION FACTOR

After identifying the exact identity of Balon in the *P. urativorans* genome, we next asked what the function of this protein is. We first hypothesized that Balon was unlikely to be a factor of protein synthesis given the lack of structural similarity to the highly conserved bacterial translation factors as shown in the previous chapter.

When comparing Balon to its most closely related structural homologs in archaea and eukaryotes, as determined by our initial homology search, we have observed a notable pattern. Despite Balon's structural resemblance to eRF1 and Pelota, the functional sites that are present in these archaeo-eukaryotic proteins are either degenerated of absent in Balon (**Figure 27**).

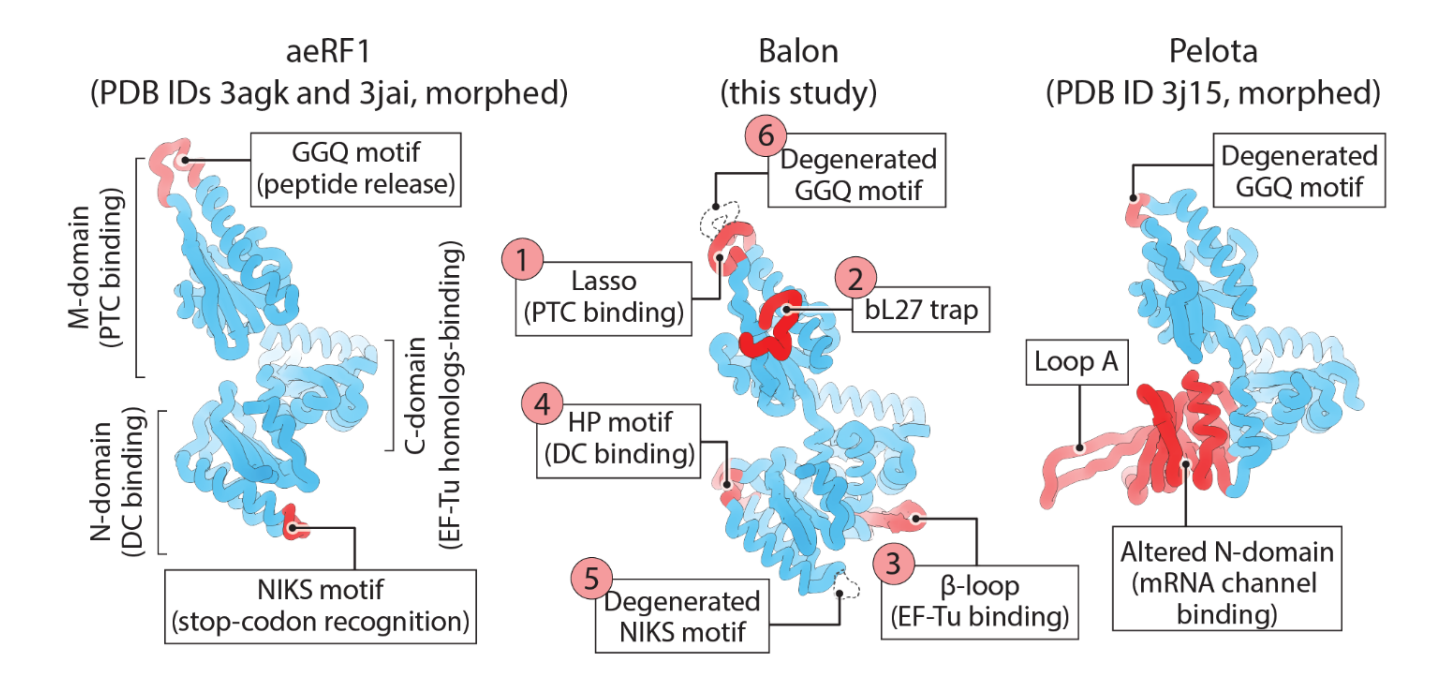


Figure 27. Balon exhibits similarities to proteins aeRF1 and Pelota, suggesting a shared evolutionary origin with the aeRF1-family of translation factors found in archaea and eukaryotes. A comparison highlights the structural resemblances between Balon, aeRF1, and Pelota. In terms of overall structure, Balon most closely resembles the translation termination factor aeRF1. It shares a similar domain organization and binds to the ribosome in a comparable manner, making contacts with the protein synthesis factor EF-Tu, as well as the active sites of the ribosome, such as the decoding centre (DC), and the peptidyl-transferase centre (PTC). However, Balon lacks essential structural elements necessary for aeRF1 activity,

such as the NIKS motif for stop-codon recognition and the GGQ motif for nascent peptide release. These functional motifs are highlighted in red. These functional motifs are highlighted in red. The red shade indicates different functional motifs within the proteins depicted in the figure (for instance the NIKS and GGQ motifs in eRF1 or the HP motif in Balon). The different shades of blue are shown to convey a better sense of volume for aesthetic purposes.

The eukaryotic translation termination factor eRF1 possesses two main sites that are critical to its role during protein synthesis, the so-called NIKS motif and GGQ motif. The NIKS motif (named after the highly conserved 4 amino acid sequence in the N-terminal domain of eRF1) is responsible for mRNA stop codon recognition (158) (159). Mutations of the NIKS motif lead to a decrease in stop codon recognition specificity and translation termination efficiency *in vitro* (160) (161). The GGQ motif, is located in the middle domain of eRF1, and is responsible for nascent peptide release (161). Mutations in this GGQ motif also lead to decrease activity of eRF1 by reducing the catalytic activity of this factor (162).

The second apparent homolog of Balon, archaeal ribosome rescue factor Pelota, possesses a  $\beta$ -loop motif in its N-terminal domain that allows it to bind the vacant A site in the mRNA channel when ribosomes become stalled during protein synthesis due to aberrant mRNAs, which include mRNAs that are truncated, lack a stop codon, or contain stable secondary structures that prevent ribosomal translation (163) (164).

Our analysis showed that, in contrast to eRF1, Balon does not possess the NIKS or GGQ motifs, suggesting that unlike eRF1, Balon is unable to recognize stop codons or promote peptide release. Instead, the middle domain of Balon bears a lasso-like protein loop that makes a direct contact around nucleotide A2602 in the 23S rRNA. This interaction positions Balon next to the outer wall of the PTC (**Figure 28C**). In this position, Balon remains excluded from the catalytic centre by the 23S rRNA residue U2585 and is therefore unable to reach the nascent peptide, further supporting the idea that the function of Balon is unlikely to catalyse termination of protein synthesis similarly to eRF1.

We also found that, in its N-terminal domain, Balon has what we have termed the HP-motif. This motif directly binds the decoding centre of the ribosome at residues

A1492 in helix h44, and A1913 in helix H69 ( $E.\ coli$  rRNA numbering) (**Figure 28B**). These interactions with the decoding centre allow Balon to stay about 10 Å away from the mRNA-binding site. This lack of contacts with the mRNA-binding site distinguishes Balon from Dom34 (Pelota's eukaryotic homolog) which directly contacts the mRNA channel with its  $\beta$ -loop when in complex with the ribosome (165).

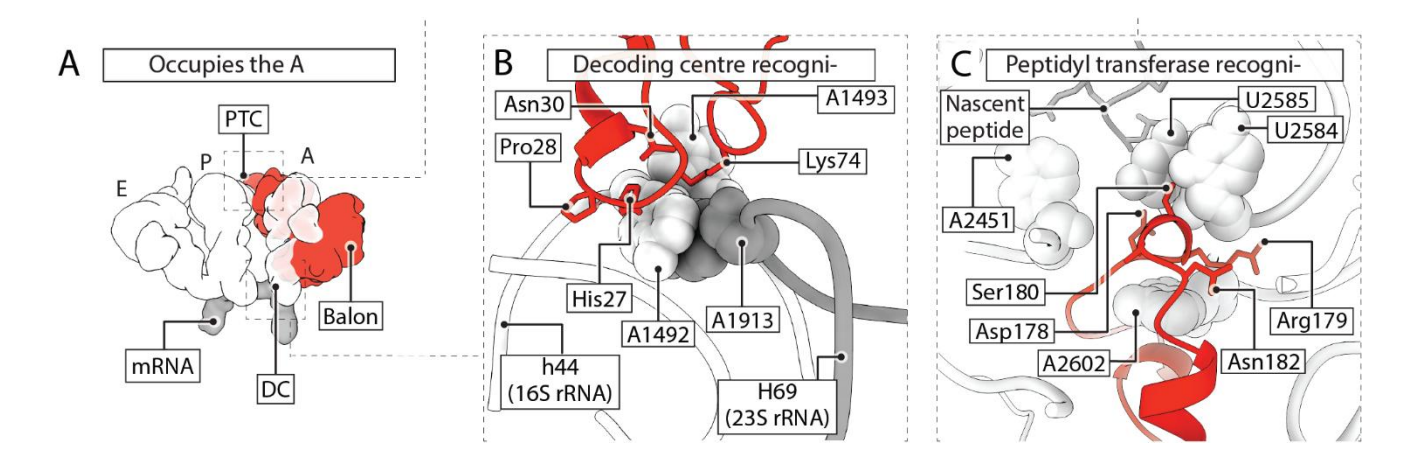
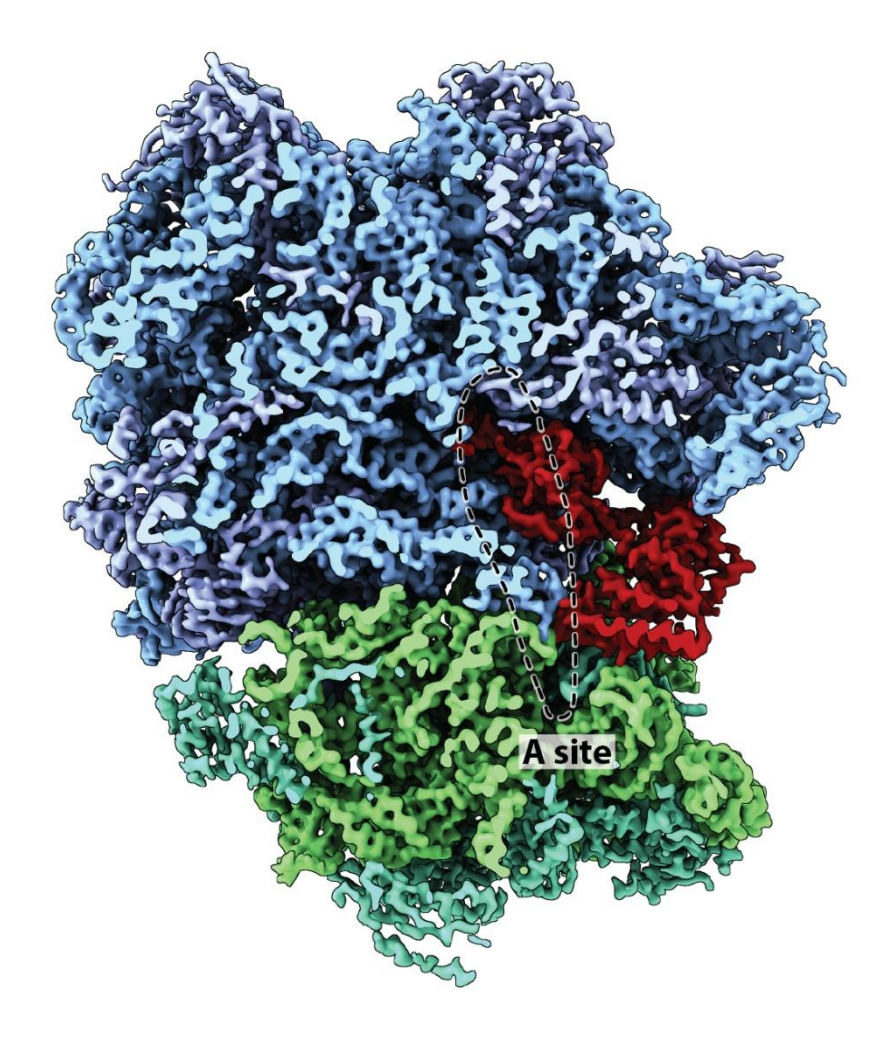


Figure 28. Balon's interactions with the ribosome is inconsistent with ribosome rescue and translation termination. (A) Superposition of Balon, tRNAs (labelled as E,P,A) and mRNA shows Balon's location relative to factors of protein synthesis. Zoomed in views of Balon in complex with the ribosome shows the binding of the HP motif to the decoding centre (B), and the interactions between the lasso loop of Balon and the residues in the vicinity of the PTC (C) illustrating in detail how Balon remains excluded from the mRNA channel and the PTC.

Once we had ruled out the possibility of Balon being a factor that supports ribosomal protein synthesis, we have proposed the following hypothesis: what if, rather than being a factor of protein synthesis, Balon plays the exact opposite function by serving as a ribosome hibernation factor?

Initially, this idea stemmed primarily from Balon's localization within the ribosome. Our cryo-EM map showed that Balon occupied most of the ribosomal A site, leaving virtually no space for translation factors to be recruited to the ribosome (**Figure 29**). In other words, Balon binding to the ribosome is incompatible with protein synthesis, which requires the ribosomal A site to be vacant to accommodate translation factors.



**Figure 29. Balon binding occludes the A site of the ribosome.** Cryo-EM map of *P. urativorans* ribosomes show that Balon (shown in red) binds at the ribosomal A site (shown with a dashed line). The A site extends along the interface of the small ribosomal subunit (green) and the large ribosomal subunit (blue). The presence of Balon at the A site prevents concurrent binding with translation factors in this active centre of the ribosome.

Aside from the structural evidence, our idea that Balon may serve as a repressor rather than participant of protein synthesis was consistent with the translational state of *P. urativorans* cells as suggested by our polysome profiling results shown in **Figure 14**. After exposing the cells to ice, thereby causing a sharp decrease in temperature, the polysome fraction (composed of actively translating ribosomes) becomes barely detectable, while monosomes (that likely correspond to non-translating ribosomes) become the dominant fraction in cold-shocked *P. urativorans*. This shift in the relative

ratio of polysomes to monosomes suggests a halt of protein synthesis, which is a major hallmark of ribosome hibernation.

In addition to the polysome profiling results, we found a third piece of evidence supporting our hypothesis that our *P. urativorans* ribosomes were in a hibernating state: the presence of protein RaiA in the P site. As mentioned in the introduction section, RaiA is a hibernation factor found across the bacterial tree of life that elicits a state of hibernation of monomeric (also known as 70S) ribosomes. Previously, concurrent binding of two hibernation factors to the ribosome has been well documented in the literature, especially in the case of gammaproteobacterial. These species rely on the simultaneous binding of hibernation factors RMF and HPF to the ribosome, leading to the formation of hibernating ribosome dimers (known as 100S ribosomes) (73).

Furthermore, our collaborators used *in vitro* translation experiments to show that Balon homologs in *M. tuberculosis* and *M. smegmatis* inhibit protein synthesis to comparable levels as hibernation factor RaiA, consistent with the idea that Balon is a *bona fide* ribosome hibernation factor (31).

In addition to Balon's incompatibility with protein synthesis due to the occlusion of active centres of the *P. urativorans* ribosome, there are other characteristics of this protein that are consistent with that of other previously identified hibernation factors.

### 3.5 THE BALON ENCODING GENE AND ITS PHYLOGENETIC AND GENOMIC LOCALIZATION

To obtain some information of the conditions under which the Balon coding gene might be expressed we decided to investigate the genomic localization of this gene across the bacterial tree of life.

In *P. urativorans* Balon is encoded by gene AOC03\_06830, which is located in the only chromosome of *P. urativorans* within nucleotides 1,582,434 to 1,583,543 and is comprised of 1,100 base pairs. This gene sits in close proximity to genes encoding for other proteins annotated as hypothetical proteins and DNA repair protein A0A0M3V901.

Next, we expanded our search to analyse the distribution and conservation of the Balon coding gene across the bacterial domain. To accomplish this, we used the homology search tool HMMER to conduct a Markov model-based homology search using UniProt as our proteomes reference source.

Interestingly, we observed the absence of Balon homologs in some of the most common bacterial model organisms, such as *E. coli*, and *S. aureus*. This may help explain why this Balon had remained undiscovered until now as ribosome hibernation studies in bacteria are dominated by a limited number of model organisms, most notably *E. coli*.

It is important to note that no Balon homologs were found in mitochondria. While one may hypothesize that there may be Balon homologs in mitochondria given the ancient proteobacterial origin of this eukaryotic organelle (166), our sequence-based homology analysis did not detect any Balon homologs outside the bacterial domain, including possible mitochondrial homologs. Interestingly, despite the evolutionary relationship between bacteria and mitochondria, it is estimated that approximately 40% of the mitochondrial proteins have no detectable prokaryotic homologs, with only 20-30% of the mitochondrial proteome having phylogenetic links to the proteobacteria (167). Nonetheless, the possibility of a Balon homolog in

mitochondria cannot be fully ruled out, however answering this question would warrant its own dedicated study.

Our homology search identified Balon homologs in 1,572 out of 8,761 representative bacteria used for this analysis, spanning 23 out of 27 major bacterial phyla (**Figure 30**), representing about 20% of all known bacterial species with a sequenced genome. These included many widely studied microorganisms, such as *T. thermophilus*, and *M. smegmatis* as well as human pathogens like *M. tuberculosis*. (**Appendix 4**). In *M. tuberculosis* and *M. smegmatis*, the Balon homologues Rv2629 and Msmeg1130 are transcriptionally induced in response to hypoxia, leading to increased survival rates and pathogenicity (168),(86),(169).

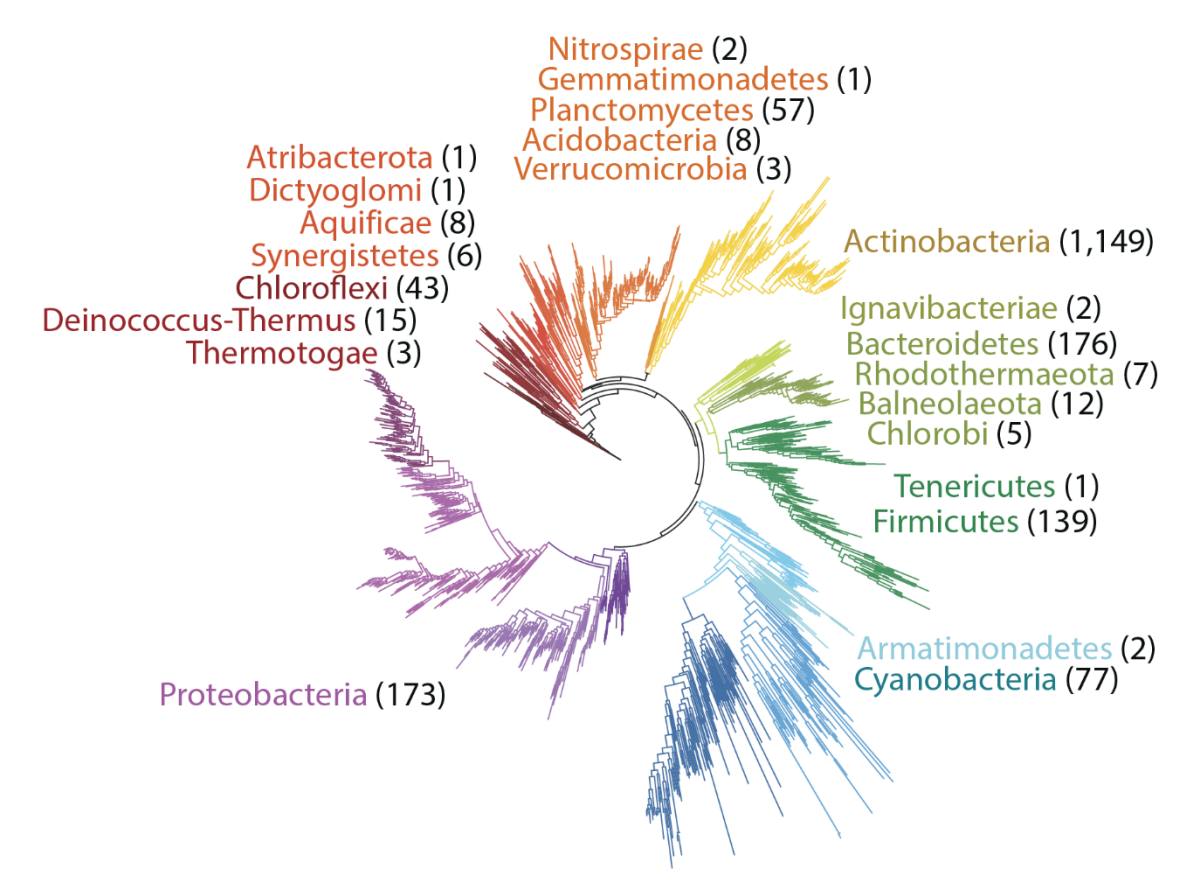


**Figure 30. Balon-coding genes are widespread among bacteria.** The bacterial tree of life coloured by phyla shows that Balon homologs are found in most bacterial lineages. We estimate that Balon is present in 23 different phyla, encompassing 1,572 representative bacteria, which is approximately 20% of all known bacteria.

We next looked for the presence of other hibernation factor coding genes in those species where we detected a Balon homolog. We found that all of the genomes that carry a gene for Balon also carry a gene for the hibernation factor RaiA or its homolog HPF (**Appendix 5**), but almost none of them also encode the hibernation factor RMF (**Appendix 6**): only 0.2% of representative bacteria simultaneously possess genes for Balon, RMF and RaiA. This suggests that Balon and RaiA could potentially bind the ribosome concurrently in other bacterial species as we observed in our cryo-EM maps of the *P. urativorans* ribosome.

It is worth noting that our homology search was restricted to proteins with a length of at least 300 amino acids to avoid overestimating the number of bacterial species with a detectable Balon homolog, and to only include in our analysis those proteins that are more likely to resemble the structure we observe in our cryo-EM maps. However, our HMMER search did initially detect Balon homologs with proteins with less than 300 residues. One notable example of this is YocB, a Balon homolog in *B. subtilis* that has been reported to be transcriptionally induced during stationary phase as well as heat and cold shock (170). YocB is only 260 amino acids long and according to its AlphaFold structure prediction it lacks the middle domain that is present in *P. urativorans*, however its N and C terminal domains do closely resemble the overall structure of Balon in *P. urativorans* (**Figure 31**).

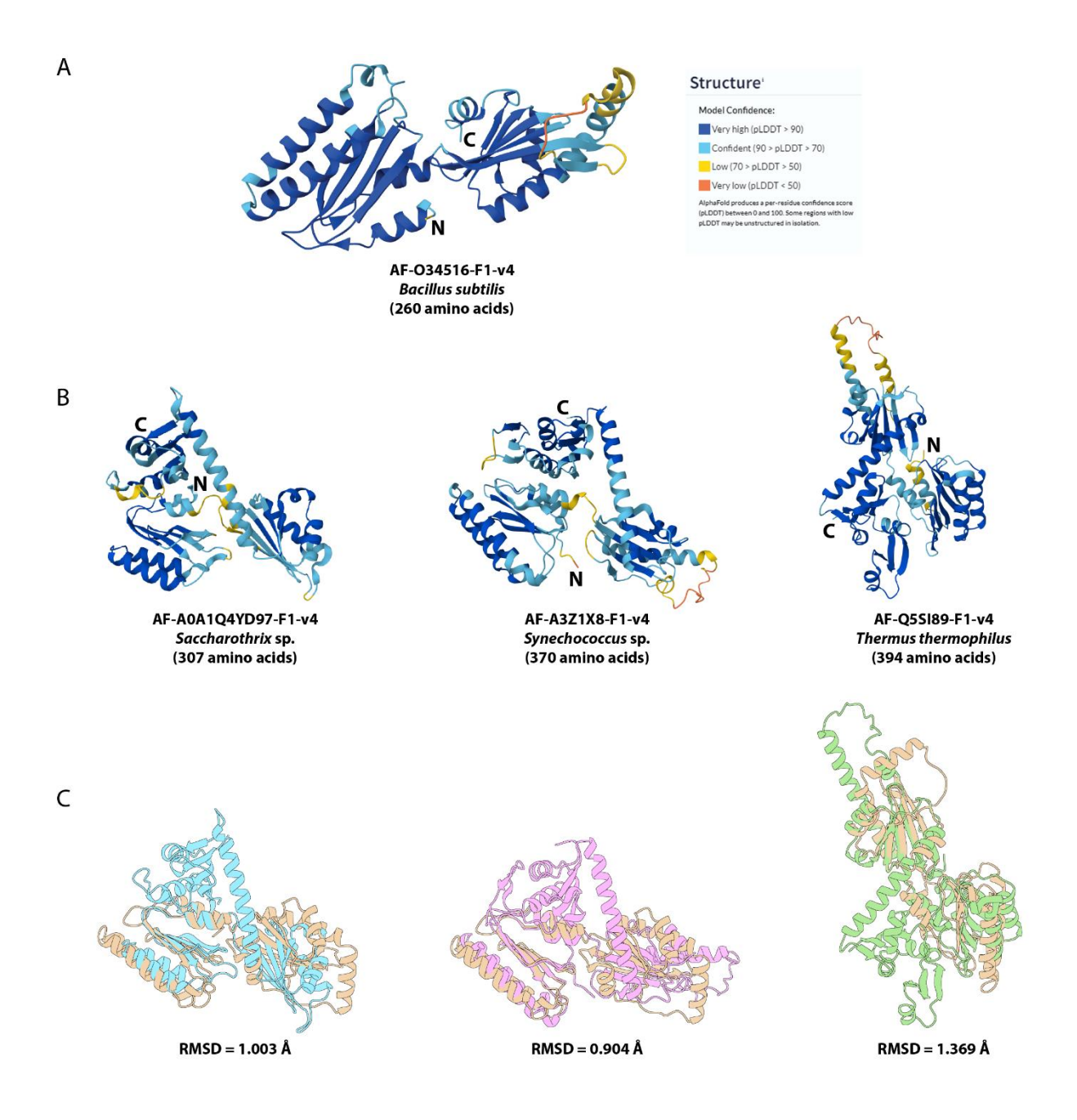


Figure 31. Comparison of AlphaFold-predicted structures of proteins detected in our homology search reveal similarity among Balon homologs in bacterial species across different phyla. (A) AlphaFold prediction of YocB, a Balon homolog in *B. subtilis*. (B) AlphaFold predicted structures of Balon homologs in *Saccharothrix* sp. (Actinobacteria), *Synechococcus* sp. (Cyanobacteria) and *T. thermophilus* (*Deinococcus-Thermus*). (C) Superimposed predicted structures of YocB (yellow) and Balon homologs in *Saccharothrix* sp. (cyan), *Synechococcus* sp. (pink), and *T. thermophilus* (green).

Proteins that were detected in our homology search which do have a comparable length to Balon in *P. urativorans* (360-420 amino acids) possessed only

about a 10% sequence conservation. However, they did present some common features at the level of sequence that could be of structural significance as we observed in our cryo-EM maps. Specifically, these homologs lack the GGQ (161) (171) and NIKS/NIKL (172) (173) motifs of archaeal and eukaryotic aeRF1 family members (**Figure 32**), suggesting that these proteins may not be involved in protein synthesis termination or ribosome rescue, and could potentially be more functionally similar to Balon than to aerF1 and Pelota, despite the structural similarity between these three protein families.

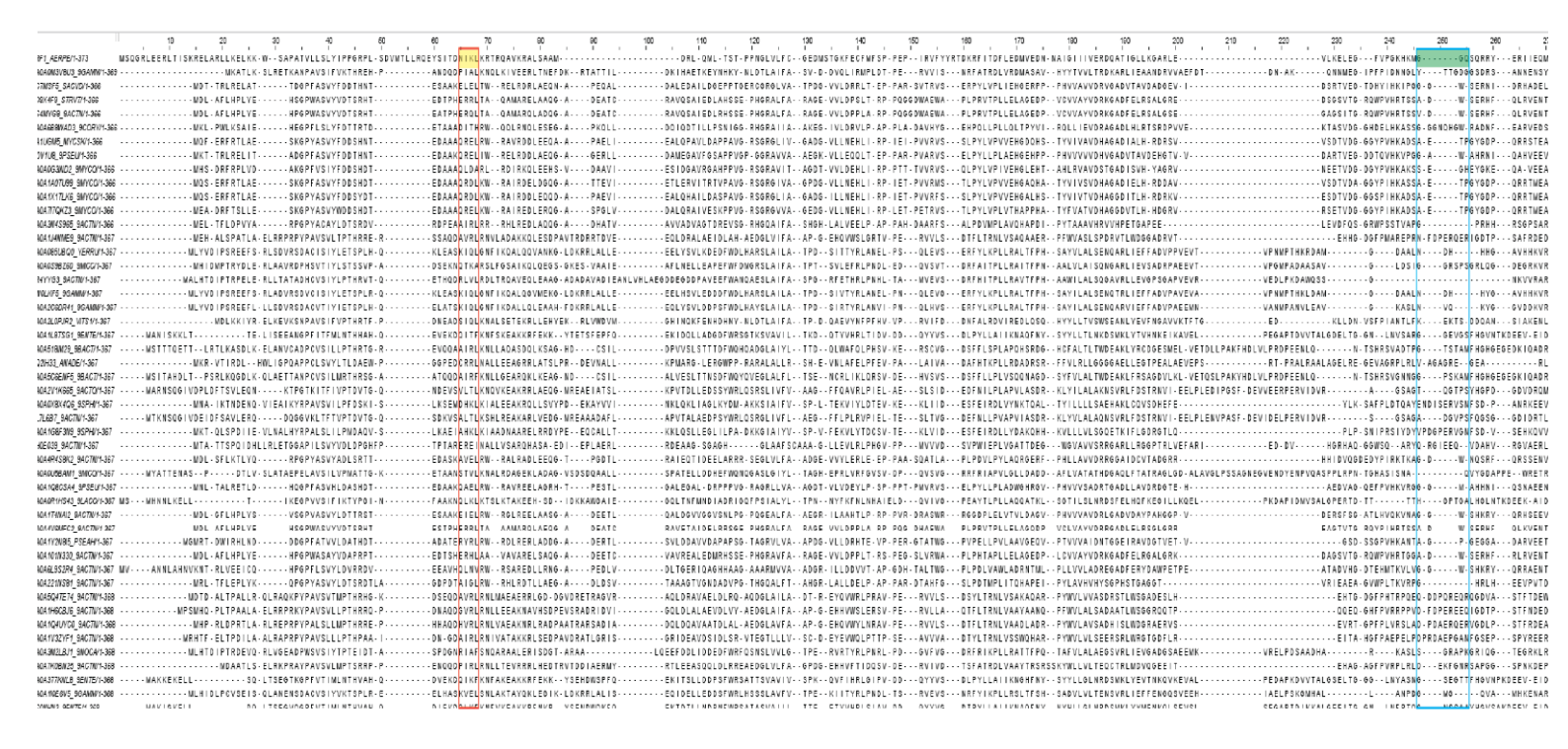


Figure 32. Balon homologs lack conservation of functional motifs present in aeRF1. Sequence alignment of aRF1 in *A. pernix* (top sequence), Balon in *P. urativorans* (2nd sequence), and Balon homologs in bacteria (remaining sequences) show that the NIKL motif in aRF1 from *A. pernix* (yellow) is mutated in Balon (red). Likewise, the GGQ motif in aRF1 from *A. pernix* (green) is degenerated in Balon (blue).

Another feature that is conserved in all Balon homologs detected is the HP motif, which in our Balon structure directly interacts with one of the most critical active centres of the ribosome, the decoding centre. This suggests that the HP motif may be particularly important in mediating Balon binding to the ribosome, explaining its high degree of conservation despite the high sequence variability among Balon homologs. In fact, when we analysed which residues show the highest degree of conservation across Balon homologs, it became clear that the most conserved residues are those that are involved in Balon binding to the ribosome as shown in our cryo-EM maps (Figure 33). This suggests that the function of Balon is similar to that of previously described hibernation factors such as RaiA, which show a low degree of sequence similarity across species and simply act as "molecular plugs" of vacant ribosomal active centres.

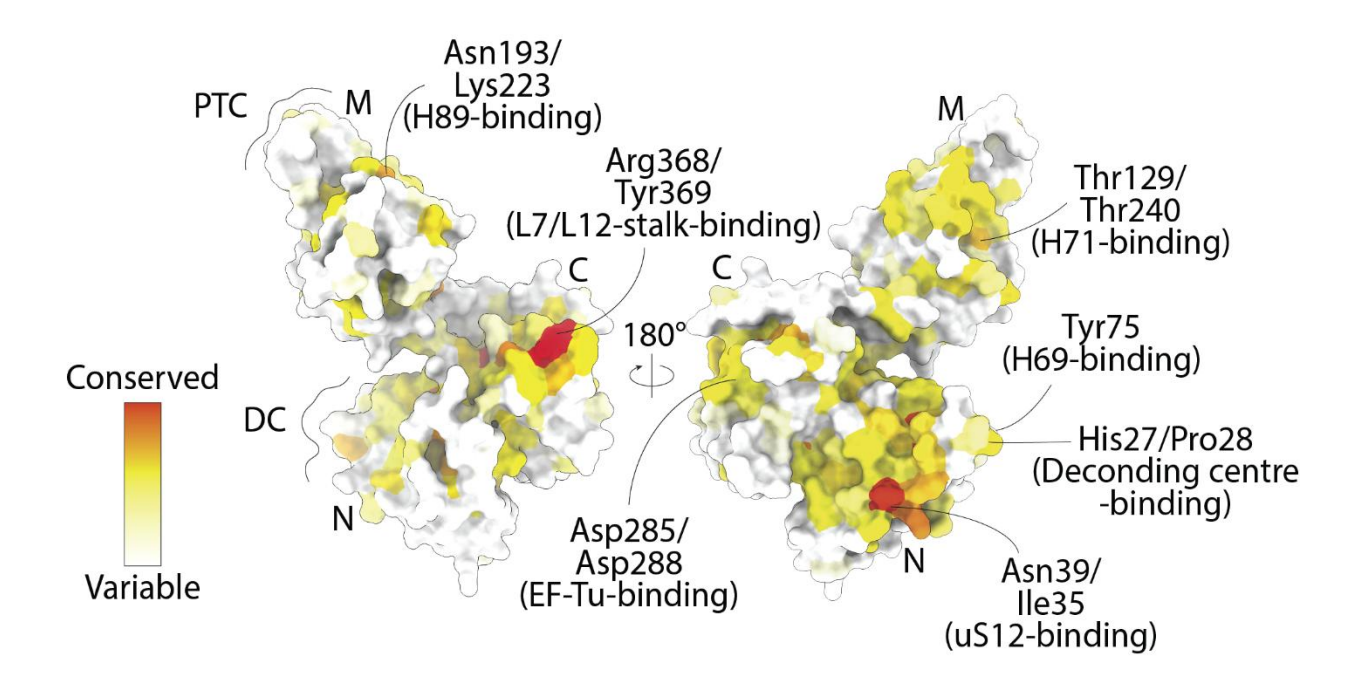


Figure 33. Atomic model of Balon (coloured by sequence conservation) illustrates high conservation of residues responsible for ribosome recognition. Sequence conservation analysis of Balon in bacterial species (1,571 sequences) shows that Balon (similar to other previously known hibernation factors) has a low level of conservation even among closely related organisms. However, residues involved in ribosome recognition and binding are almost immutable across the bacterial domain.

We next proceeded to analyse the genomic context of genes encoding Balon. We found that the Balon encoding gene is surrounded by a wide variety of genes ((**Figure 34**, **Methods section 2.9**), and that it is typically found within operons that also encode stress response factors. These factors include the ribosome hibernation factor RaiA, as well as factors related to thermal shock (e.g., Hsp20) (174), osmotic stress (e.g., OsmC, OsmY) (175) (176), acid stress (e.g., HdeD) (177), response to antibiotics (e.g., EmrB) (178), and factors involved in ribosome repair from nucleolytic damage (RtcB) (179) (180) (181) (**Figure 34**).

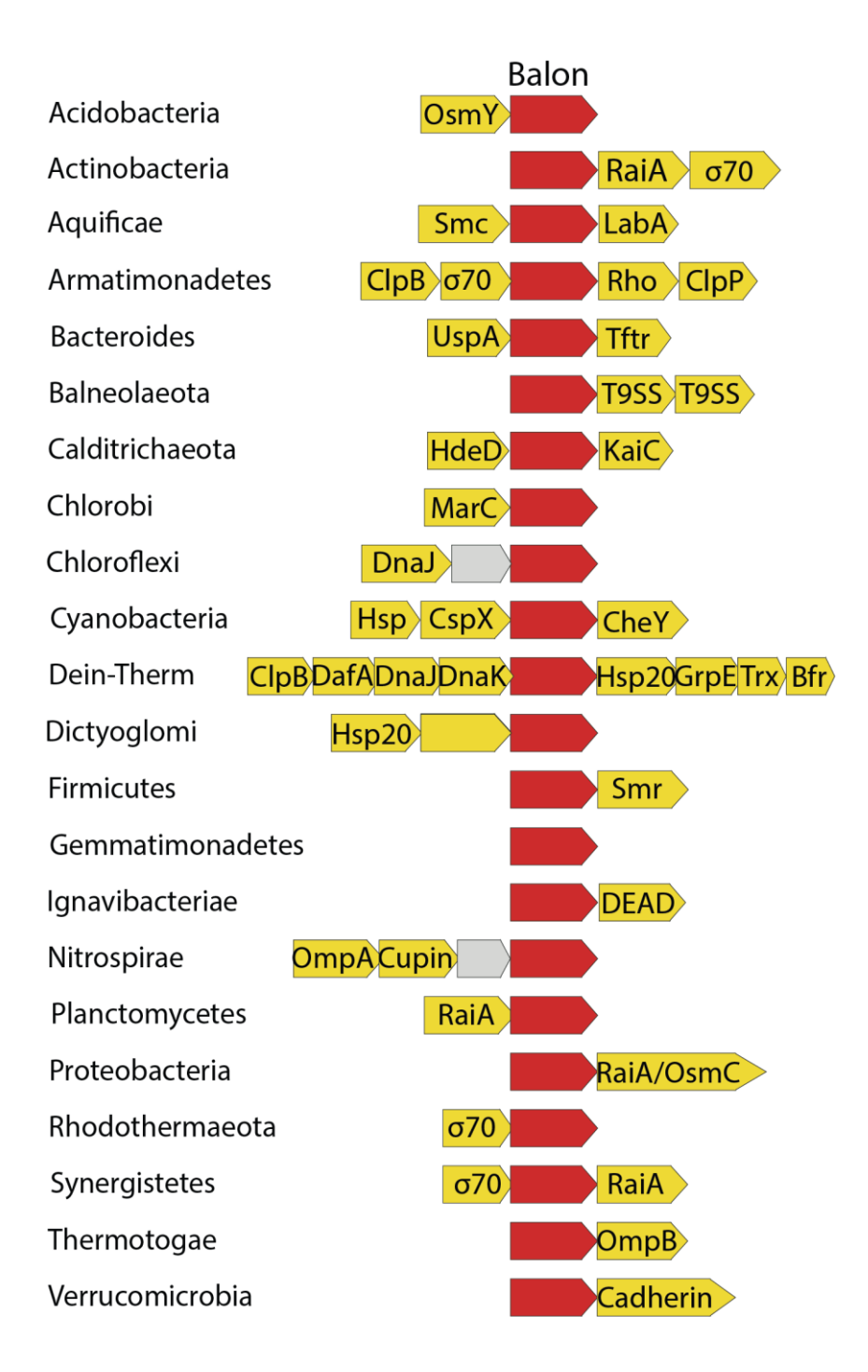


Figure 34. Balon is often encoded within stress response operons. The genetic arrangement of Balon-coding genes (depicted in orange) in selected bacterial phyla is illustrated through operon schematics. Balon-coding genes are typically found within operons that also encode stress response factors (shown in yellow). The genes of unknown function are shown in grey. These stress response factors encompass various proteins involved in heat- and cold-shock responses, such as chaperones like Hsp20, DnaK, and DnaJ. Additionally, the operons include factors related to acid tolerance (HdeD), osmotic stress tolerance (OsmB and OsmY), ribosome hibernation (RaiA), ribosome and tRNA repair (RtcB), as well as multidrug resistance proteins (Smr, MarC, EmrB).

Interestingly, we also observed that many bacterial species (603 representative species) possess multiple copies of Balon genes within their genomes, ranging from 2 to 4 copies (**Figure 35A**). For instance, species like Mycobacterium possess up to four copies of Balon-like genes. Notably, one of these genes is located near the hypoxiaresponse factor Hrp1 (182) (183), while another is adjacent to the gene encoding the multidrug transporter EmpB (184) (**Figure 35B**). Collectively, these findings suggest that Balon might serve as a stress-response protein utilized by a diverse range of bacterial species, and that its role in ribosome hibernation is not limited to cold stress.

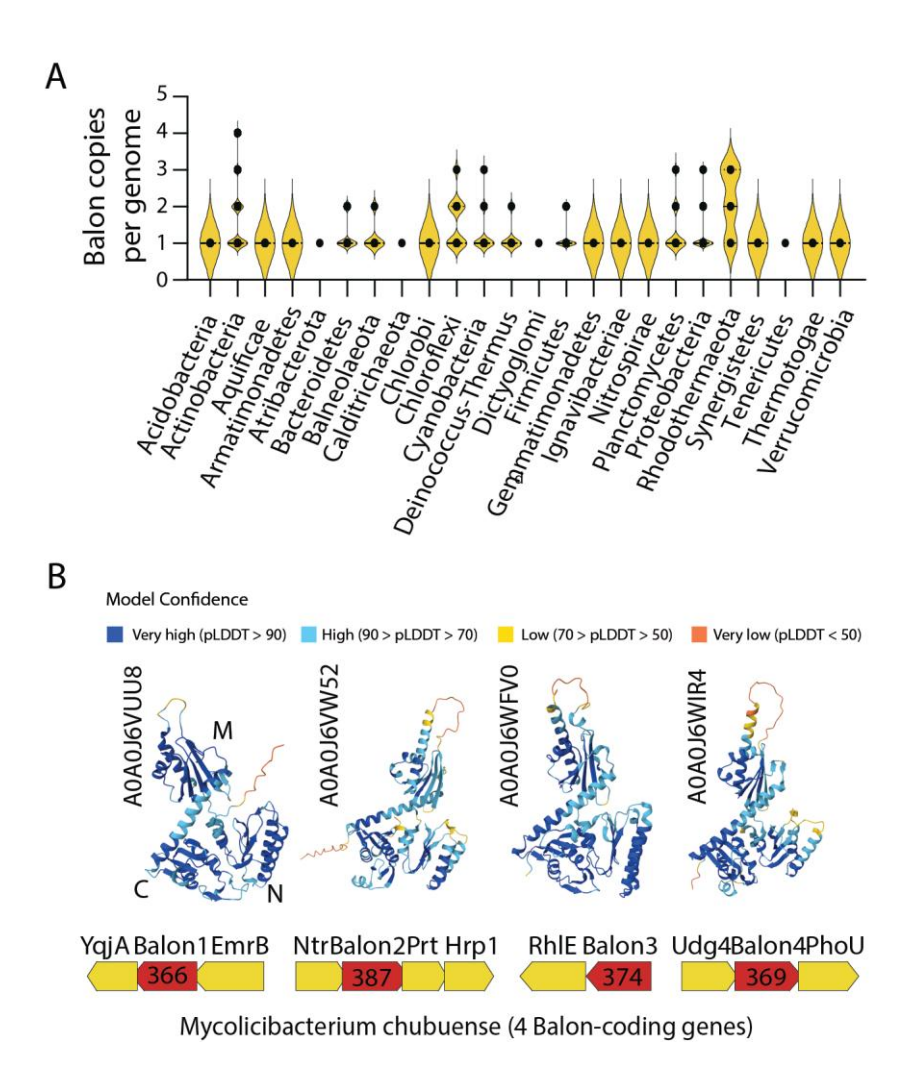
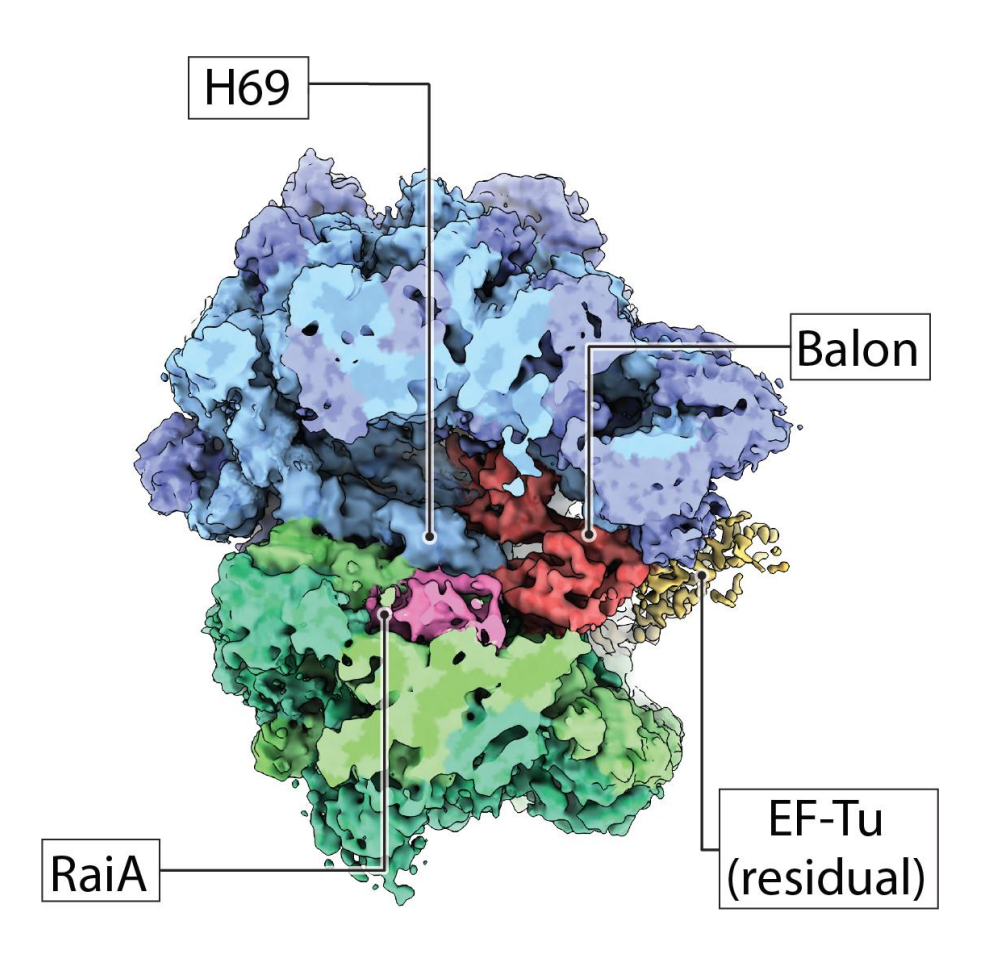


Figure 35. Bacteria may be able to express different isoforms of Balon under distinct environmental conditions. (A) In 38% of the bacterial species analysed (603 species), Balon homologs are encoded by two, three or four gene copies located in different genomic loci, suggesting their independent expression. (B) An example of the human pathogen *Mycolicibacterium chubuense* shows four copies of Balon-coding genes (protein length shown in red arrows), with one copy (Balon 1) residing in an operon with the multidrug export protein EmrB, and another copy (Balon 2) located in an operon with hypoxia-response factors. The structures (predicted by Alphafold), although similar, possess variations relative to each other.

#### 3.6 BALON BINDING TO THE RIBOSOME IS NOT LIMITED TO COLD SHOCK

To test our hypothesis that Balon binding to the ribosome is not limited to cold stress we decided to use cryo-EM to analyse ribosomes obtained from P. urativorans cells in stationary phase. To achieve this, we cultured P. urativorans at its optimal growth temperature and allowed the culture to naturally transition to stationary phase over the course of 4 days. When the culture showed no detectable signs of growth (at an  $OD_{600}$  of 1.5) we collected the cells and isolated the ribosomes as done previously, except that for this sample the cells were not exposed to ice.

After collecting and analysing the cryo-EM data we obtained a 5 Å resolution cryo-EM map of the stationary phase *P. urativorans* ribosome as shown in **Figure 36**.



**Figure 36. Balon binds the ribosome during stationary phase.** Cryo-EM map of resting *P. urativorans* cells reveals that stationary phase elicits binding to the ribosome.

When analysing the cryo-EM map it became evident that Balon was indeed bound to the A site of stationary phase *P. urativorans* ribosomes just as with the cold-shocked ribosomes. Focussed classification analysis of Balon to the ribosomes revealed that most/virtually all were bound to Balon (31), suggesting that Balon binding to the ribosome may be the primary mechanism of ribosome hibernation in *P. urativorans* during stationary phase.

In addition, we also observed clear density of the hibernation factor RaiA in the so-called P site, the active centre of the ribosome where peptide bonds are formed during protein synthesis. This indicates that these ribosomes are inactive as expected from stationary phase cells. It is worth noting that the ribosomes purified from cold shocked cells were also primarily bound to Balon in the A site, and RaiA in the P site. Whether or not both factors are essential for ribosomes to transition to a hibernating state *in vivo* remains unclear. However, concurrent binding of both Balon and RaiA under different stress conditions seems to suggest that *P. urativorans* relies on binding of both proteins to make two of the most important active centres of the ribosome inaccessible to translation factors and enter hibernation.

Another possibility is that the binding of both RaiA in addition to Balon does not aim solely to stop protein synthesis but to protect specific sites of ribosomal RNA from degradation. It is known that during stress mutant *E. coli* cells that lack hibernation factors not only show slower rates of recovery and survival, but also present detectable levels of degradation in their ribosomal RNA by endonucleases. It has been shown that one of the sites where 16S rRNA is cleaved by these endonucleases is in close proximity to the binding site of RaiA (84). If we take into account the fact that Balon alone is capable of inhibiting protein synthesis *in vitro* (31) and that Balon binding to the ribosome is incompatible with translation, the hypothesis that during stress *P. urativorans* ribosomes binds to both Balon and RaiA not necessarily to stop translation but to protect ribosomal RNA seems more likely. What is clear, however, is that RaiA seems to be a key player in Balon mediated ribosome hibernation as suggested by the absolute conservation of RaiA in bacterial species with detectable Balon homologs as discussed in the previous chapter, and as shown by the cryo-EM maps of hibernating *P. urativorans* ribosomes during cold shock and stationary phase.

# CHAPTER 4: DIFFERENT MODES OF RIBOSOME HIBERNATION

#### 4.1 BINDING STATES OF THE HIBERNATING P. URATIVORANS RIBOSOME

Our analysis of the cryo-EM maps of ribosomes from cold-shocked cells of *P. urativorans* revealed that one of the ribosomal active sites, the P site, contained some weaker density that corresponded to more than one ligand. The strength and the shape of this signal suggested that the P site was partially occupied by overlapping and mutually exclusive ligands.

To determine what additional ligands associate with the Balon-bound ribosomes we decided to conduct a focused classification analysis in order to separate our "average" cryo-EM map of P. urativorans ribosomes into different functional substates. First, by focusing on the Balon-binding site, we revealed two important pieces of information. First, that approximately 98% of the ribosome particles in our sample were associated with Balon (31), indicating that the majority of cellular ribosomes in cold-shocked bacteria associate with this apparent hibernation factor. Secondly, by focusing on the ribosomal P site, we found that our sample comprised two distinct functional states of the ribosome, as shown in **Figure 37**.

The first state, corresponding to 63% of ribosomes in our sample (31), represented ribosomes that were simultaneously bound to two hibernation factors: Balon, and the previously characterized hibernation factor RaiA. The second state, corresponding to 35% of ribosomes in our sample (31), was comprised of the ribosome in complex with Balon, tRNA and mRNA. Additionally, both binding states comprised an additional ligand, the translation elongation factor EF-Tu.

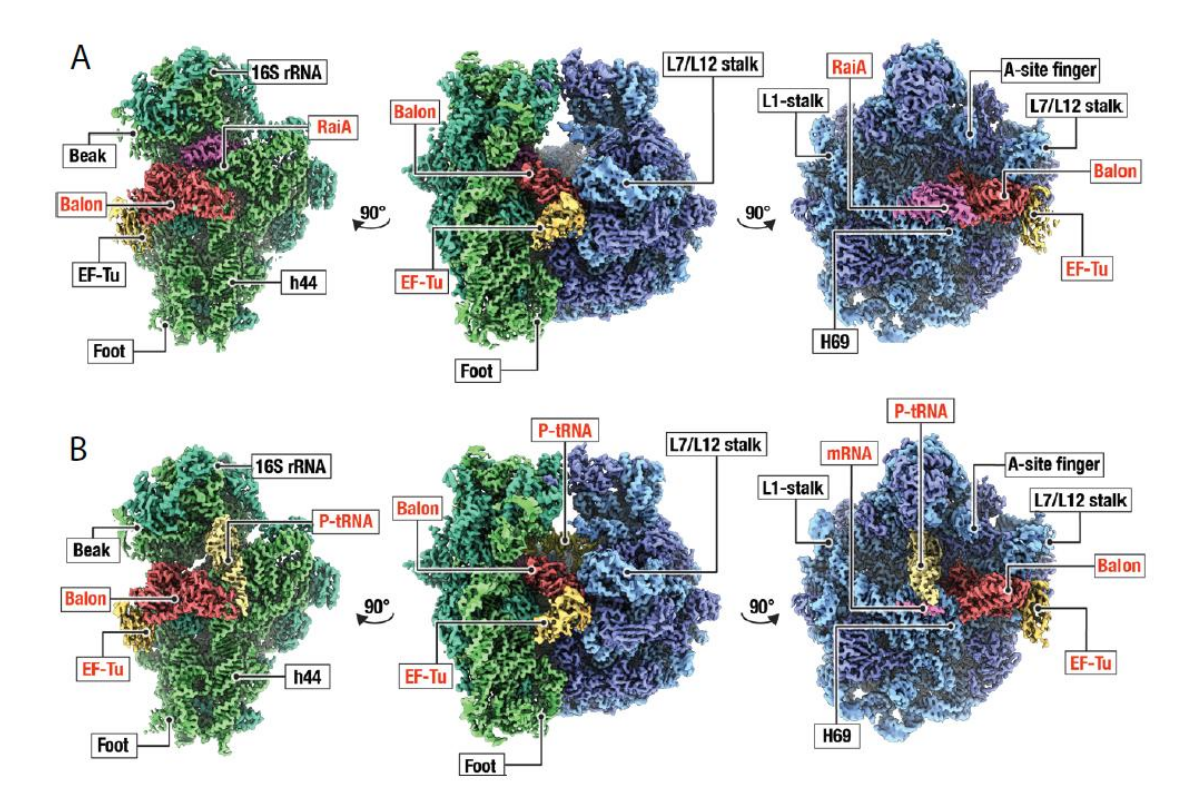


**Figure 37.** Cryo-EM maps reveal the two main states of ribosomes derived from bacteria *P. urativorans* during cold shock. Each density map (3.1 Å resolution) is color-coded and presented in three different perspectives. The left side displays the 30S subunit (green) independently with associated factors, the right side shows the 50S subunit (blue) independently with associated factors, and the middle panel depicts the complete 70S particle. (A) The first state of the ribosomes in the sample, reveals ribosomes bound to a previously unidentified translation factor called Balon, along with the known hibernation factor RaiA. (B) The second state shows ribosomes bound to Balon, mRNA, and P-site tRNA. Both ribosome states also exhibit the presence of the elongation factor EF-Tu bound to Balon.

The remainder of this chapter will provide a description of the binding states of the cold shocked hibernating *P. urativorans* ribosomes isolated from cold-shocked cells and explain the implications of these findings.

### 4.2 BINDING STATE I: THE HIBERNATING RIBOSOME IN COMPLEX WITH BALON AND RaiA

As stated earlier, we found that approximately 63% of the ribosomes in our sample had two of their active centres occupied by hibernation factors (31), with Balon bound to the A site of the ribosome and RaiA in the P site as shown in **Figure 38**.

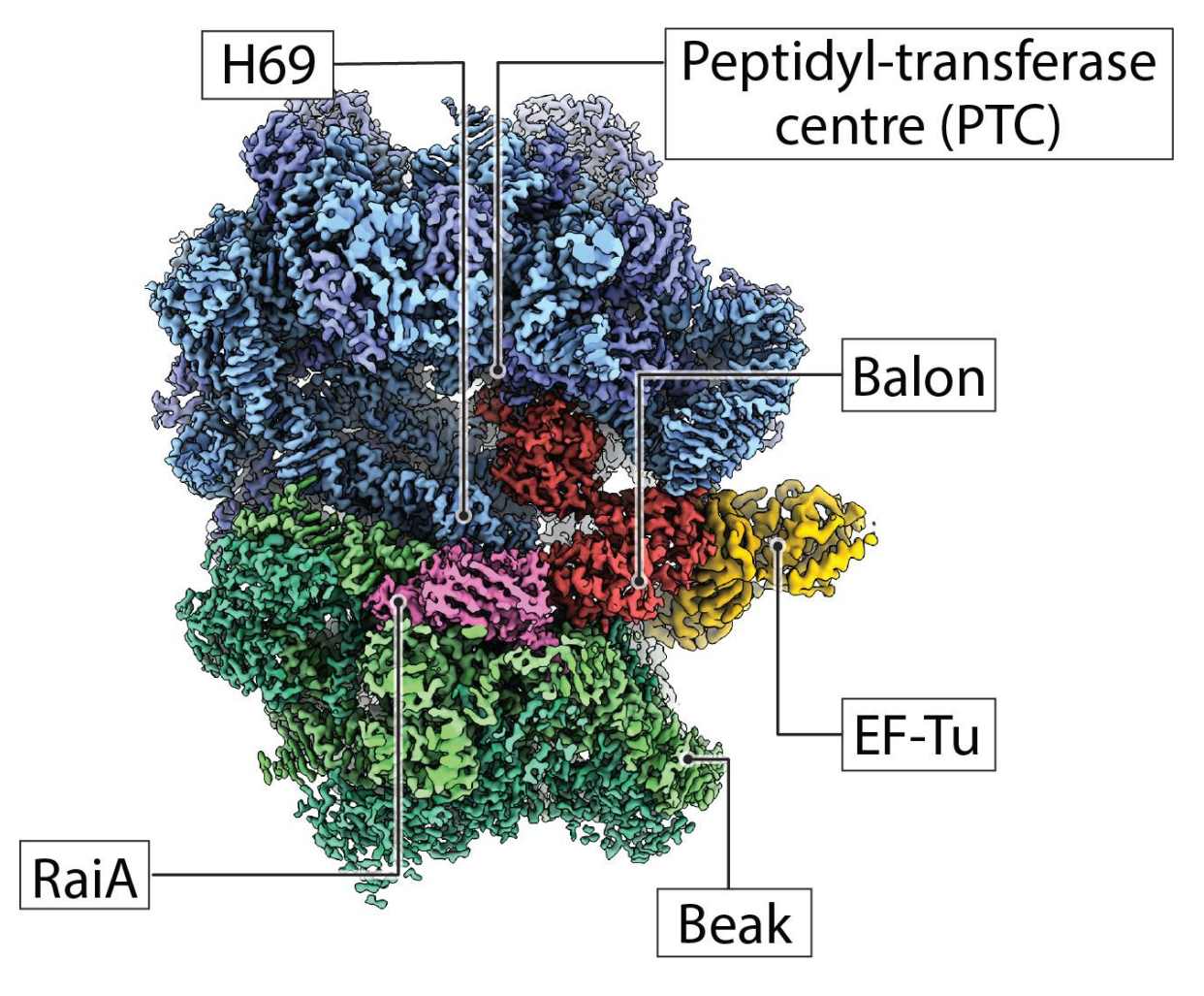


**Figure 38.** Most cold shock *P. urativorans* ribosomes are associated to two hibernation factors. Cryo-EM map after focussed classification around the P-site of *P. urativorans* ribosomes during cold shock reveals that most ribosomes are found in complex with Balon, RaiA, and EF-Tu.

Our further analysis revealed that Balon and RaiA do not directly interact with each other. Also, concurrent binding of RaiA and one of the Balon homologs (translation termination eRF1) would not be possible due to steric clash between their N-terminal domains and RaiA as shown in **Figure 39**. This suggests that while Balon is a distant homolog to archaeo-eukaryotic proteins eRF1 its function in bacteria has been repurposed by introducing structural changes in its N-terminal domain that allows Balon to bind to ribosomes concurrently with hibernation factor RaiA.

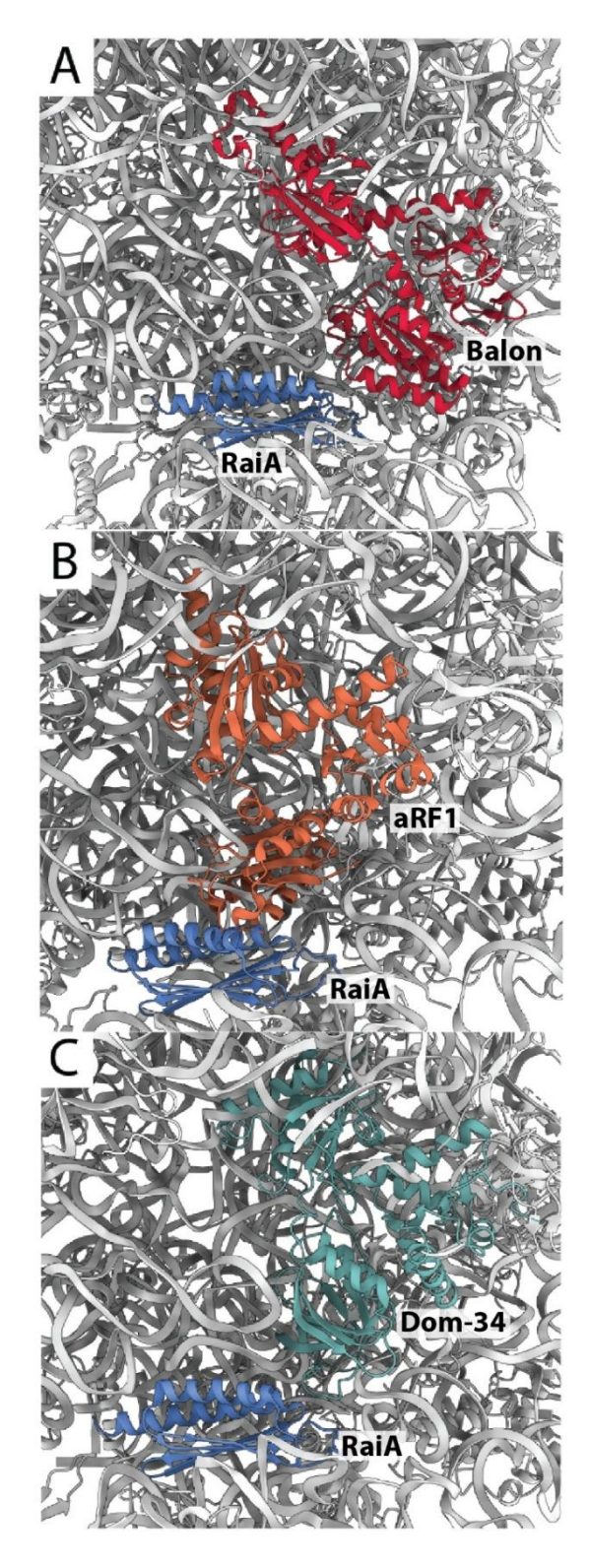


Figure 39. Balon homolog, eRF1, cannot bind the ribosome concurrently with RaiA due to steric clashes. (A) Balon does not make any direct contact with hibernation factor RaiA in complex with the ribosome making the concurrent binding of these hibernation factors to the ribosome possible (PDB 8RD8). By contrast, (B) superimposition of Balon homolog aRF1 (PDB 3AGK) shows a steric clash between the N-terminal domain of both proteins and RaiA. This clash is not observed with binding of the eukaryotic homolog of Pelota, Dom-34 (PDB 5M1J) as shown in (C).

As discussed in a previous chapter, the concurrent binding of two hibernation factors has been previously documented in gammaproteobacteria. This, along with the fact that all bacteria that bear a gene for Balon also bear a gene for RaiA, suggests that structural modifications of the N-terminal domain that differentiate Balon from eRF1 provided bacteria with one advantage: conferring Balon the capability to bind hibernating ribosomes and thereby providing an additional level of protection for ribosomes in stressed bacterial cells. Other sequence and structural modifications present in Balon in comparison to eRF1 (including the lack of the GGQ and NIKS motif as well as the bL27 trap and the presence of a Lasso-like protein loop) further support the hypothesis that Balon is a structurally distant homolog of archaea and eukaryotic translation factors that have undergone key structural changes that confer an entirely different function, that of a hibernation factor.

On a broader perspective, our finding that most ribosomes in our sample were associated with Balon is consistent with the previous studies of E. coli cells showing that ribosomes in stressed cells bind to the hibernation factors instead of the elongation factors and other factors of protein synthesis (73). Specifically, the previously established models of bacterial ribosome hibernation posit that ribosomes first become vacant (particularly in its A and P sites) before becoming associated with hibernation factors and consequently enter a state of dormancy or inactivation. Once hibernation factors disassociate from the ribosome, only then can translation factors bind the ribosome and restart protein synthesis. The most prevalent binding state of our cold shocked P. urativorans ribosomes supports this model as the occupancy of both the A site and the P site by Balon and RaiA would prevent binding of translation factors to the active centres of the ribosome and therefore disrupt protein synthesis as shown by our polysome profiling analysis.

While the current models of bacterial ribosome hibernation are still valid, as evidenced by previous research, as well as by this study, it may not be the only mechanism by which bacteria enter a state of ribosome hibernation.

## 4.3 BINDING STATE II: THE HIBERNATING RIBOSOME IN COMPLEX WITH BALON, tRNA AND mRNA

Our focussed classification analysis revealed that approximately 35% of the ribosome particles in our dataset were simultaneously bound to Balon, P-site tRNA, mRNA, and EF-Tu (31) as shown in **Figure 40**. The cryo-EM map of this functional state is the first structure that shows a hibernation factor bound to the ribosome concurrently with translation factors.

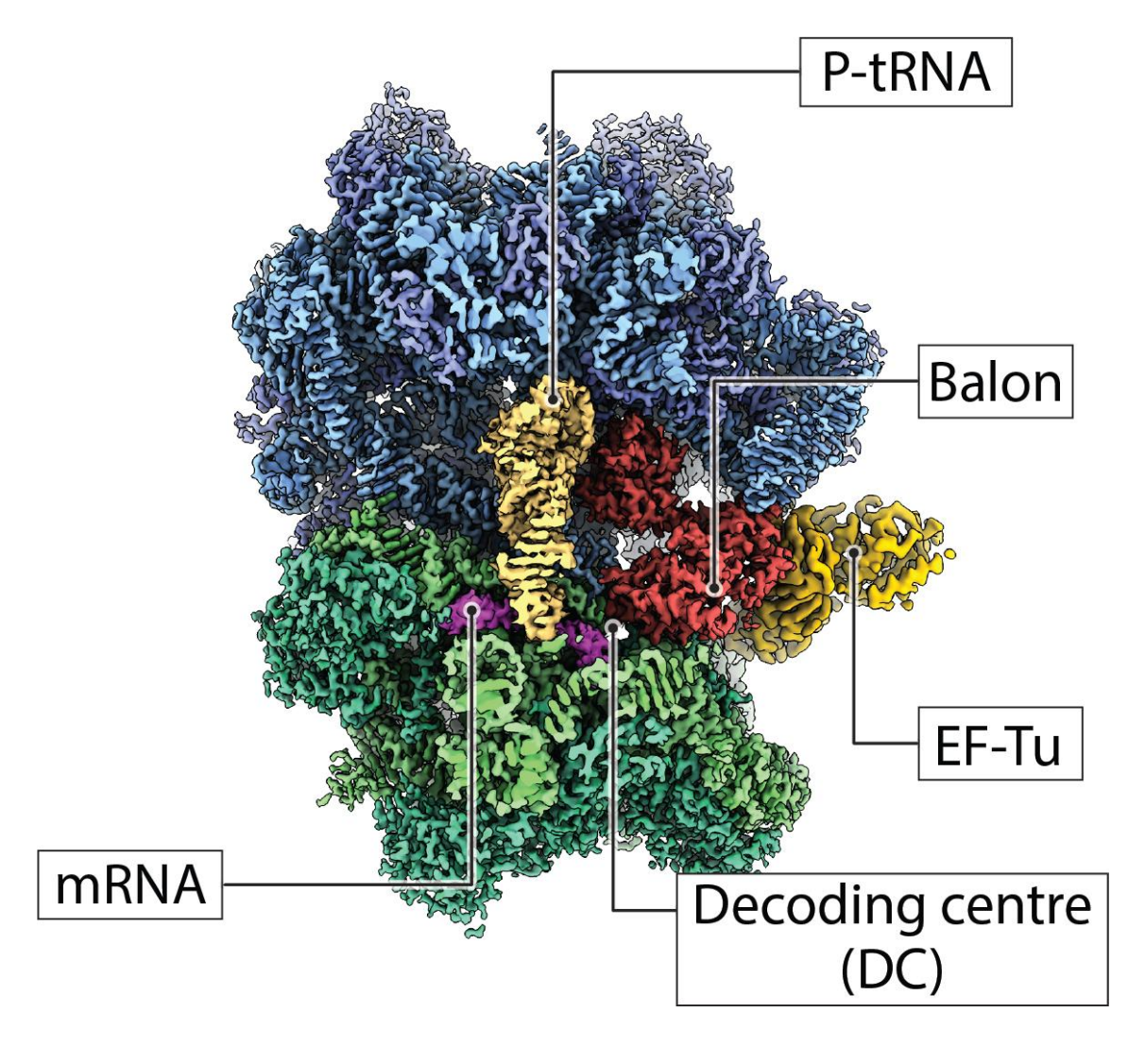
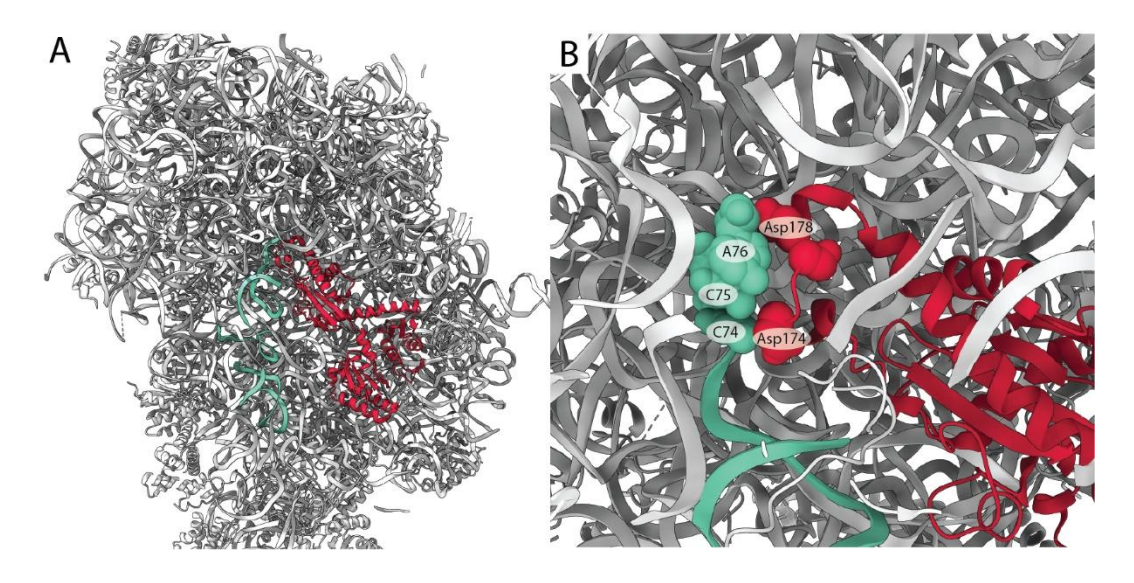


Figure 40. Focussed classification analysis of cold shock *P. urativorans* ribosomes reveals hibernating ribosomes bound to factors of protein synthesis. 35% of ribosome particles that comprised the *P. urativorans* ribosome cryo-EM map (2.6 Å resolution) obtained from cold shocked cells were bound to Balon, P-site tRNA, mRNA and EF-Tu.

Our closer inspection of this cryo-EM map revealed that the tRNA is present in the P/P conformation as shown in **Figure 41A**, suggesting that we are observing ribosomes that were arrested in the middle of the elongation stage of protein synthesis. Our closer examination revealed that there are 3 residues within the P site tRNA molecule that form direct contacts between Balon.

As shown in **Figure 41B** residue Asp 174 located in the middle domain of Balon directly contacts C74 in the tRNA, and residue Asp 178 contacts A76 in the tRNA molecule. Residues C74 and A76 are two of the residues that comprises one of the functional motifs of tRNAs molecules, the so-called CCA-end. The CCA-end is a highly conserved sequence that is located at the 3' end of all tRNA molecules and is the binding site of the amino acid residues that are delivered to the ribosome by tRNA during protein synthesis.



**Figure 41.** Cross sectional view of *P. urativorans* ribosome bound to Balon and P-site tRNA. (A) Cryo-EM focussed classification of the P site of *P. urativorans* ribosomes reveals that the tRNA molecule bound to these ribosomes is in its P/P conformation. (B) Zoomed in view in the large subunit of ribosomes containing P-site tRNA shows that Balon makes direct contact with the CCA end of tRNA.

Consistent with our interpretation of this functional state of the ribosome, its cryo-EM map showed density corresponding to a nascent peptide attached to P-site tRNA (**Figure 42**). This is consistent with the presence of mRNA in these ribosomes and suggests the possibility that these ribosomes were actively translating protein before becoming associated with Balon, and that unlike other previously described hibernation factors, Balon may be able to bind translating ribosomes.

### Bacterial ribosomes from P. urativorans bound to mRNA, peptidyl-tRNA and Balon

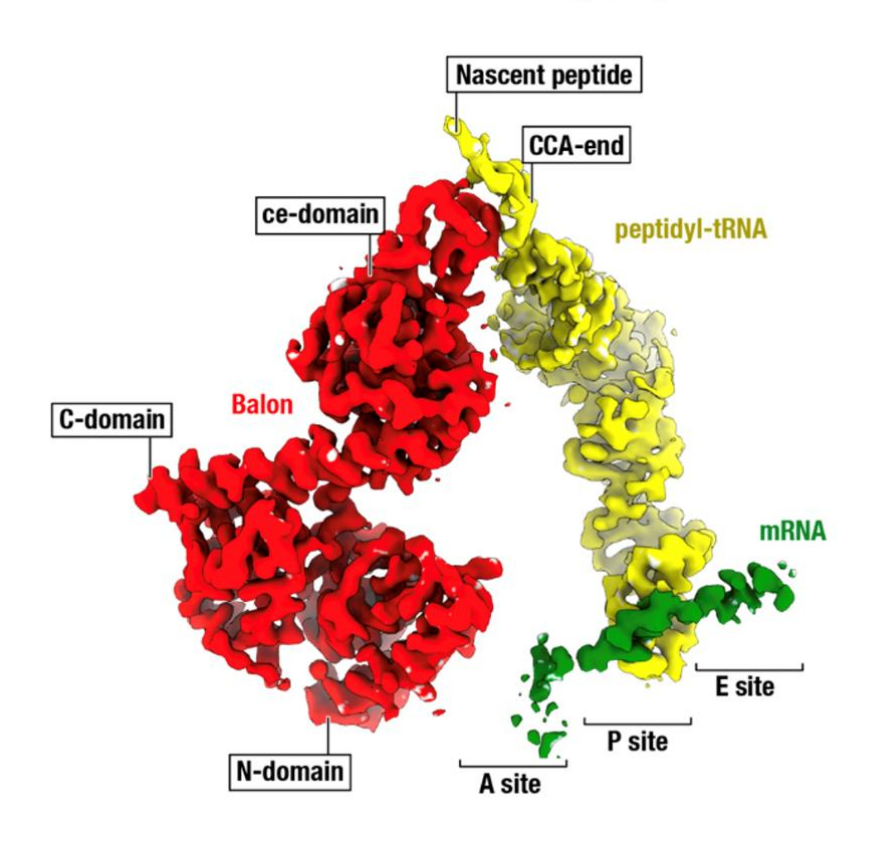


Figure 42. Balon-associated ribosomes with P-site tRNA, and mRNA also show density for the nascent peptide. *P. urativorans* ribosomes associated with hibernation factor Balon also contain density for ligands that are hallmarks of protein synthesis, such as mRNA, P-site tRNA, and the nascent peptide still attached to tRNA. This observation represents a novel binding state of the ribosome where a hibernation factor binds the ribosome concurrently with canonical factors of protein synthesis.

### Balon appears to inactivate the catalytic site of the ribosome

This cryo-EM map also allows to better appreciate another key structural feature of Balon, which we termed the bL27 trap. Previously, ribosomal protein bL27 was characterized as a bacteria-specific ribosomal protein. The molecule of bL27 has an N-terminal tail that binds near the PTC and allows water molecules to be positioned in favour of the catalytic activity of the ribosome during protein synthesis. Our map revealed that when ribosomes associate with Balon, the N-terminal tail of bL27 gets displaced away from the PTC. Instead, this N-terminal tail of bL27 associates with a protein loop in the Balon molecule we have termed the "bL27 trap" (located in the middle domain of Balon within residues Ala145 and Pro163).

Below you can see the comparison of bL27 in our structure with the active conformation of this protein as shown previously (185) that illustrates the conformational change of bL27 upon the ribosome transition from its active state to the hibernation (**Figure 43**).

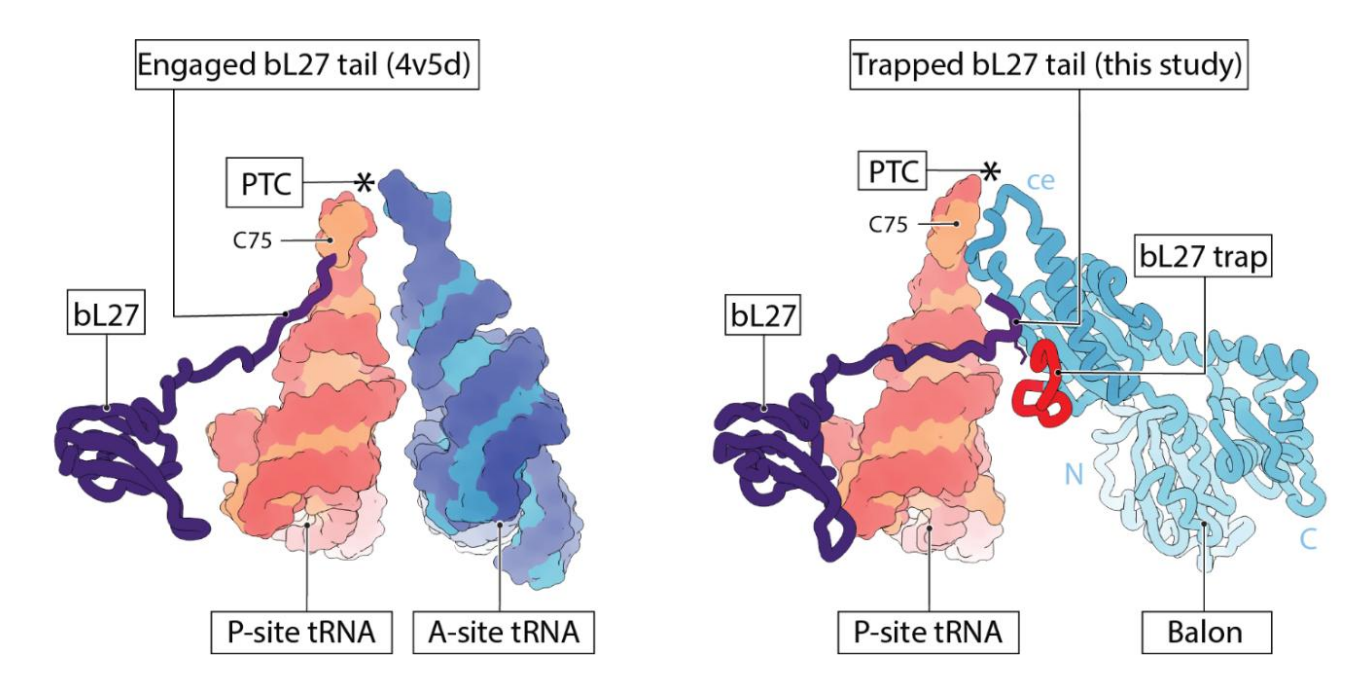
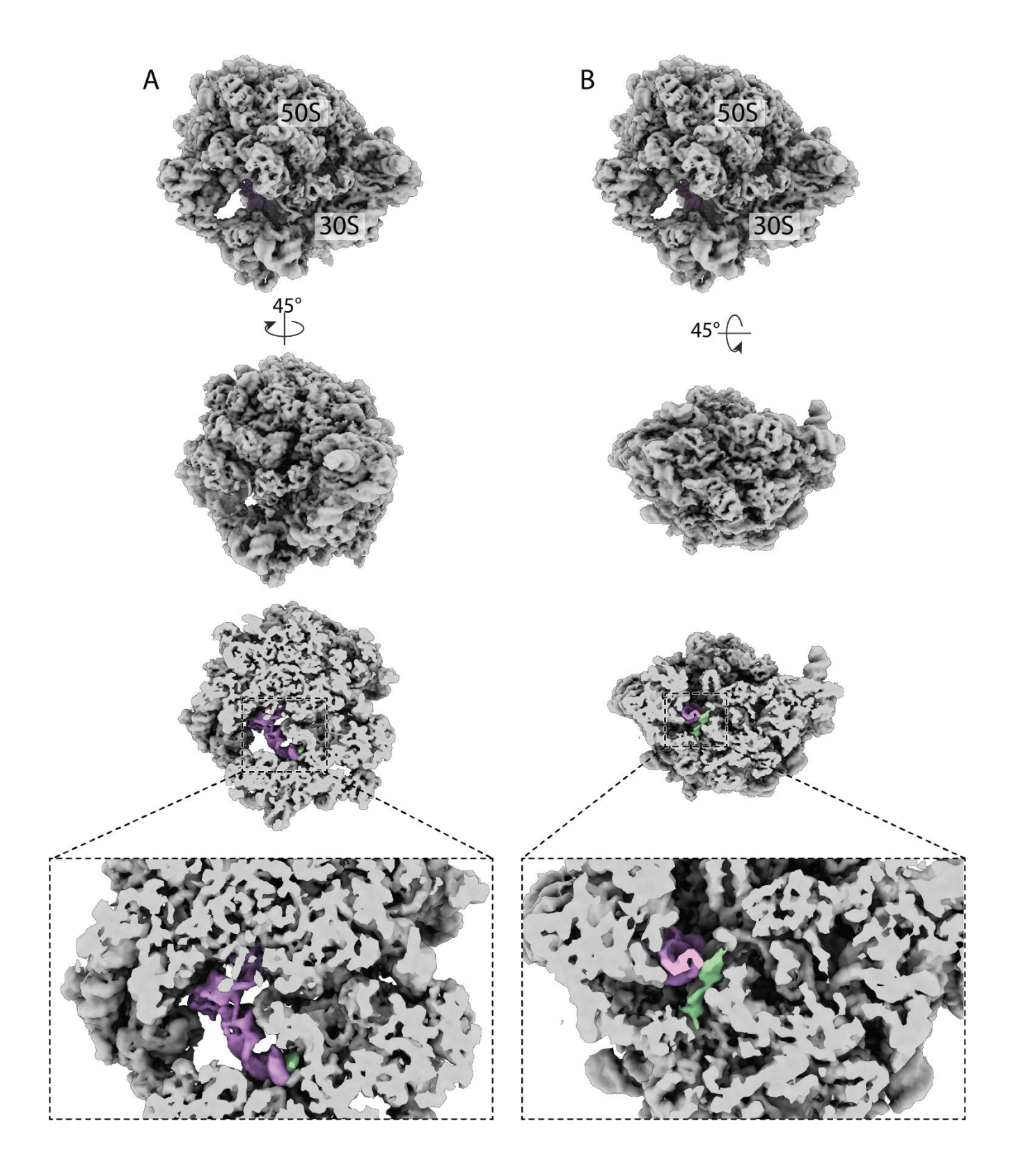


Figure 43. Comparison of the ribosomal protein bL27 in active ribosomes (left) and Balon bound ribosomes (right). Structure shown in the left panel shows the conformation of protein bL27 during protein synthesis where its N terminal tail is thought to position water molecules in a manner that is favourable for protein synthesis. By contrast, in Balon-bound (hibernating) ribosomes the N-terminal domain of bL27 adopts a different conformation.

#### Balon can associate with mRNA-bound ribosomes

Besides tRNA, our cryo-EM maps revealed another ligand of interest, mRNA. We observed that the shape of the mRNA density was not detailed enough to allow for the identification of the mRNA sequence, likely due to the presence of heterogeneous mRNAs rather than one specific mRNA type. However, the density clearly shows the stoichiometric presence of an RNA molecule in the mRNA binding channel of the ribosome associated with Balon and the P-site tRNA (**Figure 44**).



**Figure 44. Balon-associated ribosomes showed density of P-site tRNA and mRNA.** Focussed classification of Balon associated ribosomes around the P site revealed the presence of tRNA (purple) as shown in panel **A** and mRNA (green) better observed as shown in panel **B**.

While further experimentation is needed to understand the biological role of this phenomenon, our data provide the direct evidence that ribosome association with a hibernation factor and translation factors are not mutually exclusive. This is illustrated by Balon's ability to bind not only ribosomes that have become disassociated from protein synthesis factors, but also ribosomes that are still bound to translation factors. This is in contrast with current models of ribosome hibernation where ribosomes that are occupied are not contemplated as explained in the previous section.

It is important to note that our cryo-EM maps from stationary phase *P. urativorans* ribosomes did not show density for tRNA, mRNA or nascent peptide. This highlights an important distinction between different ribosome hibernation mechanisms that possibly related to the speed at which organisms are exposed to environmental stress. In the case of the cold shock sample, the cells were quickly exposed to stress in contrast to the stationary phase sample in which cells slowly transition to a state where they were exposed to the stressors that characterize stationary phase such as nutrient deprivation, changes in pH, among others.

It is possible that the binding state where we observe Balon bound to the ribosome concurrently with translation factors only occurs when cells are exposed to stress so suddenly that ribosomes do not have enough time to complete protein synthesis (and therefore disassociate from translation factors) before binding hibernation factor Balon. This finding could potentially explain how slow-growing organisms, such as *P. urativorans*, can quickly adapt to the ever-changing environmental conditions that are so prevalent in nature without the need to complete the cycle of protein synthesis.

### 4.4 BALON BINDS THE RIBOSOME IN COMPLEX WITH PROTEIN EF-Tu

### Balon potentially allows for a mechanistically distinct faster mode of hibernation

While the discovery of Balon and its implications for our understanding of ribosome hibernation and stress response in bacteria are noteworthy on their own, perhaps the most striking discovery is not Balon itself, but rather that Balon appears to be delivered to the ribosome by the translation elongation factor EF-Tu. We observed that Balon was found bound to the *P. urativorans* ribosome in complex with EF-Tu during stationary phase and cold shock as shown in **Figure 36** and **Figure 37**.

Prior to our study, the elongation factor Tu has been characterised as a canonical factor of protein synthesis that normally delivers amino-acyl tRNA to the ribosome in a process that is mediated by codon-anticodon recognition between tRNA and the decoding centre of the ribosome, and GTP hydrolysis by EF-Tu (186) (187). EF-Tu plays a critical role in protein synthesis where it recruits aminoacyl-tRNAs to the ribosome, and transitions between two conformations to do so, from its GTP-bound form to a GDP-bound. The GTP-bound EF-Tu exhibits a so-called "closed" conformation, facilitating the binding and delivery of aminoacyl-tRNAs to the ribosomal A site. If the aminoacyl-tRNA sequence matches the mRNA sequence, EF-Tu undergoes GTP hydrolysis, transitioning to the "open" or GDP-bound conformation—thereby releasing the aminoacyl-tRNA into the A site and dissociating from the ribosome (188).

EF-Tu and its overall mechanism of action are well conserved across the three domains of life (188), and while other functions have been described for this protein in the context of virulence, cell shape maintenance, and possibly immune response evasion (189) (190), its ability to deliver stress response factors to the ribosome had remained completely unknown until now.

Interestingly, previous studies showed that both Balon homologs, Pelota and aeRF1, are delivered to the ribosome by EF-Tu homologues through a mechanism that

is similar to EF-Tu delivery of tRNAs to the ribosome. Specifically, Pelota is delivered to the ribosome by the EF-Tu homologue known as protein Hbs1, and aeRF1 is recruited to the ribosome by the EF-Tu homologues known as eRF3 in eukaryotes and aEF1 $\alpha$  in archaea. Thus, Hbs1, eRF3 and aEF1 $\alpha$  are EF-Tu homologs and deliver their corresponding protein synthesis factor in a GTP-hydrolysis dependent manner (191).

The fact that Balon homologues were previously shown to be delivered to the ribosome by EF-Tu homologs, and that our cryo-EM structure revealed Balon association with EF-Tu in complex with the ribosome suggests that Balon is recruited to the ribosome in a similar manner to Pelota and aeRF3.

In our cryo-EM map, we could observe well-ordered domains III and II of EF-Tu (after focussed classification analysis), however domain I remained poorly ordered and presented some discontinued density, which was likely caused by its conformational flexibility. To resolve this problem, we have implemented further focused classification and local refinement, and the overall structure of domain I became well resolved (Figure 45).

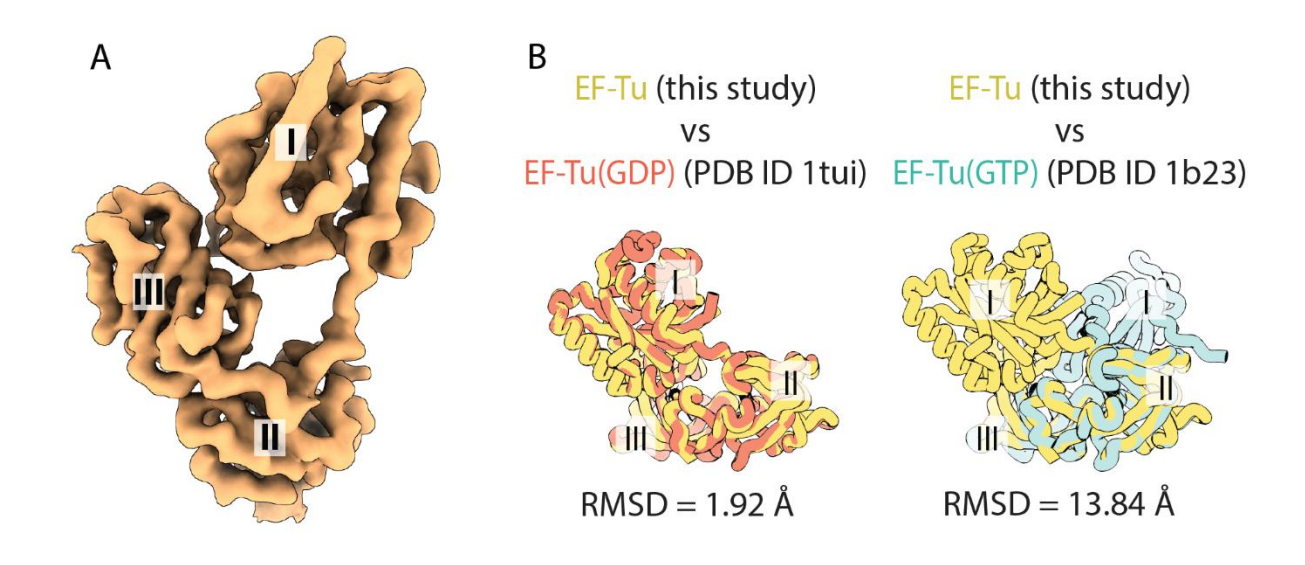


**Figure 45. EF-Tu in complex with Balon is found in its "open" conformation.** (A) Cryo-EM density of EF-Tu from *P. urativorans* ribosome in complex with Balon. (B) Structural comparison of EF-Tu structures observed in this study and determined previously. EF-Tu molecules that are bound to Balon most closely resemble the GDP-bound conformation.

We then have assessed the overall conformation of EF-Tu molecule to better understand the exact functional state of this protein in the ribosome structure. We found that the overall fold of EF-Tu in our cryo-EM maps, it closely resembles to the so-called "open" conformation of EF-Tu. Both the open (GDP bound) and closed (GTP bound) conformations of EF-Tu are highly conserved among bacteria and each conformation possesses a distinct three-dimensional fold. Furthermore, when we compare the root mean square deviation (RMSD) of EF-Tu in our model with that of previously determined EF-Tu structures, it becomes evident that the overall fold of EF-Tu in our cryo-EM maps is consistent with that of the "open" or GDP bound conformation of EF-Tu. The RMSD between EF-Tu in the *P. urativorans* structure is and EF-Tu from E. coli in the GDP bound state 1.9 Å, while the RMSD compared to the GTP bound state is 13.8 Å (**Figure 45B**). Overall, this observation suggested that the EF-Tu molecules observed in our structures represent the GDP-state of this protein and are possibly bound with GDP.

Our closer inspection of the EF-Tu-Balon interaction revealed that the C-terminal domain of Balon binds to domain III of the EF-Tu molecule in a similar fashion to aeRF1 and Pelota binding the C-terminal domains of EF-Tu homologs eRF3 and Hbs1, respectively (**Figure 46**). This binding similarity can explain the simultaneous presence of EF-Tu and Balon in our ribosome samples: in archaea, EF-Tu delivers either aeRF1 or Pelota to the ribosomal A site to terminate translation or reactivate arrested ribosomes, respectively (191), suggesting a conserved mechanism of delivery for aeRF1, Pelota, and Balon to the ribosome by EF-Tu (**Figure 46**).

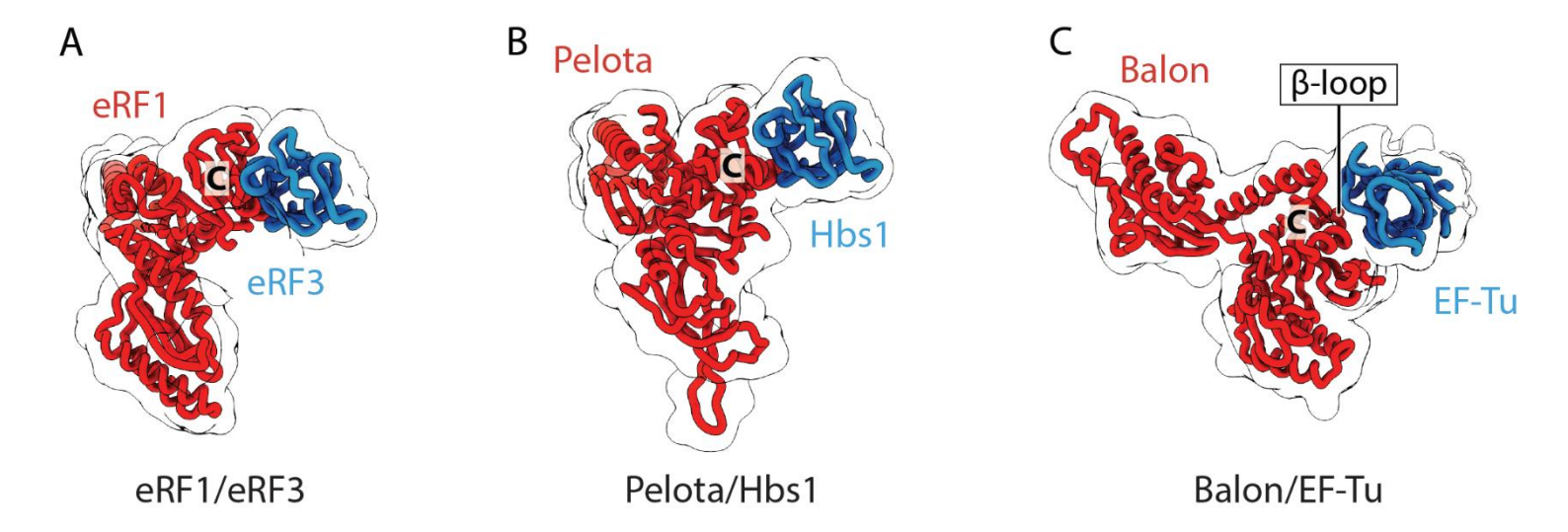


**Figure 46. Structural comparison of Balon binding to EF-Tu and their homologous proteins in archaea and eukaryotes.** Structures of (**A**) eukaryotic translation termination factor eRF1 bound to eRF3 (PDB 5LZT) (**B**) eukaryotic ribosome rescue factor Pelota bound to Hbs1 (PDB 5M1J) and (**C**) bacterial hibernation factor bound to EF-Tu suggests that Balon mediated ribosome hibernation resembles a recruitment mechanism similar to that of the recruitment of other translation factors during protein synthesis termination and rescue of stalled ribosomes.

We then assessed the molecular interactions of EF-Tu in our functional complex to better understand the physiological role and a mechanism of this interaction. We found that domain II directly contacts 16S rRNA (helix h5), similarly to previously observed domain II interactions during aminoacyl-tRNA delivery (**Figure 47**). This finding has illustrated a tRNA-mimicking properties of Balon, further explaining how this protein can be delivered to the ribosome by the tRNA-delivering factor (EF-Tu).

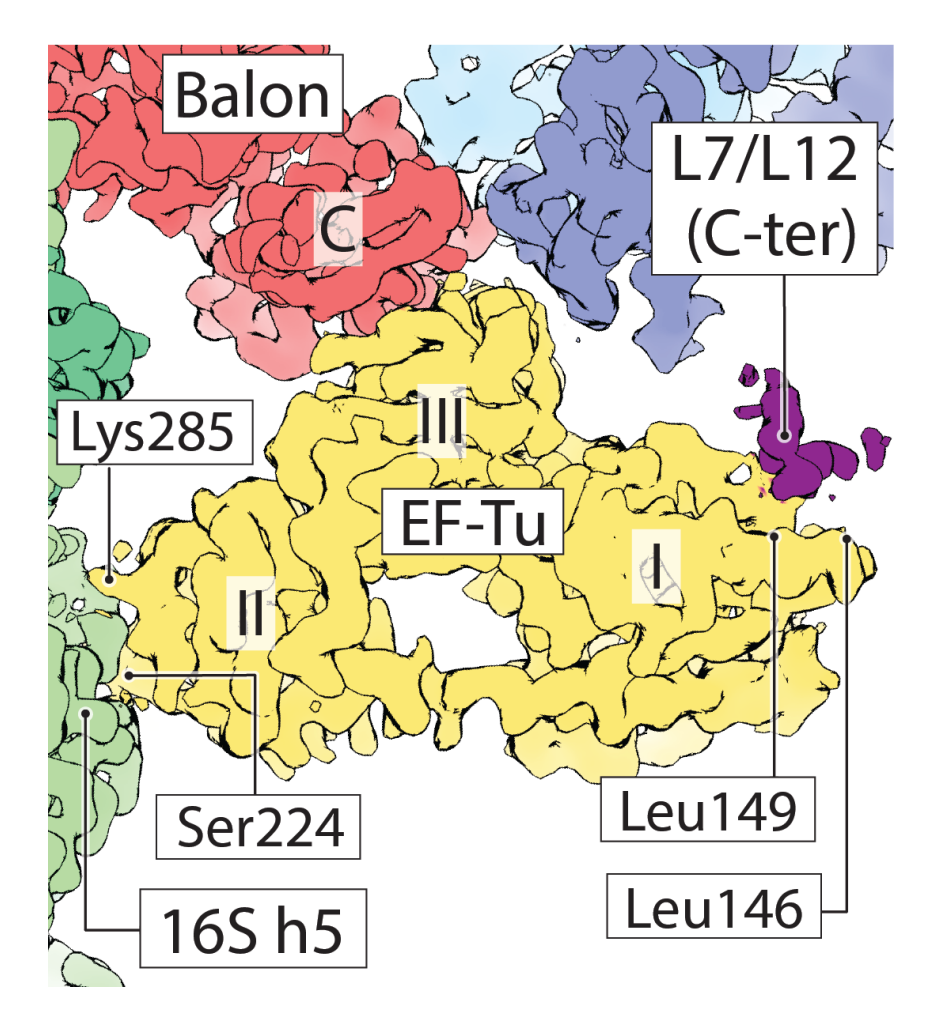


**Figure 47. EF-Tu contacts hibernation factor Balon and the small and large subunit of the ribosome.** Cryo-EM map of *P. urativorans* ribosome focusing on the EF-Tu-binding sites shows that EF-Tu is attached to Balon-bound ribosomes through contacts with Balon, the C-terminal domain of the L7/L12 stalk (protein bL12) and the 16S rRNA helix h5. Neighbouring density corresponding to 23S rRNA (light blue) and ribosomal protein uL6 (dark blue) also shown.

Strikingly, we also found that the C-terminal domain of EF-Tu, domain III, not only forms direct contacts with Balon but it also binds to the tip of the G protein-activating sarcin–ricin loop (**Figure 48**). This finding was remarkable because the sarcin-ricin loop of the ribosome is a known target for cellular toxins and nucleases, which inactivate ribosomes during stress or infection (192). Therefore, direct binding of this loop by the EF-Tu molecule could explain how cells protect the sarcin-ricin loop of the ribosome in its intact and therefore functional state during starvation or stress—thus preventing an irreversible inactivation of cellular ribosomes.

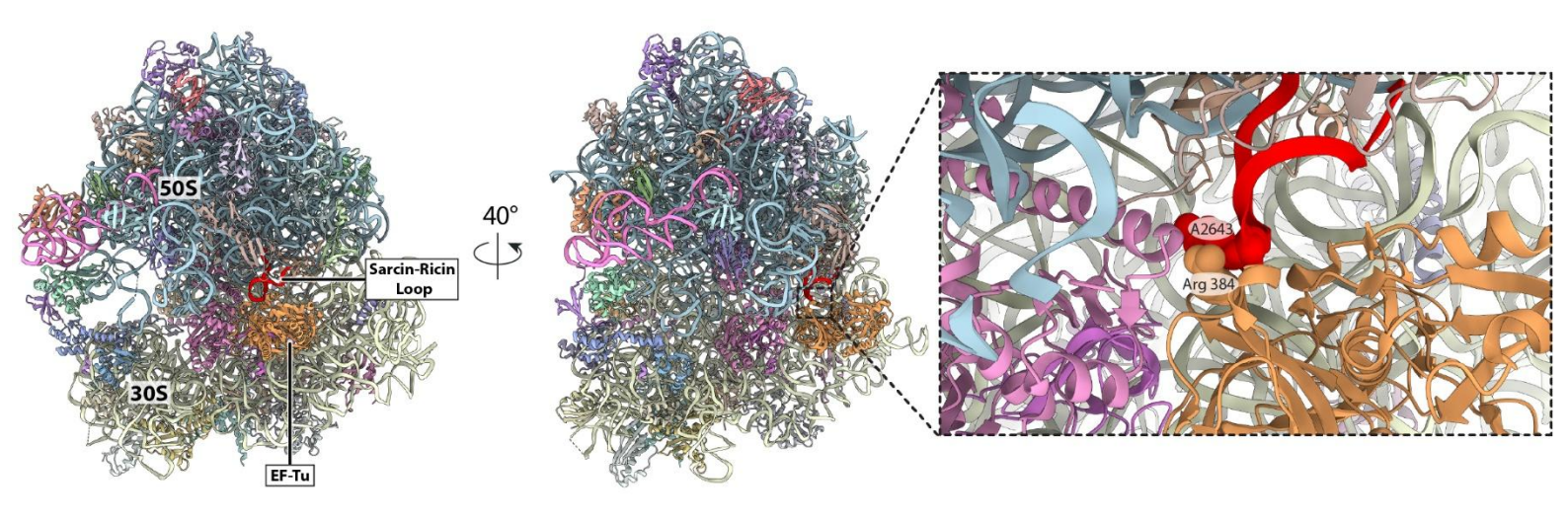


**Figure 48. Balon-associated EF-Tu interacts with the sarcin-ricin loop.** The sarcin-ricin loop is comprised of 14 nucleotides within 23S rRNA and is located in close proximity to the A site. This figure shows the sarcin-ricin loop in *P. urativorans* (red) which corresponds to residues 2636 to 2650 (2653 to 2667 in *E. coli* numbering). A zoomed-in view showing the interaction between the sarcin-ricin loop and EF-Tu (orange) reveals a direct contact between residue Arg 384 of EF-Tu and nucleotide A2643 in the sarcin-ricin loop.

We also found that the N-terminal domain of EF-Tu, domain I, which contains the nucleotide-binding site, forms previously described interactions with the C-terminal domain of the L7/L12 stalk (consisting of protein bL12) (193) (**Figure 47**). This finding was important because it provided a hint to how EF-Tu and Balon can be recruited to ribosomes in stressed cells: via the ability of EF-Tu to interact with the L7/L12-stalk of the ribosome.

Overall, our analysis suggested that Balon is delivered to the ribosome by EF-Tu through the same pathway as aminoacyl-tRNA, aeRF1, and Pelota are delivered to the ribosomes by EF-Tu and its homologs. We therefore asked: if this hypothesis is correct, then why does GDP bound EF-Tu quickly dissociate from aminoacyl-tRNAs, aeRF1, and Pelota, but not from Balon.

To answer this question, we first took a closer look at the interaction interfaces that EF-Tu forms with each of its binding partners. While Balon, eRF1, and Pelota all use their conserved C-terminal domain to interact with EF-Tu or its homologues, Balon engages with a unique surface on its C-terminal domain. This alternative EF-Tu-recognition site includes a unique  $\beta$ -loop and is about 20 Å away from the corresponding site in eRF3 and Hbs1 (**Figure 49**).

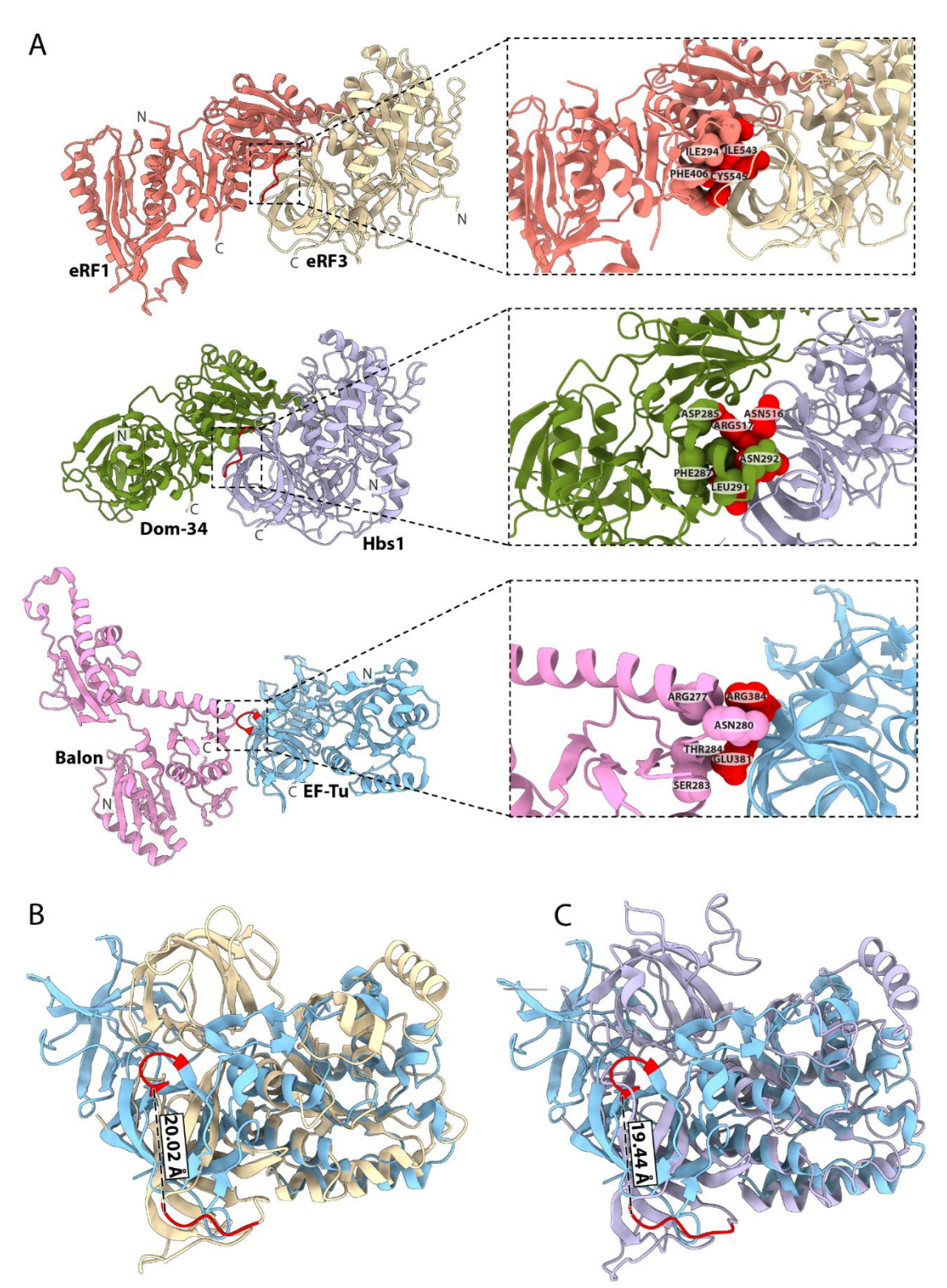


Figure 49. Balon interacts with EF-Tu at a distinct site compared to its eukaryotic homologs. (A) Balon homologs eRF1 and Dom-34 (eukaryotic homolog of Pelota) are delivered to the ribosome by G-proteins eRF3 and Hbs1 respectively. Structural comparison of eRF1 in complex with eRF3 (PDB 5LZT) and Dom-34 in complex with Hbs1 (PDB 5M1J) shows that eRF3 and Hbs1 interact with their corresponding binding partners using the same recognition site at their C-terminal domains (red). In contrast, Balon interacts with EF-Tu at a different site of its C-terminal domain shown in red. Zoomed-in views of these structures show the residues involved in these interactions. (B) Superimposed structures of EF-Tu (blue) and eRF3 (yellow) show the distance between the interfaces used by these proteins to interact with Balon and eRF1 respectively. (C) A similar distance was found between the interface used by EF-Tu (blue) to interact with Balon compared to interface used by Hsb1 (purple) to bind Dom-34.

Consequently, while in the A site, Balon cannot bind to EF-Tu while it is in its "closed" or GTP bound conformation, as this would cause a steric clash between the ribosomal sarcin–ricin loop and the closed conformation of EF-Tu (**Figure 50**).

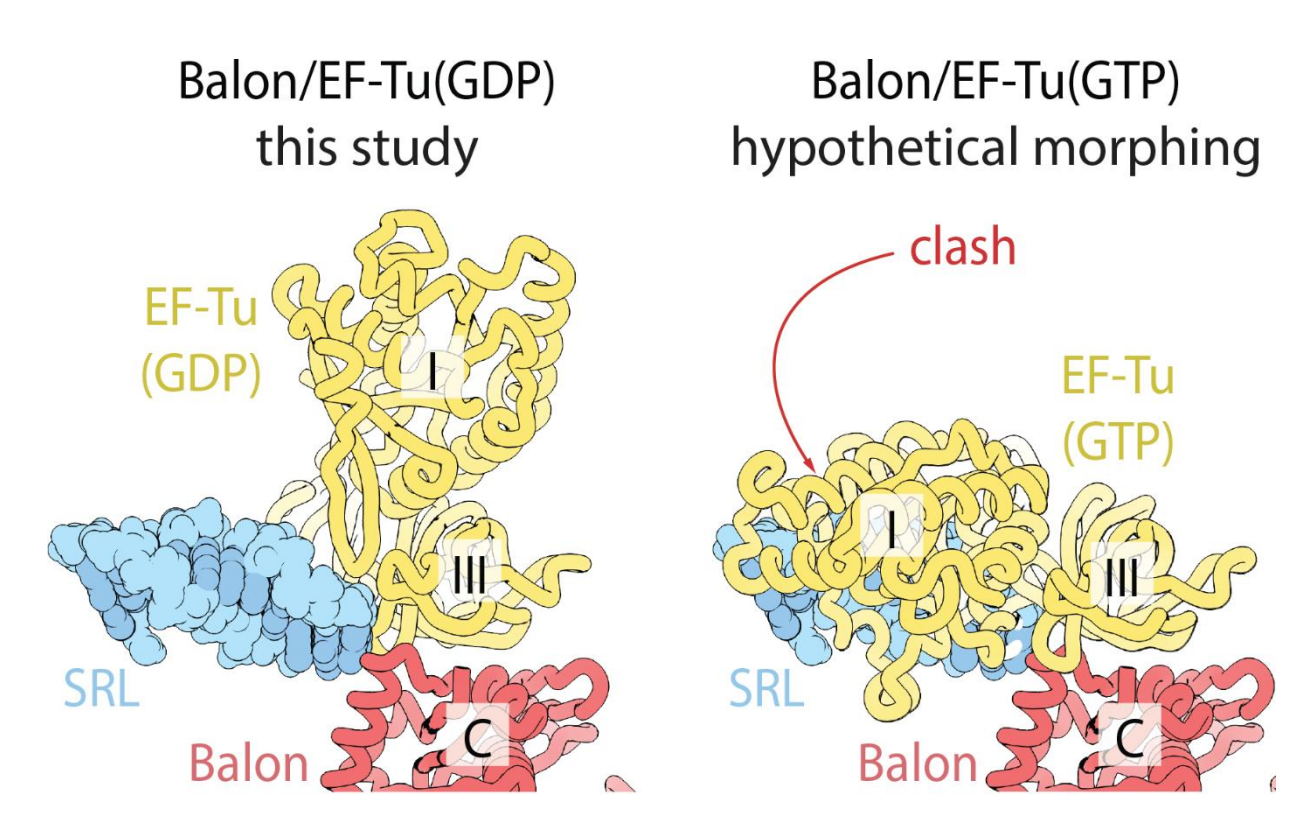


Figure 50. EF-Tu in its GTP bound or "closed" conformation in complex with Balon would not be able to bind the ribosome. Aligned structures show that EF-Tu cannot adopt the GTP-bound conformation (PDB ID 1B23) while bound to the C-terminal domain of Balon due to a clash between EF-Tu domain I and the sarcin–ricin loop.

Furthermore, the stable association between EF-Tu in its GTP bound conformation and Pelota or aeRF1 requires additional interactions with the middle domain of Pelota or aeRF1 that are possible only with the closed GTP-state of EF-Tu. However, the different relative orientation of Balon and GTP bound EF-Tu would preclude the formation of these interactions (

**Figure 51**). Without this, the Balon C-terminal domain–EF-Tu interface is limited to about 230 Å<sup>2</sup>, compared to the minimum contact area of about 500 Å<sup>2</sup> required for a

stable interaction (194). The Balon–EF-Tu complex is therefore unlikely to be stable in solution.

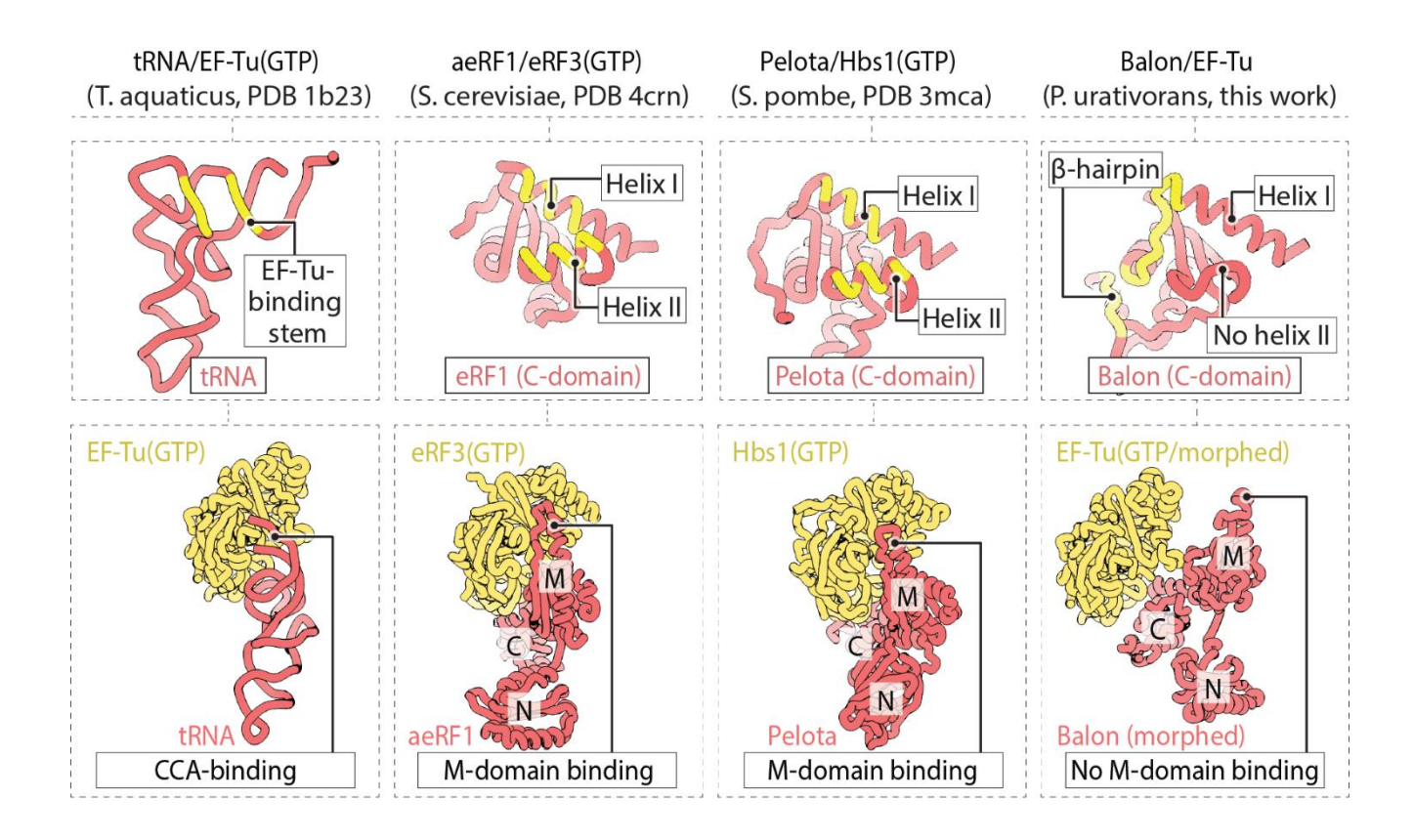


Figure 51. Balon could not establish sufficient contacts with GTP bound EF-Tu to maintain a stable interaction. Comparison of intramolecular interaction surfaces in four biological complexes, including EF-Tu-tRNA, eRF3-aeRF1, Hbs1-Pelota and EF-Tu-Balon. The upper panels highlight (in yellow) residues that recognize domain III of EF-Tu, or the EF-Tu homologues eRF3 and Hbs1. The lower panels compare complexes of EF-Tu(GTP)-tRNA, eRF3(GTP)-aeRF1 and Hbs1(GTP)-Pelota and the hypothetical complex of EF-Tu(GTP)-Balon, in which the Balon molecule is morphed to resemble the aeRF1 conformation in the eRF3(GTP)-aeRF1 complex.

Collectively, our analysis showed that whereas aeRF1, Pelota and Balon bind to the A site in complex with EF-Tu, Balon uses a dissimilar EF-Tu recognition strategy and probably follows a different delivery mechanism to the ribosomal A site. Our data imply that this mechanism involves either Balon association with the ribosomal A site and a subsequent recruitment of EF-Tu in its GDP bound state or Balon recruitment by GDP bound EF-Tu through the weak interactions between EF-Tu, Balon and the ribosomal L7/12 stalk. In either of these scenarios, Balon—unlike aminoacyl-tRNAs, aeRF1 and Pelota—does not engage with the GTP-bound form of EF-Tu, providing a possible

explanation for why Balon does not interfere with protein synthesis during normal growth conditions, when cells contain abundant levels of GTP (195).

Therefore, in contrast to aminoacyl-tRNAs, aeRF1 and Pelota, Balon loading in the A site seems to bypass not only the step of mRNA codon verification but also the step of GTP hydrolysis, offering one potential explanation as to how Balon is able to bind to ribosomes during starvation and stress. This finding reveals a previously unknown biological activity of EF-Tu, illustrating that this protein participates not only in protein synthesis but also in ribosome hibernation.

### **CHAPTER 5: CONCLUSIONS AND FUTURE WORK**

# 5.1 BALON POTENTIALLY ALLOWS FOR A MECHANISTICALLY DISTINCT FASTER MODE OF HIBERNATION

As described in the previous chapters, we have unexpectedly identified a previously unknown hibernation factor that binds the ribosome as a response to abrupt decreases in temperature and during stationary phase in the gamma proteobacterium *P. urativorans*. This hibernation factor, which we have termed Balon, is the third protein family to be structurally characterized in bacteria. It binds the A site of the ribosome, where factors of protein synthesis are recruited to during translation.

It is worth noting that unlike other bacterial hibernation factors for which we have structures in complex with the ribosome, such as RMF and RaiA/HPF, we have found that Balon has the ability to bind ribosomes that are also bound to P-site tRNA and mRNA. This suggests that Balon may be able to bind to ribosomes that are actively engaged in protein synthesis as opposed to only binding to ribosomes once they have become vacant (for instance after translation termination). While this hypothesis remains to be tested, if true, it could represent a hibernation mechanism that would allow *P. urativorans* (and possibly ~20% of other bacterial species that bear a gene for Balon) to quickly adapt to sudden changes in the environment by engaging in ribosome hibernation without the need to wait for a given round of translation to be completed.

More broadly, the fact that Balon is able to bind the ribosome concurrently with canonical factors of protein synthesis, and the possibility that it could bind actively translating ribosomes challenges our current models of ribosome hibernation which only contemplates vacant ribosomes (**Figure 52**).

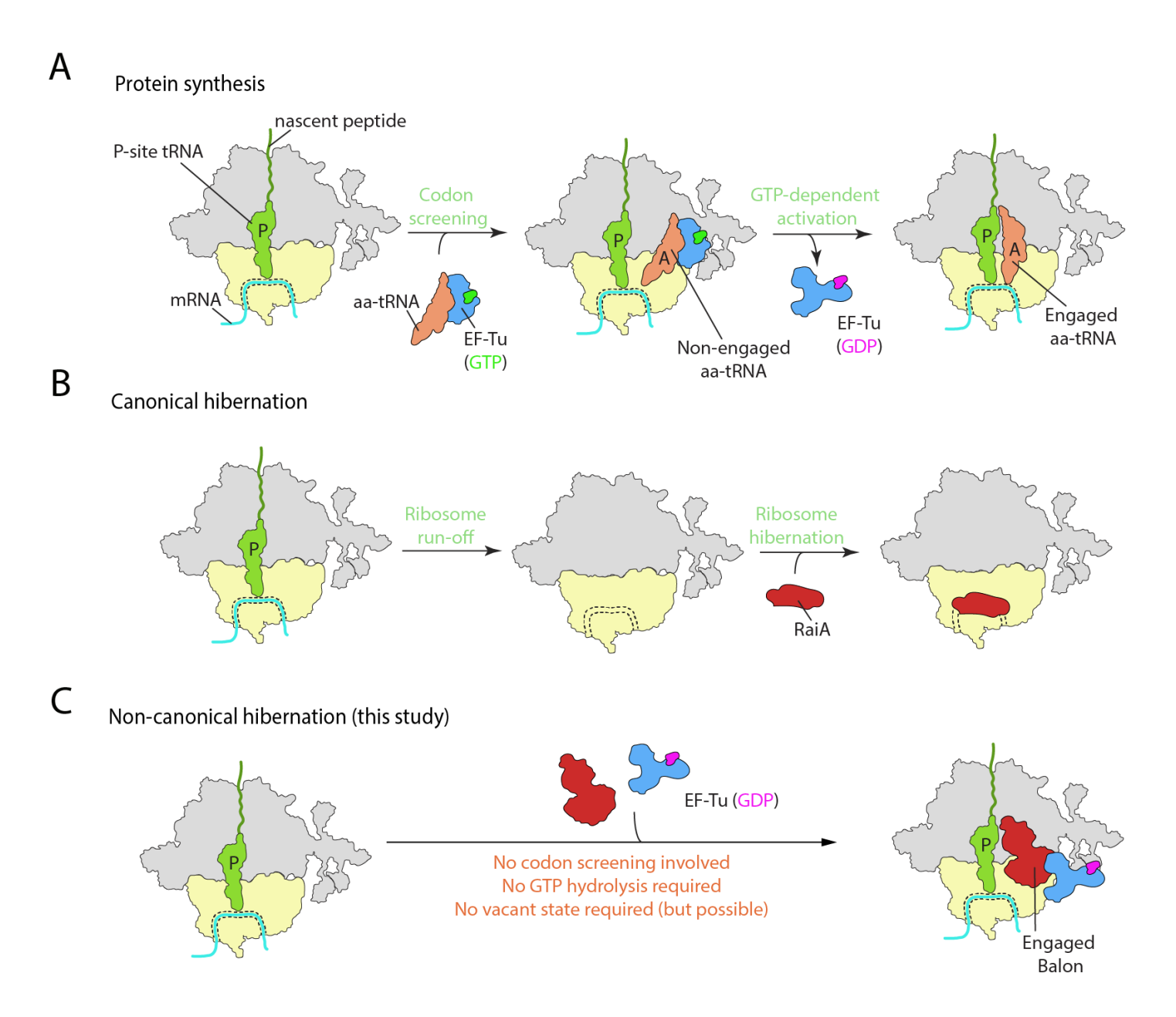


**Figure 52. Balon-mediated hibernation represents a unique mechanism of ribosome hibernation in bacteria.** (**A**) During normal protein synthesis, the elongation factor EF-Tu (in its GTP bound conformation) recruits translation factors, such as aminoacyl-tRNA, to the A site of the ribosome and rapidly dissociates from the ribosome following GTP hydrolysis. (**B**) Current models of ribosome hibernation in bacteria state that when cells are faced with starvation and other environmental stressors, ribosomes become vacant after completing a cycle of protein synthesis, before binding to hibernation factors. EF-Tu is not required for this. (**C**) As in normal protein synthesis, Balon-mediated ribosome hibernation also involves the elongation factor EF-Tu and may occur while ribosomes remain associated with mRNAs and peptidyl-tRNA.

One remaining question regarding Balon's association with the ribosome is during which step of the translation cycle could Balon inhibit protein synthesis. From our cryo-EM maps we cannot rule out the possibility that Balon can bind the ribosome

during more than one of the steps of protein synthesis. It seems plausible that Balon is able to bind during translation elongation during which the A site is primarily occupied by aminoacyl tRNAs (as they deliver amino acids to the ribosome for peptide bond formation) and elongation factor EF-G, which is responsible for translocation of tRNA from the A site to the P site, and from the P site to the E site (188). Taking into account that we do not observe density for EF-G, or E-site tRNA and that the P-site tRNA is in its P/P state one can speculate that Balon could bind the ribosome during elongation before association of EF-G results in a translocation event, and the E site becomes occupied (196). Another possibility is that Balon could bind the ribosome during translation initiation. This, however, would most likely occur during the later stages of initiation once the 70S initiation complex has been assembled. In this context, Balon could potentially bind the ribosome once initiation factor IF2 disassociates from the ribosome, the A site becomes unoccupied and the initiator tRNA, fMet-tRNAfMet is accommodated in the P site (197). It is worth noting that this scenario is not consistent with our observation of the density for the nascent peptide as initiation precedes formation of the nascent peptide chain (198). The presence of the nascent peptide also suggests that binding of Balon to the ribosome is unlikely during early stages of initiation during formation of the pre-initiation complex. Balon binding to the ribosome during translation termination seems possible as long as it occurs before the ribosomal subunits disassociate. This would likely require that Balon had a higher binding efficiency than release factors RF1 or RF2 upon conditions of stress and is able to outcompete the binding of these factors once the stop codon reaches the A site (199). While we cannot exclude the possibility that Balon could bind the ribosome during the three major steps of protein synthesis, it appears that Balon association to the ribosome is more likely to occur during elongation given the iterative nature of translation elongation which could allow for more ample opportunities for Balon to bind the ribosome. By contrast, Balon binding to the ribosome during translation initiation and termination would have to occur at specific steps within translation initiation and termination which are not cyclical and therefore provide a smaller window of opportunity for Balon to associate with the ribosome. These hypotheses, however, remain to be tested.

Overall, the significance of Balon's discovery extends beyond its role in alternative ribosome hibernation mechanisms in bacteria to include its implications for cell survival and stress response.

Given that Balon allows for the concurrent binding of canonical translation factors to the ribosome, this suggests that, unlike other hibernation factors, Balon may bind the ribosome while it is still actively engaged in protein synthesis. This would allow not only vacant or inactive ribosomes, but also actively translating ribosomes to transition to a state of hibernation. This direct transition from actively translating ribosomes to a hibernating state may offer two possible advantages to organisms that employ this mechanism of ribosome hibernation (**Figure 53**).

The first advantage that Balon mediated ribosome hibernation may have over previously described mechanisms of ribosome hibernation relates to how much time it would take for ribosomes to transition from its active state to a hibernating state. More specifically, ribosome hibernation models previously contemplated mechanisms in which ribosomes must first become vacant before transitioning to a hibernating state. This would imply that ribosomes must first finish the current round of protein synthesis they are engaged in before becoming dormant. By contrast, given that Balon mediated hibernation may allow ribosomes to bypass this intermediate vacant state, it is possible that Balon may allow for an immediately transition to a dormant state. While this may not be result in an appreciable advantage for organisms with faster rates of protein synthesis, such as E. coli (which has a rate of translation as fast as 20 amino acids per second during elongation under optimal conditions (200)), the ability to rapidly transition to a hibernating state may be advantageous for organisms that have slower rates of translation, by allowing their ribosomes to more quickly respond to stress without having to go through an entire cycle of protein synthesis to then be able to hibernate. It is important to note that the ability to rapidly employ ribosome hibernation as a response to stress may be relevant even for organisms with a relatively fast rate of protein synthesis, as it is known that environmental stress can result in a decrease in protein synthesis. S aureus, for instance, has been reported to have a translation rate of about 16 amino acids per second in nutrient-rich media. However, upon nutrient depletion the rate of protein synthesis in S. aureus drops to 10.2 amino acids per

second (201). In this scenario, Balon mediated hibernation may allow cells to better adapt to stress by taking advantage of the two biological functions of ribosome hibernation factors: protect ribosomes from degradation and modulate the energetically demanding process that is protein synthesis.

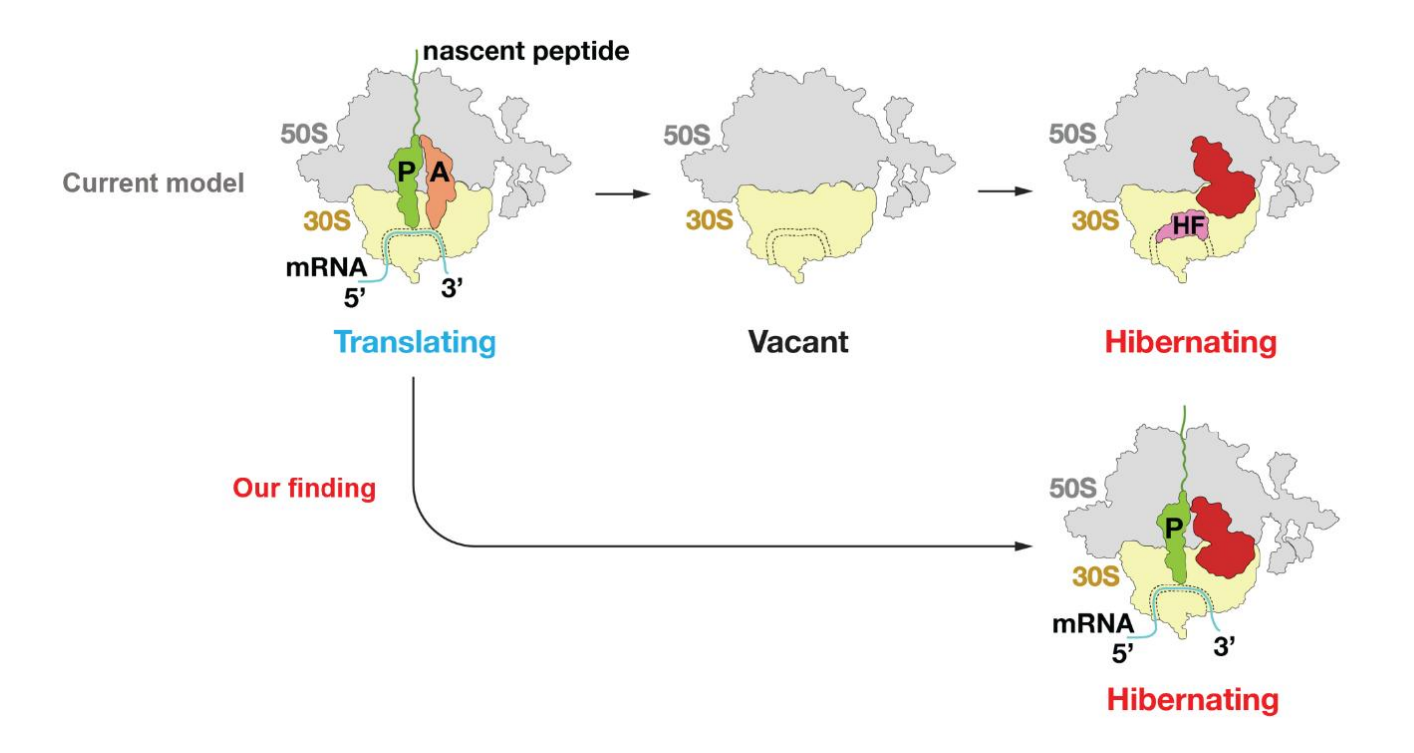


Figure 53. Balon allows ribosomes to enter hibernation using a novel mechanism of ribosome dormancy. It was previously thought that ribosomes can enter hibernation only in their vacant form. However, our study suggests that the state of hibernation is not limited to vacant ribosomes, and instead Balon could allow ribosomes to hibernate without the need to first disassociate from factors of protein synthesis.

The second advantage that Balon mediated ribosome hibernation may have over other mechanisms of ribosome hibernation relates to the number of ribosomes that may transition to a hibernating state at any given time upon stress exposure. Because Balon is able to bind ribosomes despite the presence of other ligands, such as mRNA or P-site ligands (including P-site tRNA or other hibernation factors, such as RaiA), it appears that Balon allows for more flexibility in terms of what ribosomes it can bind to. In other words, Balon binding may not be as "selective" as other hibernation factors that do not allow for the concurrent binding of mRNA or P-site ligands. As a result, it is

possible that Balon may bind a higher proportion of ribosomes in the cell and allow them to become dormant. This could potentially result in a heightened response to stress where a larger pool of ribosomes is kept in a hibernating state, instead of being degraded. If this is the case, this could represent an advantage to the cell once environmental conditions improve and a higher number of ribosomes is readily available to resume protein synthesis to baseline levels, and decrease the demand for ribosome biogenesis, an energetically costly process for the cell (202).

While cells that harbour hibernation factor Balon may have some advantages during stress response, Balon mediated ribosome hibernation may pose some disadvantages compared to mechanisms of ribosome hibernation that rely on an intermediate vacant state. One possible disadvantage of the binding state where the ribosome is associated with Balon, mRNA and P-site tRNA is that upon restoration of protein synthesis, these ribosomes may need to disassociate from these factors (and therefore become vacant) before restarting a new round of protein synthesis. This would first require the recruitment of ribosome recycling factors to the ribosome, which are proteins are responsible for splitting of the ribosomal subunits in-between rounds of protein synthesis (203). Additionally, any remnants of mRNA and the peptide chain that remain bound to Balon-associated ribosomes may possibly need to be targeted for degradation. By contrast, ribosomes that remain vacant during hibernation only need to become disassociated from the hibernation factor they are bound to, possibly facilitating the restart of protein synthesis upon the improvement of environmental conditions. It is important to note, however, that it is possible that Balon may be able to bind vacant ribosomes, as its binding site does not overlap with most of the active centres of the ribosome that are normally occupied during protein synthesis, such as the P site, the E site, and the mRNA binding channel, and it only occupies the A site. This means that while we did not observe vacant ribosomes bound to Balon under the conditions we tested, we cannot rule out the possibility that perhaps there is a small pool of vacant ribosomes that is associated with Balon under conditions of stress.

Overall, Balon mediated ribosome hibernation represents a novel strategy of ribosome dormancy in bacteria that may have notable implications to how bacteria modulate and preserve their ribosomes. While there may be possible advantages or

disadvantages of an alternative mechanism of ribosome hibernation in bacteria and its implications for cell fitness and survival, the hypotheses presented here remain to be tested.

### 5.2 OTHER POTENTIAL FUNCTIONS OF BALON

It is important to note that our findings do not preclude alternative biological functions of Balon. One potential role for this protein may involve sensing intracellular levels of GTP or the GDP/GTP ratio. Given that Balon appears to bind EF-Tu in its GDPbound state in complex with the ribosome, it is plausible that it could modulate the pool of active ribosomes in response to GTP availability, rather than completely inhibiting protein synthesis across nearly all cellular ribosomes. If true, this would suggest that Balon may play a role in regulating the metabolic response of bacterial cells in accordance with energy levels in the cell. Previously, experiments investigating the role of hibernation factor HPF in cellular responses to stress showed that HPF may be involved in the appropriate adjustment of ATP levels during long-term stationary phase. In these experiments, Listeria monocytogenes cells lacking HPF showed ATP levels that were 5 times higher than the wild type cells after prolonged stationary phase, suggesting that HPF may be involved in an energy regulation mechanism in the cell during stress (204). While we do not know if a similar phenomenon occurs in P. urativorans cells lacking Balon, we cannot rule out the possibility that during stress Balon may also be involved in modulating the translational response proportionately to the amount of GTP or the GDP/GTP in the cell.

Another possibility is that Balon may be involved in the rescue of stalled or collided ribosomes. Two or more ribosomes can collide during protein synthesis when translating an mRNA molecule with specific aberrations (205). These defects include mRNAs with secondary structures, lack of stop codons or chemically damaged mRNAs

(206). Once a ribosome becomes stalled upon encountering segments of mRNA with these defects, trailing ribosomes that are also translating the same transcript collide with the stalled or leading ribosome. These collision events have been shown to be caused by environmental stressors such as nutrient depletion or UV radiation (207). Because Balon interacts with ribosomes that are associated with mRNAs and P-site tRNA (thereby likely translating ribosomes) its involvement in ribosome collisions cannot be ruled out. In this scenario, Balon could potentially play a role in ribosome collisions as either an inhibitor of protein synthesis that allows cells to quickly halt translation by stalling ribosomes or perhaps as a factor that allows for the splitting (or rescue) of stalled ribosomes. Since Balon was initially identified and characterized in this study, additional research is necessary to elucidate the full spectrum of its biological activities.

# 5.3 BALON DISCOVERY PROVIDES AN INSIGHT INTO THE ORIGIN OF RIBOSOME HIBERNATION

On a separate note, our work provides an insight into the evolutionary origin of Balon. As discussed in the results section, Balon exhibits striking similarities to translation termination factor aeRF1 and the ribosome rescue factor Pelota in terms of structure conservation as well as binding location in the ribosome and apparent recruitment mechanism. This suggests that Balon is a distant homolog of aeRF1 and Pelota.

Interestingly, while Balon is found in the bacterial domain, both aeRF1 and Pelota are found in the archaeal and eukaryotic domains. This raises two potential scenarios that could explain the origins of Balon.

The first is that Balon, aeRF1 and Pelota evolved from a protein present in the last universal common ancestor, LUCA. As the tree of life diversified into different

domains the homologs of this protein evolved to serve different purposes in different domains of life, as evidenced by the distinct processes they partake in, and the functional motifs that allow them to play their respective roles during protein synthesis termination and ribosome rescue.

This hypothesis, however, does not fully address one critical aspect pertaining to the origins of Balon in relation to aeRF1 and Pelota. While aeRF1 and Pelota paralogues are universally conserved in the archaeal and eukaryotic domain (154), Balon is not, as we estimate that it is present in about 20% of all known bacterial species. This observation supports an alternative hypothesis: that Balon has originated in bacteria on the basis of interdomain horizontal gene transfer. It is possible that Balon may have been present in a common ancestor of archaea and eukaryotes (after their split from the bacterial domain) and later acquired by bacteria through horizontal gene transfer. While interdomain horizontal gene transfer is not a common phenomenon in nature, there have been documented cases of gene exchange between bacteria, eukaryotes and archaea (208) (209) (210).

The fact that Balon is a bacterial hibernation factor that is distant structural homolog of protein synthesis factors in archaea and eukaryotes suggests that Balon, aeRF1 and Pelota have not only a common origin, but that each of these proteins has been repurposed for a particular function within the ribosome's work cycle. For now, the exact origins of Balon remain uncertain, and answering the questions surrounding the evolution of this protein would warrant a dedicated study.

# 5.4 HOW DO RIBOSOMES RECRUIT HIBERNATION FACTORS DURING STRESS?

Another unanswered question relates to the mechanism of Balon recruitment to the ribosome in response to stress and Balon disassociation from the ribosome to resume protein synthesis.

In our study, we provided one clue to this elusive mechanism. Specifically, we have observed that Balon binds the ribosome in complex with EF-Tu during both cold shock and stationary phase. Furthermore, EF-Tu was also observed bound to Balon as a response to cold shock in both hibernating (RaiA bound) and translating (P-site tRNA bound) ribosomes. This suggests that EF-Tu is likely to be the factor responsible for recruitment of Balon to the ribosome regardless of the stressor P. urativorans cells are exposed to, and regardless of the binding state of the ribosome.

Our structural data and analysis have provided us with the necessary information to make these observations, however, they describe one particular step in the overall binding mechanism of Balon to the ribosome. For now we can only speculate about how exactly is Balon is recruited to the ribosome, whether or not it undergoes any conformational changes as it binds to the ribosome, and how and under what conditions it dissociates from the ribosome.

We hypothesize that because EF-Tu may be involved in recruiting Balon to the ribosome, and only EF-Tu in its GDP-bound state can bind Balon in complex in the ribosome as shown by our structural analysis, the availability of GDP-bound EF-Tu in the cell may be a key regulator of Balon binding to the ribosome. Testing this hypothesis would require the quantification of the intracellular concentration of EF-Tu in its GDP and GTP-bound states before and after stress. We know that there is only a 1.6 fold increase in the amount of Balon in cold shocked *P. urativorans* cells compared to noncold shocked cells (**Appendix 7**). This suggests that not only is there a baseline level of Balon before stress, but that this protein is present in the cell even when the cell is not

exposed to stress, yet it remains excluded from the ribosome. Taking this into account, it is possible that Balon may be present in the cytosol but may not be recruited to the ribosome while the cell is actively translating protein and likely most of the EF-Tu present in the cell is in its GTP-bound state.

It is currently unclear what mechanisms regulate expression of the Balon gene, and whether Balon is regulated at the transcriptional level.

Answering these questions would require further experiments that can elucidate Balon's regulatory, and binding and dissociation mechanisms. Some of these questions still remain unanswered in the field of bacterial ribosome hibernation as these exact mechanisms behind binding and dissociation remain unknown for all other hibernation factors in bacteria.

Overall, the discovery of Balon represents not only the characterization of another previously unknown bacterial hibernation factor, but it challenges our understanding of one of the mechanisms that allow bacteria to survive in hostile environments. Furthermore, it highlights the importance not limiting biological research to a few model organisms but instead explore the extraordinary diversity of life in our quest to understand nature.

### **RFFFRFNCFS**

- 1. Rittershaus ES, Baek SH, Sassetti CM. The normalcy of dormancy: common themes in microbial quiescence. Cell Host Microbe. 2013;13(6):643–51.
- 2. Vreeland RH, Rosenzweig WD, Powers DW. Isolation of a 250 million-year-old halotolerant bacterium from a primary salt crystal. Nature. 2000;407(6806):897–900.
- 3. Morono Y, Ito M, Hoshino T, Terada T, Hori T, Ikehara M, et al. Aerobic microbial life persists in oxic marine sediment as old as 101.5 million years. Nat Commun. 2020;11(1):3626.
- 4. Mammalian hibernation. Philos Trans R Soc Lond B Biol Sci. 1990;326(1237):669–86.
- 5. Lee CC. Is Human Hibernation Possible? Annu Rev Med. 2008;59(1):177–86.
- 6. Mohr SM, Bagriantsev SN, Gracheva EO. Cellular, molecular, and physiological adaptations of hibernation: the solution to environmental challenges. Annu Rev Cell Dev Biol. 2020;36(1):315–38.
- 7. McCarthy BJ. Variations in bacterial ribosomes. Biochim Biophys Acta. 1960;39(3):563-4.
- 8. Pullman ME, Monroy GC. A Naturally occurring inhibitor of mitochondrial adenosine triphosphatase. J Biol Chem. 1963;238(11):3762–9.
- 9. Hille MB. Inhibitor of protein synthesis isolated from ribosomes of unfertilised eggs and embryos of sea urchins. Nature. 1974;249(5457):556–8.
- 10. Patterson BD, Payne LA, Chen YZ, Graham D. An inhibitor of catalase induced by cold in chilling-sensitive plants. Plant Physiol. 1984;76(4):1014–8.
- 11. Gutteridge S, Parry MAJ, Burton S, Keys AJ, Mudd A, Feeney J, et al. A nocturnal inhibitor of carboxylation in leaves. Nature. 1986;324(6094):274–6.
- Chu-Ping M, Slaughter CA, DeMartino GN. Purification and characterization of a protein inhibitor of the 20S proteasome (macropain). Biochim Biophys Acta BBA-Protein Struct Mol Enzymol. 1992;1119(3):303–11.
- 13. Fernández-Tornero C. RNA polymerase I activation and hibernation: unique mechanisms for unique genes. Transcription. 2018;9(4):248–54.
- 14. Gambino R, Metafora S, Felicetti L, Raisman J. Properties of the ribosomal salt wash from unfertilized and fertilized sea urchin eggs and its effect on natural mRNA translation. Biochim Biophys Acta BBA-Nucleic Acids Protein Synth. 1973;312(2):377–91.
- 15. Huang FL, Warner AH. Control of protein synthesis in brine shrimp embryos by repression of ribosomal activity. Arch Biochem Biophys. 1974;163(2):716–27.
- 16. Ben-Shem A, Garreau De Loubresse N, Melnikov S, Jenner L, Yusupova G, Yusupov M. The structure of the eukaryotic ribosome at 3.0 Å resolution. Science. 2011 Dec 16;334(6062):1524–9.
- 17. Anger AM, Armache JP, Berninghausen O, Habeck M, Subklewe M, Wilson DN, et al. Structures of the human and *Drosophila* 80S ribosome. Nature. 2013;497(7447):80–5.

- 18. Wang YJ, Vaidyanathan PP, Rojas-Duran MF, Udeshi ND, Bartoli KM, Carr SA, et al. Lso2 is a conserved ribosome-bound protein required for translational recovery in yeast. PLoS Biol. 2018;16(9):e2005903.
- 19. Ehrenbolger K, Jespersen N, Sharma H, Sokolova YY, Tokarev YS, Vossbrinck CR, et al. Differences in structure and hibernation mechanism highlight diversification of the microsporidian ribosome. PLoS Biol. 2020;18(10):e3000958.
- 20. Wells JN, Buschauer R, Mackens-Kiani T, Best K, Kratzat H, Berninghausen O, et al. Structure and function of yeast Lso2 and human CCDC124 bound to hibernating ribosomes. PLoS Biol. 2020;18(7):e3000780.
- 21. Brown A, Baird MR, Yip MC, Murray J, Shao S. Structures of translationally inactive mammalian ribosomes. Sonenberg N, Manley JL, editors. eLife. 2018;7:e40486.
- 22. Hopes T, Norris K, Agapiou M, McCarthy CG, Lewis PA, O'Connell MJ, et al. Ribosome heterogeneity in *Drosophila melanogaster* gonads through paralog-switching. Nucleic Acids Res. 2022;50(4):2240–57.
- 23. Barandun J, Hunziker M, Vossbrinck CR, Klinge S. Evolutionary compaction and adaptation visualized by the structure of the dormant microsporidian ribosome. Nat Microbiol. 2019;4(11):1798–804.
- 24. Leesch F, Lorenzo-Orts L, Pribitzer C, Grishkovskaya I, Roehsner J, Chugunova A, et al. A molecular network of conserved factors keeps ribosomes dormant in the egg. Nature. 2023;613(7945):712–20.
- 25. Helena-Bueno K, Chan L, Melnikov S. Rippling life on a dormant planet: hibernation of ribosomes, RNA polymerases and other essential enzymes. Front Microbiol. 2024;15:1386179.
- 26. Wada A, Yamazaki Y, Fujita N, Ishihama A. Structure and probable genetic location of a" ribosome modulation factor" associated with 100S ribosomes in stationary-phase *Escherichia coli* cells. Proc Natl Acad Sci. 1990;87(7):2657–61.
- 27. Yoshida H, Maki Y, Furuike S, Sakai A, Ueta M, Wada A. YqjD is an inner membrane protein associated with stationary-phase ribosomes in *Escherichia coli*. J Bacteriol. 2012;194(16):4178–83.
- 28. Agafonov DE, Kolb VA, Nazimov IV, Spirin AS. A protein residing at the subunit interface of the bacterial ribosome. Proc Natl Acad Sci. 1999;96(22):12345–9.
- 29. Agafonov DE, Kolb VA, Spirin AS. Ribosome-associated protein that inhibits translation at the aminoacyl-tRNA binding stage. EMBO Rep. 2001;2(5):399–402.
- 30. Maki Y, Yoshida H, Wada A. Two proteins, YfiA and YhbH, associated with resting ribosomes in stationary phase *Escherichia coli*. Genes Cells. 2000;5(12):965–74.
- 31. Helena-Bueno K, Rybak MY, Ekemezie CL, Sullivan R, Brown CR, Dingwall C, et al. A new family of bacterial ribosome hibernation factors. Nature. 2024;626(8001):1125–32.
- 32. Petrov AS, Bernier CR, Hsiao C, Norris AM, Kovacs NA, Waterbury CC, Stepanov VG, Harvey SC, Fox GE, Wartell RM, Hud NV, Williams LD. Evolution of the ribosome at atomic resolution. Proc Natl Acad Sci. 2014;111(28):10251-6.
- 33. Kouba T, Koval' T, Sudzinová P, Pospíšil J, Brezovská B, Hnilicová J, et al. Mycobacterial HelD is a nucleic acids-clearing factor for RNA polymerase. Nat Commun. 2020;11(1):6419.

- 34. Pei HH, Hilal T, Chen ZA, Huang YH, Gao Y, Said N, et al. The δ subunit and NTPase HelD institute a two-pronged mechanism for RNA polymerase recycling. Nat Commun. 2020;11(1):6418.
- 35. Aibara S, Dienemann C, Cramer P. Structure of an inactive RNA polymerase II dimer. Nucleic Acids Res. 2021;49(18):10747–55.
- 36. Heiss FB, Daiß JL, Becker P, Engel C. Conserved strategies of RNA polymerase I hibernation and activation. Nat Commun. 2021;12(1):758.
- 37. Morichaud Z, Trapani S, Vishwakarma RK, Chaloin L, Lionne C, Lai-Kee-Him J, et al. Structural basis of the mycobacterial stress-response RNA polymerase auto-inhibition via oligomerization. Nat Commun. 2023;14(1):484.
- 38. Torreira E, Louro JA, Pazos I, Gonzalez-Polo N, Gil-Carton D, Duran AG, et al. The dynamic assembly of distinct RNA polymerase I complexes modulates rDNA transcription. Elife. 2017;6:e20832.
- 39. Moore BD, Seemann JR. Evidence that 2-carboxyarabinitol 1-phosphate binds to ribulose-1, 5-bisphosphate carboxylase *in vivo*. Plant Physiol. 1994;105(2):731–7.
- 40. Orr DJ, Robijns AKJ, Baker CR, Niyogi KK, Carmo-Silva E. Dynamics of Rubisco regulation by sugar phosphate derivatives and their phosphatases. J Exp Bot. 2023;74(2):581–90.
- 41. Salvucci ME, Crafts-Brandner SJ. Mechanism for deactivation of Rubisco under moderate heat stress. Physiol Plant. 2004 Dec;122(4):513–9.
- 42. Bracher A, Whitney SM, Hartl FU, Hayer-Hartl M. Biogenesis and Metabolic Maintenance of Rubisco. Annu Rev Plant Biol. 2017;68(1):29–60.
- 43. Parry MAJ, Keys AJ, Madgwick PJ, Carmo-Silva AE, Andralojc PJ. Rubisco regulation: a role for inhibitors. J Exp Bot. 2008;59(7):1569–80.
- 44. Gu J, Zhang L, Zong S, Guo R, Liu T, Yi J, et al. Cryo-EM structure of the mammalian ATP synthase tetramer bound with inhibitory protein IF1. Science. 2019;364(6445):1068–75.
- 45. Jespersen N, Ehrenbolger K, Winiger RR, Svedberg D, Vossbrinck CR, Barandun J. Structure of the reduced microsporidian proteasome bound by PI31-like peptides in dormant spores. Nat Commun. 2022;13(1):6962.
- 46. Tissières A, Watson JD. Ribonucleoprotein particles from *Escherichia coli*. Nature. 1958;182(4638):778–80.
- 47. Moen B, Janbu AO, Langsrud S, Langsrud O, Hobman JL, Constantinidou C, Kohler A, Rudi K. Global responses of *Escherichia coli* to adverse conditions determined by microarrays and FT-IR spectroscopy. Can J Microbiol. 2009;55(6):714-28.
- 48. Yoshida H, Wada A. The 100S ribosome: ribosomal hibernation induced by stress. WIREs RNA. 2014;5(5):723–32.
- 49. Huxley HE, Zubay G. Electron microscope observations on the structure of microsomal particles from *Escherichia coli*. J Mol Biol. 1960;2(1):10-IN8.
- 50. Taddei C. Ribosome arrangement during oogenesis of *Lacerta sicula* Raf. Exp Cell Res. 1972;70(2):285–92.
- 51. Burkholder GD, Comings DE, Okada TA. A storage form of ribosomes in mouse oocytes. Exp Cell Res. 1971;69(2):361–71.

- 52. Kessel RG. An electron microscope study of nuclear-cytoplasmic exchange in oocytes of *Ciona intestinalis*. J Ultrastruct Res. 1966;15(1–2):181–96.
- 53. Morimoto T, Blobel G, Sabatini DD. Ribosome crystallization in chicken embryos: II. Conditions for the formation of ribosome tetramers *in vivo*. J Cell Biol. 1972;52(2):355–66.
- 54. Yonath A. Hibernating bears, antibiotics, and the evolving ribosome (Nobel Lecture). Angew Chem Int Ed. 2010;49(26):4340–54.
- 55. Gemin O, Gluc M, Purdy M, Rosa H, Niemann M, Peskova Y, et al. Hibernating ribosomes tether to mitochondria as an adaptive response to cellular stress during glucose depletion. bioRxiv. 2023.
- 56. Sharma MR, Dönhöfer A, Barat C, Marquez V, Datta PP, Fucini P, et al. PSRP1 is not a ribosomal protein, but a ribosome-binding factor that is recycled by the ribosome-recycling factor (RRF) and elongation factor G (EF-G) 2. J Biol Chem. 2010;285(6):4006–14.
- 57. Adachi K, Sells BH. The effect of magnesium starvation on the dissociation of ribosomal proteins from *Escherichia coli* K-12 ribosomes. Biochim Biophys Acta BBA-Nucleic Acids Protein Synth. 1979;563(1):163–70.
- 58. Davis BD, Luger SM, Tai PC. Role of ribosome degradation in the death of starved *Escherichia coli* cells. J Bacteriol. 1986;166(2):439–45.
- 59. Burton RF. Biology by numbers: an encouragement to quantitative thinking. Cambridge University Press; 1998.
- 60. Schmidt A, Kochanowski K, Vedelaar S, Ahrné E, Volkmer B, Callipo L, et al. The quantitative and condition-dependent *Escherichia coli* proteome. Nat Biotechnol. 2016;34(1):104–10.
- 61. Wada A. Analysis of *Escherichia coli* ribosomal proteins by an improved two dimensional gel electrophoresis. II. Characterization of four new proteins. J Biochem (Tokyo). 1986;100(6):1595–605.
- 62. Yamagishi M, Matsushima H, Wada A, Sakagami M, Fujita N, Ishihama A. Regulation of the *Escherichia coli* rmf gene encoding the ribosome modulation factor: growth phase-and growth rate-dependent control. EMBO J. 1993;12(2):625–30.
- 63. Wada A, Igarashi K, Yoshimura S, Aimoto S, Ishihama A. Ribosome modulation factor: stationary growth phase-specific inhibitor of ribosome functions from *Escherichia coli*. Biochem Biophys Res Commun. 1995;214(2):410–7.
- 64. Yoshida H, Maki Y, Kato H, Fujisawa H, Izutsu K, Wada C, et al. The ribosome modulation factor (RMF) binding site on the 100S ribosome of *Escherichia coli*. J Biochem (Tokyo). 2002;132(6):983–9.
- 65. Polikanov YS, Blaha GM, Steitz TA. How hibernation factors RMF, HPF, and YfiA turn off protein synthesis. Science. 2012;336(6083):915–8.
- 66. Shine J, Dalgarno L. The 3'-terminal sequence of *Escherichia coli* 16S ribosomal RNA: complementarity to nonsense triplets and ribosome binding sites. Proc Natl Acad Sci. 1974;71(4):1342–6.
- 67. Sengupta J, Agrawal RK, Frank J. Visualization of protein S1 within the 30S ribosomal subunit and its interaction with messenger RNA. Proc Natl Acad Sci. 2001;98(21):11991–6.
- 68. Laursen BS, Sørensen HP, Mortensen KK, Sperling-Petersen HU. Initiation of protein synthesis in bacteria. Microbiol Mol Biol Rev. 2005;69(1):101–23.

- 69. Yusupova GZ, Yusupov MM, Cate JHD, Noller HF. The path of messenger RNA through the ribosome. Cell. 2001;106(2):233–41.
- 70. Omotajo D, Tate T, Cho H, Choudhary M. Distribution and diversity of ribosome binding sites in prokaryotic genomes. BMC Genomics. 2015;16:1–8.
- 71. Wen JD, Kuo ST, Chou HHD. The diversity of Shine-Dalgarno sequences sheds light on the evolution of translation initiation. RNA Biol. 2021;18(11):1489–500.
- 72. Brodersen DE, Clemons Jr WM, Carter AP, Wimberly BT, Ramakrishnan V. Crystal structure of the 30 S ribosomal subunit from *Thermus thermophilus*: structure of the proteins and their interactions with 16 S RNA. J Mol Biol. 2002;316(3):725–68.
- 73. Prossliner T, Skovbo Winther K, Sørensen MA, Gerdes K. Ribosome hibernation. Annu Rev Genet. 2018;52:321–48.
- 74. Ueta M, Ohniwa RL, Yoshida H, Maki Y, Wada C, Wada A. Role of HPF (hibernation promoting factor) in translational activity in *Escherichia coli*. J Biochem (Tokyo). 2008;143(3):425–33.
- 75. Maki Y, Yoshida H, Wada A. Two proteins, YfiA and YhbH, associated with resting ribosomes in stationary phase *Escherichia coli*. Genes Cells. 2000;5(12):965–74.
- 76. Ueta M, Yoshida H, Wada C, Baba T, Mori H, Wada A. Ribosome binding proteins YhbH and YfiA have opposite functions during 100S formation in the stationary phase of *Escherichia coli*. Genes Cells. 2005;10(12):1103–12.
- 77. Ogle JM, Carter AP, Ramakrishnan V. Insights into the decoding mechanism from recent ribosome structures. Trends Biochem Sci. 2003;28(5):259–66.
- 78. Ueta M, Wada C, Daifuku T, Sako Y, Bessho Y, Kitamura A, et al. Conservation of two distinct types of 100S ribosome in bacteria. Genes Cells. 2013;18(7):554–74.
- 79. Franken LE, Oostergetel GT, Pijning T, Puri P, Arkhipova V, Boekema EJ, et al. A general mechanism of ribosome dimerization revealed by single-particle cryo-electron microscopy. Nat Commun. 2017;8(1):722.
- 80. Puri P, Eckhardt TH, Franken LE, Fusetti F, Stuart MCA, Boekema EJ, et al. *Lactococcus lactis* YfiA is necessary and sufficient for ribosome dimerization. Mol Microbiol. 2014;91(2):394–407.
- 81. Khusainov I, Vicens Q, Ayupov R, Usachev K, Myasnikov A, Simonetti A, et al. Structures and dynamics of hibernating ribosomes from *Staphylococcus aureus* mediated by intermolecular interactions of HPF. EMBO J. 2017;36(14):2073–87.
- 82. Ueta M, Wada C, Wada A. Formation of 100S ribosomes in *Staphylococcus aureus* by the hibernation promoting factor homolog SaHPF. Genes Cells. 2010;15(1):43–58.
- 83. El-Sharoud WM, Niven GW. The influence of ribosome modulation factor on the survival of stationary-phase *Escherichia coli* during acid stress. Microbiology. 2007;153(1):247–53.
- 84. Prossliner T, Gerdes K, Sørensen MA, Winther KS. Hibernation factors directly block ribonucleases from entering the ribosome in response to starvation. Nucleic Acids Res. 2021;49(4):2226–39.
- 85. Lipońska A, Yap MNF. Hibernation-promoting factor sequesters *Staphylococcus aureus* ribosomes to antagonize RNase R-mediated nucleolytic degradation. MBio. 2021;12(4):10.

- 86. Trauner A, Lougheed KE, Bennett MH, Hingley-Wilson SM, Williams HD. The dormancy regulator DosR controls ribosome stability in hypoxic mycobacteria. J Biol Chem. 2012;287(28):24053–63.
- 87. Akanuma G, Kazo Y, Tagami K, Hiraoka H, Yano K, Suzuki S, et al. Ribosome dimerization is essential for the efficient regrowth of *Bacillus subtilis*. Microbiology. 2016;162(3):448–58.
- 88. Feaga HA, Kopylov M, Kim JK, Jovanovic M, Dworkin J. Ribosome dimerization protects the small subunit. J Bacteriol. 2020;202(10):10.
- 89. Dimitrova-Paternoga L, Kasvandik S, Beckert B, Granneman S, Tenson T, Wilson DN, et al. Structural basis of ribosomal 30S subunit degradation by RNase R. Nature. 2024;1–8.
- 90. Basu A, Yap MNF. Disassembly of the *Staphylococcus aureus* hibernating 100S ribosome by an evolutionarily conserved GTPase. Proc Natl Acad Sci. 2017;114(39):E8165–73.
- 91. Bisset KA. The Cytology of Micrococcus cryophilus. J Bacteriol. 1954;67(1):41-4.
- 92. McLean RA, Sulzbacher WL, Mudd S. *Micrococcus cryophilus*, spec. nov.; a large coccus especially suitable for cytologic study. J Bacteriol. 1951;62(6):723–8.
- 93. Bowman JP, Cavanagh J, Austin JJ, Sanderson K. Novel *Psychrobacter* species from Antarctic ornithogenic soils. Int J Syst Evol Microbiol. 1996;46(4):841–8.
- 94. Aislabie J, Jordan S, Ayton J, Klassen JL, Barker GM, Turner S. Bacterial diversity associated with ornithogenic soil of the Ross Sea region, Antarctica. Can J Microbiol. 2009;55(1):21–36.
- 95. Krucon T, Dziewit L, Drewniak L. Insight into ecology, metabolic potential, and the taxonomic composition of bacterial communities in the periodic water pond on King George Island (Antarctica). Front Microbiol. 2021;12:708607.
- 96. Cabezas A, Azziz G, Bovio-Winkler P, Fuentes L, Braga L, Wenzel J, et al. Ubiquity and diversity of cold adapted denitrifying bacteria isolated from diverse Antarctic ecosystems. Front Microbiol. 2022;13:827228.
- 97. Kämpfer P, Glaeser SP, Irgang R, Fernández-Negrete G, Poblete-Morales M, Fuentes-Messina D, et al. Psychrobacter pygoscelis sp. nov. isolated from the penguin *Pygoscelis papua*. Int J Syst Evol Microbiol. 2020;70(1):211–9.
- 98. Kudo T, Kidera A, Kida M, Kawauchi A, Shimizu R, Nakahara T, et al. Draft genome sequences of *Psychrobacter* strains JCM 18900, JCM 18901, JCM 18902, and JCM 18903, isolated preferentially from frozen aquatic organisms. Genome Announc. 2014;2(2):10.
- 99. Yassin AF, Busse HJ. *Psychrobacter lutiphocae* sp. nov., isolated from the faeces of a seal. Int J Syst Evol Microbiol. 2009;59(8):2049–53.
- 100. Kämpfer P, Jerzak L, Wilharm G, Golke J, Busse HJ, Glaeser SP. *Psychrobacter ciconiae* sp. nov., isolated from white storks (*Ciconia ciconia*). Int J Syst Evol Microbiol. 2015;65(3):772–7.
- 101. Welter DK, Ruaud A, Henseler ZM, De Jong HN, Van Coeverden de Groot P, Michaux J, et al. Free-living, psychrotrophic bacteria of the genus *Psychrobacter* are descendants of pathobionts. Msystems. 2021;6(2):10.
- 102. Psychrobacter. Encyclopedia of Food Microbiology (Second Edition) (2014), pp. 261-268.
- 103. Rodrigues DF, da C Jesus E, Ayala-del-Río HL, Pellizari VH, Gilichinsky D, Sepulveda-Torres L, et al. Biogeography of two cold-adapted genera: *Psychrobacter* and *Exiguobacterium*. ISME J. 2009 Jun;3(6):658–65.

- 104. Morita RY. Psychrophilic bacteria. Bacteriol Rev. 1975;39(2):144-67.
- 105. Morita RY. Psychrophiles and Psychrotrophs. E LS. 2001.
- 106. Cgibbon LM, Russell NJ. The turnover of phospholipids in the psychrophilic bacterium *Micrococcus cryophilus* during adaptation to changes in growth temperature. Microbiology. 1985;131(9):2293–302.
- 107. Chintalapati S, Kiran MD, Shivaji S. Role of membrane lipid fatty acids in cold adaptation. Cell Mol Biol. 2004;50(5):631–42.
- 108. Hirano A, Shiraki K, Arakawa T. Polyethylene glycol behaves like weak organic solvent. Biopolymers. 2012;97(2):117–22.
- 109. Emsley P, Lohkamp B, Scott WG, Cowtan K. Features and development of Coot. Acta Crystallogr D Biol Crystallogr. 2010;66(4):486–501.
- 110. Jumper J, Evans R, Pritzel A, Green T, Figurnov M, Ronneberger O, et al. Highly accurate protein structure prediction with AlphaFold. Nature. 2021;596(7873):583–9.
- 111. Polikanov YS, Melnikov SV, Söll D, Steitz TA. Structural insights into the role of rRNA modifications in protein synthesis and ribosome assembly. Nat Struct Mol Biol. 2015;22(4):342–4.
- 112. Pettersen EF, Goddard TD, Huang CC, Meng EC, Couch GS, Croll TI, et al. UCSF ChimeraX: Structure visualization for researchers, educators, and developers. Protein Sci. 2021;30(1):70–82.
- 113. Liebschner D, Afonine PV, Baker ML, Bunkóczi G, Chen VB, Croll TI, et al. Macromolecular structure determination using X-rays, neutrons and electrons: recent developments in Phenix. Acta Crystallogr Sect Struct Biol. 2019;75(10):861–77.
- 114. Madej T, Lanczycki CJ, Zhang D, Thiessen PA, Geer RC, Marchler-Bauer A, et al. MMDB and VAST+: tracking structural similarities between macromolecular complexes. Nucleic Acids Res. 2014;42(D1):D297–303.
- 115. Williams CJ, Headd JJ, Moriarty NW, Prisant MG, Videau LL, Deis LN, et al. MolProbity: More and better reference data for improved all-atom structure validation. Protein Sci. 2018;27(1):293–315.
- 116. Potter SC, Luciani A, Eddy SR, Park Y, Lopez R, Finn RD. HMMER web server: 2018 update. Nucleic Acids Res. 2018;46(W1):W200–4.
- 117. Sievers F, Wilm A, Dineen D, Gibson TJ, Karplus K, Li W, et al. Fast, scalable generation of high-quality protein multiple sequence alignments using Clustal Omega. Mol Syst Biol. 2011;7(1):539.
- 118. Ishihama Y, Oda Y, Tabata T, Sato T, Nagasu T, Rappsilber J, et al. Exponentially modified protein abundance index (emPAI) for estimation of absolute protein amount in proteomics by the number of sequenced peptides per proteins. Mol Cell Proteomics. 2005;4(9):1265–72.
- 119. Netzer WJ, Hartl FU. Protein folding in the cytosol: chaperonin-dependent and -independent mechanisms. Trends Biochem Sci. 1998;23(2):68–73.
- 120. Wilson DN, Nierhaus KH. The ribosome through the looking glass. Angew Chem Int Ed Engl. 2003;42(30):3464–86.
- 121. Dever TE, Ivanov IP. Roles of polyamines in translation. J Biol Chem. 2018;293(48):18719–29.
- 122. Nierhaus KH. Mg $^{2+}$ , K $^{+}$ , and the Ribosome. J Bacteriol. 2014;196(22):3817–9.

- 123. Gor K, Duss O. Emerging quantitative biochemical, structural, and biophysical methods for studying ribosome and protein–RNA complex assembly. Biomolecules. 2023;13(5):866.
- 124. Farías-Rico JA, Mourra-Díaz CM. A short tale of the origin of proteins and ribosome evolution. Microorganisms. 2022 Oct;10(11):2115.
- 125. Rodrigues DF, Tiedje JM. Coping with our cold planet. Appl Environ Microbiol. 2008;74(6):1677-86
- 126. Cold adaptation of microorganisms. Philos Trans R Soc Lond B Biol Sci. 1990;326(1237):595–611.
- 127. Shu WS, Huang LN. Microbial diversity in extreme environments. Nat Rev Microbiol. 2022;20(4):219–35.
- 128. Gianese G, Argos P, Pascarella S. Structural adaptation of enzymes to low temperatures. Protein Eng. 2001;14(3):141–8.
- 129. Zeldovich KB, Berezovsky IN, Shakhnovich EI. Protein and DNA sequence determinants of thermophilic adaptation. PLoS Comput Biol. 2007;3(1):e5.
- 130. Goncearenco A, Ma BG, Berezovsky IN. Molecular mechanisms of adaptation emerging from the physics and evolution of nucleic acids and proteins. Nucleic Acids Res. 2014;42(5):2879–92.
- 131. Santiago M, Ramírez-Sarmiento CA, Zamora RA, Parra LP. Discovery, molecular mechanisms, and industrial applications of cold-active enzymes. Front Microbiol. 2016;7.
- 132. Bhatia RK, Ullah S, Hoque MZ, Ahmad I, Yang YH, Bhatt AK, et al. Psychrophiles: A source of cold-adapted enzymes for energy efficient biotechnological industrial processes. J Environ Chem Eng. 2021;9(1):104607.
- 133. Xu H, Xu D, Liu Y. Molecular Biology Applications of Psychrophilic Enzymes: Adaptations, Advantages, Expression, and Prospective. Appl Biochem Biotechnol. 2024;6.
- 134. Liu Y, Zhang N, Ma J, Zhou Y, Wei Q, Tian C, et al. Advances in cold-adapted enzymes derived from microorganisms. Front Microbiol. 2023;14:1152847.
- 135. Yusupov MM, Yusupova GZh, Baucom A, Lieberman K, Earnest TN, Cate JHD, et al. Crystal structure of the ribosome at 5.5 Å resolution. Science. 2001 May 4;292(5518):883–96.
- 136. Oshima T, Imahori K. Description of *Thermus thermophilus* (Yoshida and Oshima) comb. nov., a nonsporulating thermophilic bacterium from a Japanese thermal spa. Int J Syst Bacteriol. 1974;24(1):102–12.
- 137. Sas-Chen A, Thomas JM, Matzov D, Taoka M, Nance KD, Nir R, et al. Dynamic RNA acetylation revealed by quantitative cross-evolutionary mapping. Nature. 2020;583(7817):638–43.
- 138. Atomi H, Fukui T, Kanai T, Morikawa M, Imanaka T. Description of *Thermococcus kodakaraensis* sp. nov., a well studied hyperthermophilic archaeon previously reported as *Pyrococcus* sp. KOD1. Archaea. 2004;1(4):263.
- 139. Cheng J, Kellner N, Berninghausen O, Hurt E, Beckmann R. 3.2-Å-resolution structure of the 90S preribosome before A1 pre-rRNA cleavage. Nat Struct Mol Biol. 2017;24(11):954–64.
- 140. Kellner N, Schwarz J, Sturm M, Fernandez-Martinez J, Griesel S, Zhang W, et al. Developing genetic tools to exploit *Chaetomium thermophilum* for biochemical analyses of eukaryotic macromolecular assemblies. Sci Rep. 2016;6(1):20937.

- 141. Rivera MC, Maguire B, Lake JA. Isolation of ribosomes and polysomes. Cold Spring Harb Protoc. 2015;2015(3).
- 142. Zhang Y, Gross CA. Cold shock response in bacteria. Annu Rev Genet. 2021;55:377–400.
- 143. Maki Y, Yoshida H. Ribosomal hibernation-associated factors in *Escherichia coli*. Microorganisms. 2021;10(1):33.
- 144. Glaeser RM, Hall RJ. Reaching the information limit in Cryo-EM of biological macromolecules: experimental aspects. Biophys J. 2011;100(10):2331–7.
- 145. Nilsson M, Bülow L, Wahlund KG. Use of flow field-flow fractionation for the rapid quantitation of ribosome and ribosomal subunits in *Escherichia coli* at different protein production conditions. Biotechnol Bioeng. 1997;54(5):461–7.
- 146. Scott M, Gunderson CW, Mateescu EM, Zhang Z, Hwa T. Interdependence of cell growth and gene expression: origins and consequences. Science. 2010;330(6007):1099–102.
- 147. Mathieson W, Thomas GA. Simultaneously extracting DNA, RNA, and protein using kits: Is sample quantity or quality prejudiced? Anal Biochem. 2013;433(1):10–8.
- 148. Rheinberger J, Oostergetel G, Resch GP, Paulino C. Optimized cryo-EM data-acquisition workflow by sample-thickness determination. Acta Crystallogr Sect Struct Biol. 2021;77(5):565–71.
- 149. Bertoline LMF, Lima AN, Krieger JE, Teixeira SK. Before and after AlphaFold2: An overview of protein structure prediction. Front Bioinforma. 2023;3:1120370.
- 150. Zhou J, Lancaster L, Donohue JP, Noller HF. How the ribosome hands the A-site tRNA to the P site during EF-G-catalyzed translocation. Science. 2014;345(6201):1188–91.
- 151. Reuveni S, Ehrenberg M, Paulsson J. Ribosomes are optimized for autocatalytic production. Nature. 2017;547(7663):293–7.
- 152. Petropoulos AD, McDonald ME, Green R, Zaher HS. Distinct roles for release factor 1 and release factor 2 in translational quality control. J Biol Chem. 2014;289(25):17589–96.
- 153. Inagaki Y, Ford Doolittle W. Evolution of the eukaryotic translation termination system: origins of release factors. Mol Biol Evol. 2000;17(6):882–9.
- 154. Atkinson GC, Baldauf SL, Hauryliuk V. Evolution of nonstop, no-go and nonsense-mediated mRNA decay and their termination factor-derived components. BMC Evol Biol. 2008;8(1):290.
- 155. Franckenberg S, Becker T, Beckmann R. Structural view on recycling of archaeal and eukaryotic ribosomes after canonical termination and ribosome rescue. Curr Opin Struct Biol. 2012;22(6):786–96.
- 156. Buskirk AR, Green R. Ribosome pausing, arrest and rescue in bacteria and eukaryotes. Philos Trans R Soc B Biol Sci. 2017;372(1716):20160183.
- Hellen CU. Translation termination and ribosome recycling in eukaryotes. Cold Spring Harb Perspect Biol. 2018;10(10):a032656.
- 158. Song H, Mugnier P, Das AK, Webb HM, Evans DR, Tuite MF, et al. The crystal structure of human eukaryotic release factor eRF1—mechanism of stop codon recognition and peptidyl-tRNA hydrolysis. Cell. 2000;100(3):311–21.

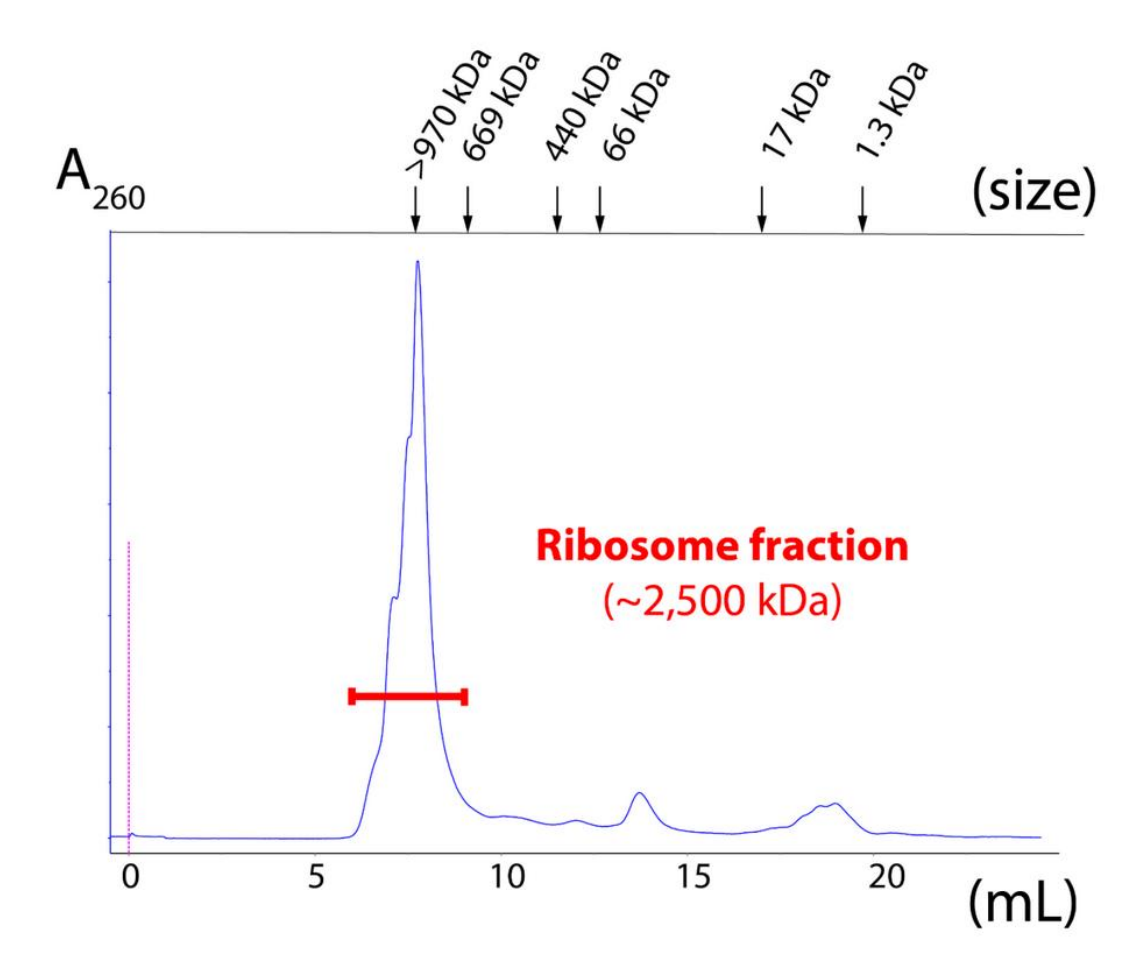
- 159. Brown A, Shao S, Murray J, Hegde RS, Ramakrishnan V. Structural basis for stop codon recognition in eukaryotes. Nature. 2015;524(7566):493–6.
- 160. Merritt GH, Naemi WR, Mugnier P, Webb HM, Tuite MF, von der Haar T. Decoding accuracy in eRF1 mutants and its correlation with pleiotropic quantitative traits in yeast. Nucleic Acids Res. 2010 Sep;38(16):5479–92.
- 161. Frolova LY, Tsivkovskii RY, Sivolobova GF, Oparina NY, Serpinsky OI, Blinov VM, et al. Mutations in the highly conserved GGQ motif of class 1 polypeptide release factors abolish ability of human eRF1 to trigger peptidyl-tRNA hydrolysis. RNA. 1999;5(8):1014–20.
- 162. Seit-Nebi A, Frolova L, Justesen J, Kisselev L. Class-1 translation termination factors: invariant GGQ minidomain is essential for release activity and ribosome binding but not for stop codon recognition. Nucleic Acids Res. 2001;29(19):3982–7.
- 163. Becker T, Franckenberg S, Wickles S, Shoemaker CJ, Anger AM, Armache JP, et al. Structural basis of highly conserved ribosome recycling in eukaryotes and archaea. Nature. 2012;482(7386):501–6.
- 164. Kobayashi K, Kikuno I, Kuroha K, Saito K, Ito K, Ishitani R, et al. Structural basis for mRNA surveillance by archaeal Pelota and GTP-bound EF1α complex. Proc Natl Acad Sci.2010;107(41):17575–9.
- 165. Hilal T, Yamamoto H, Loerke J, Bürger J, Mielke T, Spahn CM. Structural insights into ribosomal rescue by Dom34 and Hbs1 at near-atomic resolution. Nat Commun. 2016;7(1):13521.
- 166. Martijn J, Vosseberg J, Guy L, Offre P, Ettema TJG. Deep mitochondrial origin outside the sampled alphaproteobacteria. Nature. 2018 May;557(7703):101–5.
- 167. Roger AJ, Muñoz-Gómez SA, Kamikawa R. The Origin and Diversification of Mitochondria. Curr Biol. 2017;27(21):R1177–92.
- 168. HD Park. Rv3133c/dosR is a transcription factor that mediates the hypoxic response of *Mycobacterium tuberculosis*. Mol Microbiol. 2003;48:833–43.
- 169. Liu D, Hao K, Wang W, Peng C, Dai Y, Jin R, et al. Rv2629 overexpression delays *Mycobacterium smegmatis* and *Mycobacteria tuberculosis* entry into log-phase and increases pathogenicity of *Mycobacterium smegmatis* in mice. Front Microbiol. 2017;8:296597.
- 170. Pedreira T, Elfmann C, Stülke J. The current state of Subti Wiki, the database for the model organism *Bacillus subtilis*. Nucleic Acids Res. 2022;50(D1):D875–82.
- 171. Loh PG, Song H. Structural and mechanistic insights into translation termination. Curr Opin Struct Biol. 2010;20(1):98–103.
- 172. Frolova L, Seit-Nebi A, Kisselev LEV. Highly conserved NIKS tetrapeptide is functionally essential in eukaryotic translation termination factor eRF1. RNA. 2002;8(2):129–36.
- 173. Kobayashi K, Saito K, Ishitani R, Ito K, Nureki O. Structural basis for translation termination by archaeal RF1 and GTP-bound EF1α complex. Nucleic Acids Res. 2012;40(18):9319–28.
- 174. Haslbeck M, Vierling E. A first line of stress defense: small heat shock proteins and their function in protein homeostasis. J Mol Biol. 2015;427(7):1537–48.
- 175. Gutierrez C, Devedjian JC. Osmotic induction of gene osmC expression in *Escherichia coli* K12. J Mol Biol. 1991;220(4):959–73.

- 176. Yim HH, Villarejo M. osmY, a new hyperosmotically inducible gene, encodes a periplasmic protein in *Escherichia coli*. J Bacteriol. 1992;174(11):3637–44.
- 177. Masuda N, Church GM. Regulatory network of acid resistance genes in *Escherichia coli*. Mol Microbiol. 2003;48(3):699–712.
- 178. Lomovskaya O, Lewis KIM. Emr, an *Escherichia coli* locus for multidrug resistance. Proc Natl Acad Sci U.S.A. 1992;89(19):8938–42.
- 179. Filipowicz W. Making ends meet: a role of RNA ligase RTCB in unfolded protein response. EMBO J. 2014;33(24):2887–9.
- 180. Temmel H, Müller C, Sauert M, Vesper O, Reiss A, Popow J, et al. The RNA ligase RtcB reverses MazF-induced ribosome heterogeneity in *Escherichia coli*. Nucleic Acids Res. 2017;45(8):4708–21.
- 181. Tian Y, Zeng F, Raybarman A, Fatma S, Carruthers A, Li Q, et al. Sequential rescue and repair of stalled and damaged ribosome by bacterial PrfH and RtcB. Proc Natl Acad Sci. 2022;119(29):e2202464119.
- 182. Sharpe ML, Gao C, Kendall SL, Baker EN, Lott JS. The structure and unusual protein chemistry of hypoxic response protein 1, a latency antigen and highly expressed member of the DosR regulon in *Mycobacterium tuberculosis*. J Mol Biol. 2008;383(4):822–36.
- 183. Sun C, Yang G, Yuan J, Peng X, Zhang C, Zhai X, et al. *Mycobacterium tuberculosis* hypoxic response protein 1 (Hrp1) augments the pro-inflammatory response and enhances the survival of *Mycobacterium smegmatis* in murine macrophages. J Med Microbiol. 2017;66(7):1033–44.
- 184. Yousefian N, Ornik-Cha A, Poussard S, Decossas M, Berbon M, Daury L, et al. Structural characterization of the EmrAB-TolC efflux complex from *E. coli*. Biochim Biophys Acta BBA-Biomembr. 2021;1863(1):183488.
- 185. Voorhees RM, Weixlbaumer A, Loakes D, Kelley AC, Ramakrishnan V. Insights into substrate stabilization from snapshots of the peptidyl transferase center of the intact 70S ribosome. Nat Struct Mol Biol. 2009;16(5):528–33.
- 186. Nissen P, Nyborg J. EF-G and EF-Tu Structures and Translation Elongation in Bacteria. 2004.
- 187. Schuette JC, Murphy IV FV, Kelley AC, Weir JR, Giesebrecht J, Connell SR, et al. GTPase activation of elongation factor EF-Tu by the ribosome during decoding. EMBO J. 2009;28(6):755–65.
- 188. Loveland AB, Demo G, Korostelev AA. Cryo-EM of elongating ribosome with EF-Tu• GTP elucidates tRNA proofreading. Nature. 2020;584(7822):640–5.
- 189. Harvey KL, Jarocki VM, Charles IG, Djordjevic SP. The diverse functional roles of elongation factor Tu (EF-Tu) in microbial pathogenesis. Front Microbiol. 2019;10:2351.
- 190. Defeu Soufo HJ, Reimold C, Linne U, Knust T, Gescher J, Graumann PL. Bacterial translation elongation factor EF-Tu interacts and colocalizes with actin-like MreB protein. Proc Natl Acad Sci. 2010;107(7):3163–8.
- 191. Saito K, Kobayashi K, Wada M, Kikuno I, Takusagawa A, Mochizuki M, et al. Omnipotent role of archaeal elongation factor 1 alpha (EF1α) in translational elongation and termination, and quality control of protein synthesis. Proc Natl Acad Sci. 2010;107(45):19242–7.
- 192. Zamakhaev M, Grigorov A, Bespyatykh J, Azhikina T, Goncharenko A, Shumkov M. VapC toxin switches *M. smegmatis* cells into dormancy through 23S rRNA cleavage. Arch Microbiol. 2023;205(1):28.

- 193. Diaconu M, Kothe U, Schlünzen F, Fischer N, Harms JM, Tonevitsky AG, et al. Structural basis for the function of the ribosomal L7/12 stalk in factor binding and GTPase activation. Cell. 2005;121(7):991–1004.
- 194. Day ES, Cote SM, Whitty A. Binding efficiency of protein–protein complexes. Biochemistry. 2012;51(45):9124–36.
- 195. Leiva LE, Zegarra V, Bange G, Ibba M. At the crossroad of nucleotide dynamics and protein synthesis in bacteria. Microbiol Mol Biol Rev. 2023;87(1):e00044-22.
- 196. Xu B, Liu L, Song G. Functions and Regulation of Translation Elongation Factors. Front Mol Biosci. 2022;8.
- 197. Kaledhonkar S, Fu Z, Caban K, Li W, Chen B, Sun M, et al. Late steps in bacterial translation initiation visualized using time-resolved cryo-EM. Nature. 2019;570(7761):400–4.
- 198. Jha S, Komar AA. Birth, life and death of nascent polypeptide chains. Biotechnol J. 2011;6(6):623–40.
- 199. Petry S, Weixlbaumer A, Ramakrishnan V. The termination of translation. Curr Opin Struct Biol. 2008;18(1):70–7.
- 200. Pedersen S. *Escherichia coli* ribosomes translate in vivo with variable rate. EMBO J. 1984;3(12):2895–8.
- 201. Se M, Jj I. Translational control of protein synthesis in *Staphylococcus aureus*. J Bacteriol. 1975;122(3).
- 202. Zegarra V, Bedrunka P, Bange G, Czech L. How to save a bacterial ribosome in times of stress. Semin Cell Dev Biol. 2023;136:3–12.
- 203. Sm S, Mg G. Mechanisms of ribosome recycling in bacteria and mitochondria: a structural perspective. RNA Biol. 2022;19(1).
- 204. Kline BC, McKay SL, Tang WW, Portnoy DA. The *Listeria monocytogenes* hibernation-promoting factor is required for the formation of 100S ribosomes, optimal fitness, and pathogenesis. J Bacteriol. 2015;197(3):581–91.
- 205. Meydan S, Guydosh NR. A cellular handbook for collided ribosomes: surveillance pathways and collision types. Curr Genet. 2021;67(1):19–26.
- 206. Iyer KV, Müller M, Tittel LS, Winz ML. Molecular highway patrol for ribosome vollisions. ChemBioChem. 2023;24(20):e202300264.
- 207. Wu CCC, Peterson A, Zinshteyn B, Regot S, Green R. Ribosome collisions trigger general stress responses to regulate cell fate. Cell. 2020;182(2):404-416.e14.
- 208. Koonin EV, Makarova KS, Aravind L. Horizontal Gene Transfer in Prokaryotes: Quantification and Classification1. Annu Rev Microbiol. 2001;55:709–42.
- 209. Cote-L'Heureux A, Maurer-Alcalá XX, Katz LA. Old genes in new places: A taxon-rich analysis of interdomain lateral gene transfer events. PLOS Genet. 2022;18(6):e1010239.
- 210. Sutherland KM, Ward LM, Colombero CR, Johnston DT. Inter-domain horizontal gene transfer of nickel-binding superoxide dismutase. Geobiology. 2021;19(5):450–9.

### **APPENDICES**

**Appendix 1.** Size-exclusion chromatography confirms the presence of cold-adapted ribosomes in the purified samples. An aliquot of a ribosome-containing sample from *P. urativorans* (the only abundant cellular structures with a molecular weight exceeding 2.5 MDa).



Appendix 2. Cryo-EM data collection, refinement and validation statistics.

Refinement	Structure 1	Structure 2	Structure 3
	70S P. urativorans ribosome/Balon/RaiA	70S P. urativorans ribosome/Balon/tRNA/mRNA	70S P. urativorans ribosome/Balon/EF- Tu
Model resolution (Å)	3.06	3.1	3.4
FSC threshold	0.5	0.5	0.5
Model resolution range (Å)	2.6 – 50	3.1 – 50	3.36 – 50
Map sharpening <i>B</i> factor (Ų)	-44.95	-40.01	-30
Model composition			
Non-hydrogen atoms	141,221	141,064	144,733
Protein residues	6,211	6,097	6,331
Ligands: Mg <sup>2+</sup>	1	1	1
B factors (Ų) (min/max/mean)			
Protein	3.7/98.4/32.6	3.6/98.4/32.5	3.6/98.4/32.5
Nucleotide	0.8/97.9/30.5	0.8/163.2/31.3	0.8/99.9/31.2
Ligand	30.0/30.0/30.0	-	30.00/30.00/30.00
R.m.s. deviations			
Bond lengths (Å)	0.007	0.006	0.009
Bond angles (°)	0.744	0.695	0.766
Validation			
MolProbity score	2.35	2.17	1.73
Clashscore	7.57	7.75	6.79
Poor rotamers (%)	0.16	4.08	0.13
Ramachandran plot			
Favoured (%)	94.81	95.88	94.83
Allowed (%)	4.03	4.06	5.07
Disallowed (%)	0.16	0.07	0.11

**Appendix 3.** Mass spectrometry analysis of ribosome sample from cold adapted *P. urativorans* (available as Excel file)

Appendix 4. List of bacterial species bearing a Balon gene (available as Excel file)

Appendix 5. List of bacterial species bearing a RaiA or HPG gene (available as Excel file)

Appendix 6. List of bacterial species bearing an RMF gene (available as Excel file)

Appendix 7. Mass spec ice treated vs non ice treated cells (available as Excel file)

### **PUBLICATIONS**

# Rippling life on a dormant planet: hibernation of ribosomes, RNA polymerases and other essential enzymes

Karla Helena-Bueno<sup>1,2,\*</sup>, Lewis I. Chan<sup>1,2,\*</sup>, Sergey V. Melnikov<sup>1\*</sup>

#### **Abstract**

Throughout the tree of life, cells and organisms enter states of dormancy or hibernation as a key feature of their biology: from a bacterium arresting its growth in response to starvation, to a plant seed anticipating placement in fertile ground, to a human oocyte poised for fertilization to create a new life. Recent research shows that when cells hibernate, many of their essential enzymes hibernate too: they disengage from their substrates and associate with a specialized group of proteins known as hibernation factors. Here, we summarize how hibernation factors protect essential cellular enzymes from undesired activity or irreparable damage in hibernating cells. We show how molecular hibernation, once viewed as rare and exclusive to certain molecules like ribosomes, is in fact a widespread property of biological molecules that is required for the sustained persistence of life on Earth.

<sup>&</sup>lt;sup>1</sup> Biosciences Institute, Newcastle University, Newcastle upon Tyne, UK

<sup>&</sup>lt;sup>2</sup> These authors contributed equally

<sup>\*</sup>Co-corresponding authors

### A new family of bacterial ribosome hibernation factors

**Karla Helena-Bueno**<sup>1,12</sup>, Mariia Yu. Rybak<sup>2,12</sup>, Chinenye L. Ekemezie<sup>1</sup>, Rudi Sullivan<sup>3</sup>, Charlotte R. Brown<sup>1</sup>, Charlotte Dingwall<sup>1</sup>, Arnaud Baslé<sup>1</sup>, Claudia Schneider<sup>1</sup>, James P. R. Connolly<sup>1</sup>, James N. Blaza<sup>4,5,6</sup>, Bálint Csörgő<sup>7</sup>, Patrick J. Moynihan<sup>3</sup>, Matthieu G. Gagnon<sup>2,8,9,10\*</sup>, Chris H. Hill<sup>5,6,11\*</sup>, Sergey V. Melnikov<sup>1\*</sup>,

#### Abstract

To conserve energy during starvation and stress, many organisms use hibernation factor proteins to inhibit protein synthesis and protect their ribosomes from damage. In bacteria, two families of hibernation factors have been described, but the low conservation of these proteins and the huge diversity of species, habitats and environmental stressors have confounded their discovery. Here, by combining cryogenic electron microscopy, genetics and biochemistry, we identify Balon, a new hibernation factor in the cold-adapted bacterium Psychrobacter urativorans. We show that Balon is a distant homologue of the archaeo-eukaryotic translation factor aeRF1 and is found in 20% of representative bacteria. During cold shock or stationary phase, Balon occupies the ribosomal A site in both vacant and actively translating ribosomes in complex with EF-Tu, highlighting an unexpected role for EF-Tu in the cellular stress response. Unlike typical A-site substrates, Balon binds to ribosomes in an mRNAindependent manner, initiating a new mode of ribosome hibernation that can commence while ribosomes are still engaged in protein synthesis. Our work suggests that Balon-EF-Tu-regulated ribosome hibernation is a ubiquitous bacterial stressresponse mechanism, and we demonstrate that putative Balon homologues in Mycobacteria bind to ribosomes in a similar fashion. This finding calls for a revision of the current model of ribosome hibernation inferred from common model organisms and holds numerous implications for how we understand and study ribosome hibernation.

<sup>&</sup>lt;sup>1</sup> Biosciences Institute, Newcastle University, Newcastle upon Tyne, UK

<sup>&</sup>lt;sup>2</sup> Department of Microbiology & Immunology, University of Texas Medical Branch, USA

<sup>&</sup>lt;sup>3</sup> School of Biosciences, University of Birmingham, Birmingham, UK

<sup>&</sup>lt;sup>4</sup>Department of Chemistry, University of York, York, UK

<sup>&</sup>lt;sup>5</sup>York Structural Biology Laboratory, University of York, York, UK

<sup>&</sup>lt;sup>6</sup> York Biomedical Research Institute, University of York, York, UK

<sup>&</sup>lt;sup>7</sup> Synthetic and Systems Biology Unit, Institute of Biochemistry, HUN-REN Biological Research Centre, Szeged, Hungary

<sup>&</sup>lt;sup>8</sup> Department of Biochemistry & Molecular Biology, University of Texas Medical Branch, USA

<sup>&</sup>lt;sup>9</sup> Sealy Center for Structural Biology & Molecular Biophysics, University of Texas Medical Branch, USA

<sup>&</sup>lt;sup>10</sup> Institute for Human Infections & Immunity, University of Texas Medical Branch, USA

<sup>&</sup>lt;sup>11</sup>Department of Biology, University of York, York, UK

<sup>&</sup>lt;sup>12</sup> These authors contributed equally

<sup>\*</sup> Co-corresponding authors

## A conserved ribosomal protein has entirely dissimilar structures in different organisms

Léon Schierholz<sup>1,4</sup>, Charlotte R. Brown<sup>2,4</sup>, **Karla Helena-Bueno**<sup>2,4</sup>, Vladimir N. Uversky<sup>3</sup>, Robert P. Hirt<sup>2</sup>, Jonas Barandun<sup>1\*</sup>, Sergey V. Melnikov<sup>2\*</sup>

<sup>1</sup>Department of Molecular Biology, Laboratory for Molecular Infection Medicine Sweden, Umeå Centre for Microbial Research and Science for Life Laboratory, Umeå University, Sweden.

<sup>3</sup>Department of Molecular Medicine and USF Health Byrd Alzheimer's Research Institute, Morsani College of Medicine, University of South Florida, Tampa, FL, USA.

#### **Abstract**

Ribosomes from different species can markedly differ in their composition by including dozens of ribosomal proteins that are unique to specific lineages but absent in others. However, it remains unknown how ribosomes acquire new proteins throughout evolution. Here, to help answer this question, we describe the evolution of the ribosomal protein msL1/msL2 that was recently found in ribosomes from the parasitic microorganism clade, microsporidia. We show that this protein has a conserved location in the ribosome but entirely dissimilar structures in different organisms: in each of the analyzed species, msL1/msL2 exhibits an altered secondary structure, an inverted orientation of the N-termini and C-termini on the ribosomal binding surface, and a completely transformed 3D fold. We then show that this fold switching is likely caused by changes in the ribosomal msL1/msL2-binding site, specifically, by variations in rRNA. These observations allow us to infer an evolutionary scenario in which a small, positively charged, de novo-born unfolded protein was first captured by rRNA to become part of the ribosome and subsequently underwent complete fold switching to optimize its binding to its evolving ribosomal binding site. Overall, our work provides a striking example of how a protein can switch its fold in the context of a complex biological assembly, while retaining its specificity for its molecular partner. This finding will help us better understand the origin and evolution of new protein components of complex molecular assemblies-thereby enhancing our ability to engineer biological molecules, identify protein homologs, and peer into the history of life on Earth.

<sup>&</sup>lt;sup>2</sup>Biosciences Institute, Newcastle University, Newcastle upon Tyne, UK.

<sup>&</sup>lt;sup>4</sup>These authors contributed equally

<sup>\*</sup>Co-corresponding authors

## Ribosomal proteins can hold a more accurate record of bacterial thermal adaptation compared to rRNA

Antonia van den Elzen<sup>1,2</sup>, **Karla Helena-Bueno**<sup>1,2</sup>, Charlotte R. Brown<sup>1,2</sup>, Lewis I. Chan<sup>1</sup>, Sergey V. Melnikov<sup>1\*</sup>

#### Abstract

Ribosomal genes are widely used as 'molecular clocks' to infer evolutionary relationships between species. However, their utility as 'molecular thermometers' for estimating optimal growth temperature of microorganisms remains uncertain. Previously, some estimations were made using the nucleotide composition of ribosomal RNA (rRNA), but the universal application of this approach was hindered by numerous outliers. In this study, we aimed to address this problem by identifying additional indicators of thermal adaptation within the sequences of ribosomal proteins. By comparing sequences from 2021 bacteria with known optimal growth temperature, we identified novel indicators among the metal-binding residues of ribosomal proteins. We found that these residues serve as conserved adaptive features for bacteria thriving above 40°C, but not at lower temperatures. Furthermore, the presence of these metalbinding residues exhibited a stronger correlation with the optimal growth temperature of bacteria compared to the commonly used correlation with the 16S rRNA GC content. And an even more accurate correlation was observed between the optimal growth temperature and the YVIWREL amino acid content within ribosomal proteins. Overall, our work suggests that ribosomal proteins contain a more accurate record of bacterial thermal adaptation compared to rRNA. This finding may simplify the analysis of unculturable and extinct species.

<sup>&</sup>lt;sup>1</sup>Biosciences Institute, Newcastle University, Newcastle upon Tyne, UK

<sup>&</sup>lt;sup>2</sup>These authors contributed equally

<sup>\*</sup>Corresponding author

### **PREPRINTS**

### Gosha: a database of organisms with defined optimal growth temperatures

Karla Helena-Bueno<sup>1,2</sup>, Charlotte R. Brown<sup>1,2</sup>, Sergey Melnikov<sup>1\*</sup>

- <sup>1</sup>Biosciences Institute, Newcastle University, Newcastle upon Tyne, UK
- <sup>2</sup>These authors contributed equally
- \*Corresponding author

#### **Abstract**

Currently, we are witnessing an explosive accumulation of genomic sequences for organisms across all branches of life. However, typically the genomic data lack the information about optimal growth conditions of corresponding organisms. As a result, it becomes challenging to use the genomic data for studying the adaptations of organisms and biological molecules to diverse environments. To address this problem, we have created a database Gosha, available at http://melnikovlab.com/gshc. This database brings together information about the genomic sequences and optimal growth temperatures for 25,324 species, including ~89% of the bacterial species with known genome sequences. Using this database, one can annotate genomic sequences from thousands of species and correlate variations in genes and genomes with optimal growth temperatures. The database interface allows users to retrieve optimal growth temperatures for bacteria, eukaryotes and archaea, providing a tool to explore how organisms, genomes, and individual proteins and nucleic acids adapt to certain temperatures. We hope that this database will contribute to medicine and biotechnology by helping to create a better understanding of molecular adaptations to heat and cold, leading to new ways to preserve biological samples, engineer useful enzymes, and develop biological materials and organisms with the desired tolerance to heat and cold.